Development of a Thermospray Nebulizer Interface for Liquid Chromatography with Flame Ionization Detection and Detector Response Studies of Volatile and non-Volatile Compounds

Christian Becker

DOI: 10.17185/duepublico/70525
URN: urn:nbn:de:hbz:464-20190919-123654-6

Development of a Thermospray Nebulizer Interface for Liquid Chromatography with Flame Ionization Detection and Detector Response Studies of Volatile and non-Volatile Compounds

Dissertation

zur Erlangung des akademischen Grades eines
Doktors der Naturwissenschaften
– Dr. rer. nat. –

vorgelegt von

Christian Becker
geboren in Moers

Institut für Instrumentelle Analytische Chemie
der
Universität Duisburg-Essen

Die vorliegende Arbeit wurde im Zeitraum von April 2012 bis Mai 2015 im Arbeitskreis von Prof. Dr. Torsten C. Schmidt am Lehrstuhl für Instrumentelle Analytische Chemie der Universität Duisburg-Essen durchgeführt.

Tag der Disputation: 19.07.2019

Gutachter:	Prof. Dr. Torsten C. Schmidt
	Prof. Dr. Oliver J. Schmitz
Vorsitzender:	Prof. Dr. Matthias Epple

Contents

Chapter 3 (Continued)

A thermospray nebulizer interface for liquid chromatography - flame ionization detection: Development and optimization

Chapter 4

Response analysis: A brief introduction to the applied response factor equations and the most common response factor prediction models 51

Chapter 5

Determination of liquid chromatography/flame ionization detection response factors for alcohols, ketones and sugars 61

Chapter 6

Determination of liquid chromatography/flame ionization detection response factors for N-heterocycles, carboxylic acids, halogenated compounds and others 79

Chapter 6 (Continued)

Determination of liquid chromatography/flame ionization detection response factors for N-heterocycles, carboxylic acids, halogenated compounds and others

Summary

Liquid chromatography (LC) is the analytical tool of choice for the investigation of by-products in pharmaceutical and chemical industry. The UV- and refractive index detector (RFID) encounter to the most common detectors for these purposes. The detection of unknown by-products deliver no sufficient information, since both detectors only can be used for a limited spectrum of analytes. Furthermore, without knowledge of the chemical structure, a semi-quantitative analysis is barely possible.

The flame ionization detector (FID) is advantageous to provide semi-quantitative data in the detection and quantification of, e.g., synthesis by-products in pharmaceuticals and chemical products. In contrast to commonly applied detectors, the FID signal is proportional to the carbon content of the analyte and allows the estimation of an analyte concentration directly out of the obtained signal. Several attempts to employ the FID for liquid chromatography have been carried out until yet [1].

This thesis described the development of a novel LC/FID interface and a FID response study of more than 100 compounds in order to achieve a better understanding of differences between gas chromatography (GC)/FID and LC/FID response data. The thesis was divided into 3 major sections: 1. a detailed study of previously described interfaces, 2. the development and optimization of a novel interface and 3. the analysis and comparison of response data obtained by GC/FID and LC/FID.

The historical conveyor type systems were designed to overcome the problems arise in FI detection by use of organic solvents in liquid chromatography. Therefore the systems dependent choice of non-volatile analytes in the beginning of LC/FID coupling change to volatile analytes by implementation of only water liquid chromatography [1]. Previously invented interfaces were studied to find out the advantages and disadvantages between the different types of interfaces, such as conveyor based interfaces, capillary jet interfaces or spray chamber interfaces. The focus was set on direct coupling techniques which can be operated without pre-evaporation steps of signal disturbing organic solvents, as known from conveyor type interfaces. The advantages and disadvantages of these interfaces were critically reviewed to design and present a novel interface.

In the development and optimization of the here designed interface the influence of the nebulizer material on flame stability and capillary blockage was shown. Previously reported problems such as blocking of the transfer capillary were solved using a stainless steel nebulizer body and transfer capillary. The effects of the working parameters such as backpressure, gas flow, distance between nebulizer nozzle and FID collector or FID temperature on the signal were analyzed.

The novel interface was validated for selected compounds known from literature. The linear correlation of the concentration and obtained FID signal of 21 N-heterocycles and 6 alcohols was found to be R^2 = 0.991 to 0.999. The limits of detection of N-heterocycles ranged from 0.24 ng (pyrimidine-N-oxide) to 1.26 ng (s-triazin) absolute injected carbon. Obtained results for chromatographic separation of the alcohols propanol, butanol, pentanol and hexanol, used within previous studies in the field of LC/FID coupling were presented and compared to literature. The developed interface showed a substantial improvement of the absolute injected carbon concentration down to 0.28 ng (ethanol) in comparison to previously invented interfaces.

The use of different theoretical and practical response models was discussed to assist the response studies performed in the final section of the thesis. The scope was set on the experimental derived Effective Carbon Number (ECN_{Exp}) [2, 3] and experimental relative sensitivity (RF_{Exp}) [2, 4], respectively.

The influences of functional groups and substitutes, such as hydroxyl groups, halogens and ketones were discussed regarding former GC/FID studies. For some functional groups, effects on the obtained signals were found to be more negligible by extension of the carbon backbone. The influence of mono-alcohols decreased from C1 to C7. The effects of mono-, di- and poly-substituted compounds were compared and a substantial effect of the substitute location and the response factor was observed for, e.g., butan-1,2-ole.

Inflame processes for pyrimidine and pyridazine were proposed by the support of literature data. The response data of structural isomers obtained by theoretical response models (e.g. pyridine) were compared to experimental data of literature and within this study. The differences of theoretical isomer response data (e.g. pyridine, pyrimidine) to experimental

data were explained by the occurring inflame processes. In the end the response data were compared to GC/FID response data as far as they are available.

The present work is a great step forward for the analysis of volatile and non-volatile compounds using LC/FID. For the first time the responses of more the 100 different compounds were detected using LC/FID and compared to GC/FID response data if available. Much more LC feasible compounds are available, therefore further work is necessary to investigate all of this compounds and compare them to GC/FID responses. Further research in pharmaceutical industry is required to show the advantages of the semi-quantitative analysis of by-products by LC/FID.

Zusammenfassung

Die Flüssigchromatographie (LC) ist die Methode der Wahl für die Untersuchung von pharmazeutischen bzw. chemischen Produkten und derer Synthese-Nebenprodukte. Der UV-Detektor und Brechungsindexdetektor (RFID) zählen zu den am häufigsten verwendeten Detektoren für diese Untersuchungen. Beide Detektoren liefern jedoch nur unzureichende Informationen über die zu untersuchenden Nebenprodukte, da sie nur für ein kleines Spektrum an Verbindungen angewandt werden können und bei nicht Kenntnis der Struktur nur eine limitierte Aussagekraft in der quantitativen Analyse von Nebenprodukten vorweisen.

Der Flammenionisationsdetektor (FID) bietet deutliche Vorteile in der semi-quantitativen und qualitativen Analyse von u.a. Synthese-Nebenprodukten in der pharmazeutischen und chemischen Industrie. Im Gegensatz zu den häufig verwendeten UV- und RFI-Detektoren besitzt der FID ein konzentrationsabhängiges Detektorsignal, welches proportional zu dem Kohlenstoffgehalt der Verbindung ist. Die Proportionalität zwischen Signal und Kohlenstoffgehalt ermöglicht eine semi-quantitative Konzentrationsbestimmung auch unbekannter Nebenprodukte. Es wurden bereits zahlreiche Versuche unternommen, diesen in der Gaschromatographie verwendeten Vorteil des FID auch für die LC nutzbar zu machen [1].

Diese Arbeit beschreibt die Entwicklung eines neuen LC/FID Interface und die damit durchgeführten Responsestudien an über 100 verschiedenen Substanzen, um ein besseres Verständnis der Unterschiede zwischen GC/FID und LC/FID Responsen zu erhalten. Die Arbeit unterteilt sich in drei Segmente: 1. eine detaillierte Studie von bereits in der Literatur erwähnten LC/FID Systemen, 2. die Entwicklung und Optimierung eines neuen LC/FID Interfaces und 3. die Analyse von verschiedenen leichtflüchtigen bis schwerflüchtigen Substanzen und der Vergleich der experimentellen Responsen zwischen GC/FID und LC/FID.

In der Vergangenheit wurden LC/FID Interfaces so entwickelt, dass sie die in der LC verwendeten organischen Lösungsmittel durch Förderbänder und Verdampfer-Einheiten beseitigen konnten. Daher waren die ersten LC/FID Systeme auf die Analyse von schwerflüchtigen Substanzen limitiert, welche nicht im Lösungsmittelverdampfungsschritt

entfernt wurden. Das Design änderte sich jedoch mit der Einführung von rein wässrigen LC Methoden. Die Einführung dieser Methode ermöglichte die direkte Kopplung von LC und FID durch z.B. Kapillar-Jet-Interfaces oder die Zerstäuber-Sprüh-Kammer

Eines der am häufigsten berichteten Probleme von Kapillarbasierten Interfaces ist das Verstopfen der Transferkapillare für den Eintrag der wässrigen mobilen Phase in den FID. Für die Untersuchung dieses Problems wurden verschiedene Materialien und Systemaufbauten getestet. Die Untersuchungen zeigten, dass der Effekt durch ein rein stahlbasiertes System mit Transferkapillaren, welche einen größeren Innendurchmesser als die bis dahin verwendeten Glaskapillaren haben, nahezu vollständig beseitigt werden kann. Da die Verwendung solcher Kapillaren jedoch eine Restriktion innerhalb des Systems erfordert, wurde der Einfluss von verschiedenen Rückdrucken untersucht. Weitere Parameter, welche im Verlauf der Entwicklung optimiert wurden, waren u.a. der Gas Fluss, die Einbauhöhe des Interface und die FID Temperatur.

Das entwickelte Interface wurde durch Messung von diversen aus der Literatur bekannten Substanzen getestet. Eine lineare Korrelation von Kohlenstoffgehalt und FID Response wurde bei 21 untersuchten N-Heterozyklischen Verbindungen und sechs Alkoholen nachgewiesen. Die Korrelation für alle untersuchten Substanzen lag hierbei zwischen R^2 0.991 und 0.999. Die Nachweisgrenzen der heterozyklischen Verbindungen lagen zwischen 0.24 ng (Pyrimidin-n-oxyd) und 1.24 ng (s-Triazin) absolut injizierte Substanzmenge. Die chromatographische Auftrennung der untersuchten Alkohole zeigte eine deutliche Verbesserung der Nachweisgrenzen mit Hilfe des hier präsentierten Interface auf 0.28 ng (Ethanol) im Vergleich zu bestehenden LC/FID Systemen.

In der zweiten Sektion der Arbeit wurden die der Analyse zugrundeliegenden Responseberechnungen und einige theoretische Responsevorhersagemodelle diskutiert. Der Fokus der angewandten Response Modelle lag auf der experimentellen effektiven Kohlenstoffzahl (ECN_{EXP}) [2, 3] und der experimentellen relativen Sensitivität (RF_{Exp}) [2, 4].

Die Einflüsse verschiedener funktioneller Gruppen wie beispielsweise OH-Gruppen, Halogene und Ketone wurde in der zweiten Sektion mit Bezug auf publizierte GC/FID Studien diskutiert. Hierbei konnte festgestellt werden, dass der Einfluss der OH-Gruppe in

mono-substituierten Alkoholen mit steigender Kohlenstoffzahl von C1 bis C7 deutlich abnimmt. Die Studien haben gezeigt, dass nicht nur der Substituent, sondern die Position innerhalb einer Verbindung einen signifikanten Einfluss auf das Responseverhalten einer Verbindung hat.

Die aus der Literatur bekannten Verbrennungsprozesse für verschiedene Verbindungen wurden verwendet, um einen detaillierteren Einblick auf die erhaltenen Unterschiede im Responseverhalten von beispielsweise Pyrimidin und Pyridazin zu erhalten. Die Diskrepanzen zwischen theoretischen und experimentellen Werten für Isomere konnten so aufgezeigt werden. Gängige theoretische Responseberechnungsmodelle berücksichtigen diese Unterschiede von Isomeren bisher nicht. Abschließend wurden die in dieser Arbeit erhaltenen experimentellen Responsedaten mit den experimentellen Werten aus GC/FID Responsestudien verglichen.

Diese Arbeit bedeutet einen großen Schritt für die Analyse von volatilen und nicht-volatilen Substanzen mittels LC/FID. Erstmals wurden die LC/FID Responsen von mehr als hundert verschiedenen Substanzen gemessen und wenn möglich mit den Responsedaten aus GC/FID Responsestudien verglichen. Die Bandbreite an GC und LC fähigen Substanzen ist jedoch groß, daher wird es in zukünftige Projekten notwendig sein noch weitere Verbindungen zu analysieren und die erhaltenen Responsedaten mit denen aus GC/FID Studien zu vergleichen. Um eine Akzeptanz der hier vorgestellten Detektion und der damit verbundenen semi-quantitativen Analyse von Nebenprodukten während der Synthese von z.B. pharmazeutischen Produkten zu schaffen, ist es notwendig, weitere Studien im Gebiet der pharmazeutischen Industrie durch zu führen.

References

[1] C. Becker, M.A. Jochmann, T.C. Schmidt, An Overview of Approaches in Liquid Chromatography Flame ionization Detection, TrAC Trends in Analytical Chemistry, 110 (2018) 143-149.
[2] J.T. Scanlon, D.E. Willis, Calculation of Flame Ionization Detector Relative Response Factors Using the Effective Carbon Number Concept, J. Chromatogr. Sci., 23 (1985) 333-340.
[3] J.C. Sternberg, Gallaway, W.S. and Jones, D.T.L., The Mechanism of Response of Flame Ionization Detectors, in: Gas Chromatography: Third International Symposium Held Under the Auspices of the Analysis Instrumentation Division of the Instrument Society of America, June 13-16, 1961, Academic, 1962, pp. 231-267.
[4] W.A. Dietz, Response Factors for Gas Chromatographic Analyses, J. Chromatogr. Sci., 5 (1967) 68-71.

Chapter 1

Introduction and scope

1.1 Liquid chromatography/flame ionization detection as analytical tool

On-line monitoring of pharmaceutical products and by-products requires fast and sensitive analytical methods. Since most pharmaceuticals are non-volatile, common gas chromatography (GC) systems cannot be used without time consuming sample pre-treatment steps such as derivatization. Especially during the synthesis of new pharmaceuticals or pesticides, unwanted by-products can occur. The different characteristics of the main synthetic products and their by-products can cause undesired, time consuming analytical problems in industry and science. Commonly, non-volatile compounds are analyzed using liquid chromatography (LC) while the volatile compounds like residual solvents are analyzed by GC. Due to the substance specific characteristics of the partially unknown by-products, e.g., the lack of a chromophoric group or analyte volatility, combinations of different detectors are required. In addition, quantitative analysis requires reference standards, which can be expensive or have to be synthesized since they are not commercially available at all.

Quantitative response analysis by flame ionization detection (FID) after GC separation has been established as a powerful and fast technique in, e.g., fragrance and petroleum industries [1]. The selectivity for carbon and the sensitivity to organic compounds make the FID capable to quantify a wide range of analytes. Studies on FID response showed a linear correlation between carbon content and response signal [2-5]. The only limitation of FID analysis was the required volatility of the analytes for GC separation. A suitable solution to overcome the lack of FID analysis of non-volatile analytes was the introduction of LC/FID hyphenations, starting already in the 1960s.

The biggest challenge in the development of LC/FID was the coupling itself, as the separation takes place in the liquid phase and detection requires transfer of the analytes into the gas phase. Organic solvents as eluent in LC made a direct and fast coupling impossible [6]. Solvents needed to be vaporized or separated to minimize interferences or saturation of the FID, caused by carbon overload. The first interfaces bridging this gap were

introduced in the 1960s [7-9] and based on a pre-evaporation of organic solvents. In the coming decades advanced systems such as supercritical fluid interfaces [10] and capillary based interfaces were presented, finally leading to spray chamber interfaces introduced in 2012 [11, 12].

Capillary based interfaces and the nebulizer spray chamber changed the spectrum and scope of the analytes of LC/FID analysis. Investigation of volatile compounds such as alcohols, aldehydes or ketones became possible by LC/FID. Furthermore, non-volatile compound analysis by FID became possible, too [6]. However, for some compounds the responses of the existing LC/FID interfaces are different from the ones obtained in GC/FID [2, 12]. Non-volatile analytes, such as carbohydrates and amino acids, were observed to have non-linear responses and spray chamber type nebulizers are known to cause memory effects if used in non-volatile compound analysis [11, 12]. Therefore, a robust and direct interface is required to close the gap between GC/FID and LC/FID.

Although capillary based LC/FID couplings have been thoroughly investigated over the past 30 years and have been successfully applied to analyze a multitude of compounds, the interfaces still can be improved. In GC/FID, responses of more than 200 different substances are evaluated and categorized according to their substance classification [1, 5, 13-15]. Based on such data, several prediction methods for FID response were explored. In contrast, studies on LC/FID responses are rare and the influence of the mobile phase as well as the comparability of GC/FID and LC/FID response studies has not been investigated yet. Applications and investigations on the response behavior of heterocyclic compounds, pharmaceuticals and organic acids have barely been described before.

1.2 Aims and scope

Past research projects showed the potential of LC/FID as a low cost universal and robust detector for semi-quantitative analysis of different compound groups. Solving the low durability of fused silica capillary based coupling approaches, LC/FID can become a green alternative to organic solvent and reference material based analysis.

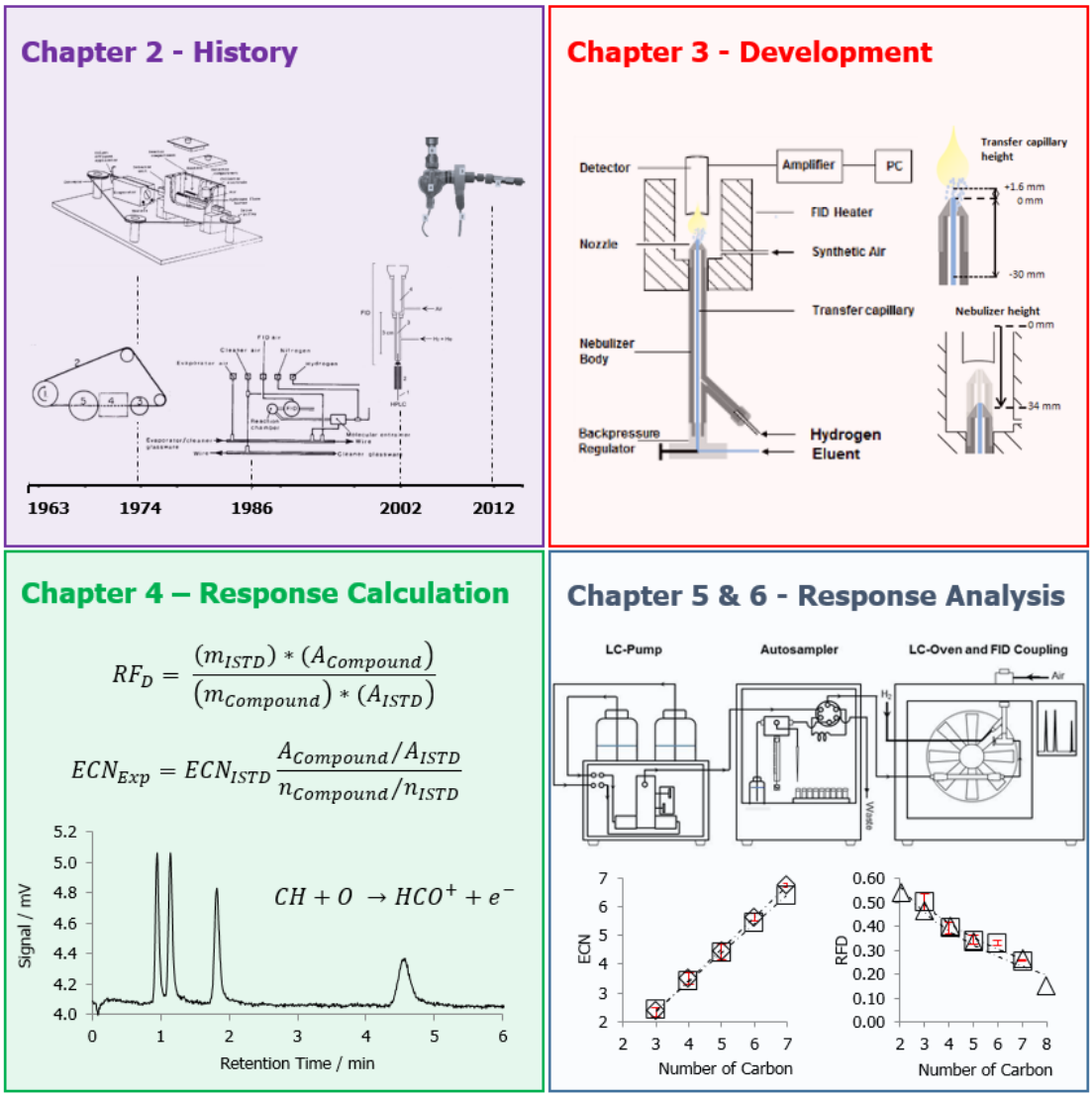

Figure 1.1. Graphical presentation of the main chapters and contents of this work. Chapter 2 contains the review of former approachesin LC/FID coupling. Chapter 3 shows schematically the optimization of the self-made nebulizer. The theoretical background of response factor analysis discussed in Chapter 4. Chapter 5 and 6 show the system setup used within this work and diagrams of the response behavior of alcohols.

The present study is divided into five main chapters (Figure 1.1) and a final conclusion and outlook. The main chapters focus on the recent developments of LC/FID (Chapter 2), the

development and improvement of a self-made capillary based interface (Chapter 3), the theoretical background of FID response analysis (Chapter 4) and the systematic study of LC/FID responses of more than 100 compounds (Chapter 5 and 6).

Chapter 2 is a critical review and discussion of former interface systems and the obtained results and limitations. The detailed study of previous LC/FID couplings helps to figure out problems encountered and innovations done over the past decades. Therefore, the history of LC/FID from the first coupling approaches by moving wires and disks, to capillary based interfaces and nebulizer spray chambers is presented.

Based on the technical data and results of previous LC/FID couplings, a novel interface for the analysis of volatile and non-volatile compounds is presented in **Chapter 3**. The applicability of the self-made LC/FID interface was investigated within this study. The effects of different mobile phase flow rates on the FID parameters such as gas flows and temperature were investigated by several authors [16]. Within this chapter, several other parameters (e.g., backpressure, capillary size and column flow) were investigated. Significant influence on the efficiency of the interface and the sensitivity of the analyte signal were observed. In addition, the relationship between robustness and capillary material was investigated.

Two points still need to be investigated in LC/FID analysis: the responses of a broad variety of compounds and the related in-flame processes for a better understanding of the observed response. Only limited results are available for the former and the available results mainly focus on investigation of alcohols and related volatile compounds. The latter is only discussed rudimentary in FID related publications. Many GC/FID studies are dealing with response behavior of organic analytes such as alcohols and alkanes. Dietz [17] and Sternberg et al. [5] presented comprehensive studies of response data for more than 120 compounds. However, the scope of these investigations was set on GC relevant analytes. As a proof of concept, different response factor calculations relevant for GC were applied to the data obtained here. To provide an overview of the fundamental equations of response factor calculation, **Chapter 4** introduces the response models applied within this work. The presented models are namely the Effective Carbon Number of a component, here defined as ECN_{Exp} [18], the theoretical effective carbon number ECN_{Theo} according to

Sternberg et al. [5], the relative sensitivity or divisor response factor according to Dietz RF_D [17] and the relative sensitivity calculated by the here presented data RF_{Exp}. Furthermore, discrepancies between theoretical response of structural isomers and experimental data described in literature are discussed in this chapter.

In **Chapter 5** the response data and proposed in-flame processes of alcohols, poly-alcohols, alditols, ketones and sugars are presented. **Chapter 6** focuses on the response and relevant combustion processes of nitrogen heterocycles, halogenated compounds, organic acids and others. Both chapters present the response data of more than 100 compounds, thus, by far exceeding the previously available number and variability of compounds in LC/FID response studies.

Chapter 7 concludes this work with a brief general discussion of the presented work, future trends and perspectives of LC/FID as analytical tool.

1.3 References

[1] E. Tissot, S. Rochat, C. Debonneville, A. Chaintreau, Rapid GC-FID quantification technique without authentic samples using predicted response factors, Flavour and Fragrance Journal, 27 (2012) 290-296.
[2] R.G. Ackman, J.C. Sipos, Flame ionization detector response for carbonyl carbon atom in carboxylic group of fatty acids + esters, J. Chromatogr., 16 (1964) 298-305.
[3] T. Holm, Aspects of the mechanism of the flame ionization detector, J. Chromatogr. A, 842 (1999) 221-227.
[4] H.Y. Tong, F.W. Karasek, Flame ionization detector response factors for compound classes in quantitative analysis of complex organic mixtures, Anal. Chem., 56 (1984) 2124-2128.
[5] J.C. Sternberg, Gallaway, W.S. and Jones, D.T.L., The Mechanism of Response of Flame Ionization Detectors, in: Gas Chromatography: Third International Symposium Held Under the Auspices of the Analysis Instrumentation Division of the Instrument Society of America, June 13-16, 1961, Academic, 1962, pp. 231-267.
[6] C. Becker, M.A. Jochmann, T.C. Schmidt, An Overview of Approaches in Liquid Chromatography Flame ionization Detection, TrAC Trends in Analytical Chemistry, (2018).
[7] O.S. Privett, W.L. Erdahl, An improved flame ionization detector for high performance liquid chromatography, Anal. Biochem., 84 (1978) 449-461.
[8] R.P.W. Scott, J.G. Lawrence, An improved moving wire Liquid chromatography detector, J. Chromatogr. Sci., 8 (1970) 65-71.
[9] A.T.R. James, J.R.; Scott, R.P.W. , Chern. And., 18 (1964) 146 - 756.
[10] M.G. Rawdon, Modified flame ionization detector for supercritical fluid chromatography, Anal. Chem., 56 (1984) 831-832.
[11] E. Young, R.M. Smith, B.L. Sharp, J.R. Bone, Liquid chromatography-flame ionisation detection using a nebuliser/spray chamber interface. Part 1. Design and testing, J. Chromatogr. A, 1236 (2012) 16-20.
[12] E. Young, R.M. Smith, B.L. Sharp, J.R. Bone, Liquid chromatography-flame ionisation detection using a nebuliser/spray chamber interface. Part 2. Comparison of functional group responses, J. Chromatogr. A, 1236 (2012) 21-27.
[13] B. Lučić, N. Trinajstić, S. Sild, M. Karelson, A.R. Katritzky, A New Efficient Approach for Variable Selection Based on Multiregression: Prediction of Gas Chromatographic Retention Times and Response Factors, Journal of Chemical Information and Computer Sciences, 39 (1999) 610-621.
[14] J.Y. de Saint Laumer, E. Cicchetti, P. Merle, J. Egger, A. Chaintreau, Quantification in gas chromatography: prediction of flame ionization detector response factors from combustion enthalpies and molecular structures, Anal. Chem., 82 (2010) 6457-6462.
[15] G. Musumarra, D. Pisano, A.R. Katritzky, A.R. Lapucha, F.J. Luxem, R. Murugan, M. Siskin, G. Brons, Prediction of gas chromatographic response factors by the PLS method, Tetrahedron Comput. Methodol., 2 (1989) 17-36.
[16] D. Guillarme, S. Heinisch, J.Y. Gauvrit, P. Lanteri, J.L. Rocca, Optimization of the coupling of high-temperature liquid chromatography and flame ionization detection application to the separations of alcohols, J. Chromatogr. A, 1078 (2005) 22-27.

[17] W.A. Dietz, Response Factors for Gas Chromatographic Analyses, J. Chromatogr. Sci., 5 (1967) 68-71.
[18] J.T. Scanlon, D.E. Willis, Calculation of Flame Ionization Detector Relative Response Factors Using the Effective Carbon Number Concept, J. Chromatogr. Sci., 23 (1985) 333-340.

Chapter 2

An overview of approaches in liquid chromatography flame ionization detection‡

Several attempts to combine liquid chromatography (LC) with flame ionization detection (FID) have been made since the 1960s. Elaborated systems were developed to overcome problems such as detector overload by use of organic solvents in LC or transfer of non-volatile analytes into FID. Almost twenty years after the first successful applications by solvent evaporation based techniques, subcritical water high temperature liquid chromatography opened the door for novel approaches to combine LC with FID. Direct coupling without pre-evaporation steps of signal disturbing organic solvents became possible and new instrumental developments resulted in capillary jet interface systems. These systems are suitable for a broad range of volatile and non-volatile analytes, which led to a significant increase of publications. This review discusses the most important developments of LC/FID coupling and summarizes its field of applications.

‡Adapted from: C. Becker, M.A. Jochmann, T.C. Schmidt, An Overview of Approaches in Liquid Chromatography Flame ionization Detection, TrAC, 110 (2019) 143-149.

2.1 Introduction

Several LC based analytical methods with various detectors are available for a detailed characterization as well as quantification of pharmaceutical impurities [1]. According to the ICH Q3A Guideline the pharmaceutical impurities are classified into (i) inorganic impurities, (ii) organic impurities and (iii) residual solvents. One of the most frequently used detectors for the analysis of organic impurities is the UV- or Diode array (DA) detector [1, 2]. However, UV- and DA-detection methods are only useful if the analytes have a suitable chromophore [3, 4].

Substances without chromophore are commonly detected by Refractive Index (RI) or Evaporative Light Scattering Detectors (ELSD). The ELSD is well applicable as LC detector in case of non-volatile compounds, and analysis of, e.g., lipids, sugars [5] and pharmaceuticals [6] highlighted its broad application range. However, a quantification by ELSDs is limited [2] because the ELSD is known to have a non-linear response which increases exponentially with increasing sample size, whereby the exponent depends substantially on the exact design of the nebulizer [7]. RI in contrast to ELS detection, has a limited sensitivity, is temperature dependent and shows interferences as well as baseline drifts by application of solvent gradients [5].

All of these detection modes have their limitations in qualitative and quantitative analysis and, therefore, reviews on analysis of pharmaceuticals and their by-products revealed Mass Spectrometry (MS) analysis as method of choice [7]. These drawbacks demonstrate that there is a need for a robust and almost maintenance free detector to overcome the above-mentioned limitations of quantification during synthesis of pharmaceutical and chemical products. The FID with its carbon related response rather support a fast semi-quantitative screening of pharmaceutical and chemical products in general, then determining the chemical structure as done by MS methods.

The FID commonly applied in gas chromatography (GC), is known to be a robust and precise detector for the analysis of carbon containing materials. It provides linear response in the order of 10^4 to 10^7 and delivers a signal proportional to the carbon content of the analyte, and allows the estimation of analyte concentration directly out of the obtained

signal [8-10]. Use of reference materials, as required for other LC detectors, is not necessary for semi-quantitative impurity screening and investigation of volatile and non-volatile analytes by LC/FID. Furthermore, in contrast to GC/FID, LC/FID analysis of non-volatile analytes requires no time consuming sample preparation and pre-treatment such as derivatization.

In the following, we will discuss early LC/FID interfaces that used a chain, moving wire or disk for uptake of an organic mobile phase prior to detection to prevent FID signal saturation. In the early 1990´s the introduction of subcritical water high temperature LC methods paved the way for LC/FID interfaces in the coming decades [11]. Direct LC/FID hyphenation became possible. In contrast to organic solvents, water causes no detector overload. Therefore, aqueous LC represents a valuable application field for LC/FID coupling for the analysis of, e.g., alcohols [12, 13], pharmaceuticals [14] or lipids [15]. The drop cell interface [16, 17], fused silica (FS) based capillary jet interfaces [12, 18, 19], stainless steel (SS) capillary jet interfaces [20] or the nebulizer/spray chamber [21, 22] have become promising techniques, capable to detect a wide variety of volatile and non-volatile compounds.

2.2 Early developments

2.2.1 Conveyor interfaces

The first types of LC/FID interfaces are known as conveyor type interfaces (Figure 2.1), named according to the mechanism of solvent uptake and evaporation processing by a moving wire or belt. The first LC/FID interface was issued by Haahti and Nikkari in 1963 [23]. Conveyor type interfaces had three major parts in common: first - a circulating (or feeding) chain, wire or belt; second - an air stripping chamber to evaporate the eluent with inert gases such as argon [24] or helium used in later systems [25, 26]; and third - a pyrolyzation chamber, for pyrolysis of analytes attached onto the wire or belt. The pyrolysis products then were swept into the FID using helium or hydrogen as carrier gas.

The system by Haahti and Nikkaris suffered from loss of analytes and high electrical noise generated by the chain mesh [27]. Later on this problem was targeted by use of a platinum

chain which vertically passed through the FID flame, by that the collector electrode was located concentric to the chain [28]. A more complex interface was published in 1964. The authors used a transport wire instead of a chain for solvent uptake. These early designs suffered of poor reliability and the transport mechanisms were susceptible to failures [29].

The concept was improved and in 1967 the Pye LCM Liquid Chromatograph became the first commercially available LC/FID interface [30]. To enhance the limit of detection, an oxidizing chamber was implemented. After evaporation of the solvent, the sample undergoes combustion to carbon dioxide and water. The carbon dioxide then is reduced in the presence of hydrogen and a nickel catalyst to methane [29, 30]. The pre-combustion/reduction enhanced the sensitivity by one order of magnitude.

Within the following decades, slight changes of the operation principles were made, e.g., a modified version of the Pye LC by improvement of the belt and eluent applicator [31]. Other authors transferred the eluent onto the belt using a spray mechanism [32] or exchanged the belt by a wire [25]. The modifications enhanced the obtained detection limits by a factor of up to 50 in comparison with earlier systems [32].

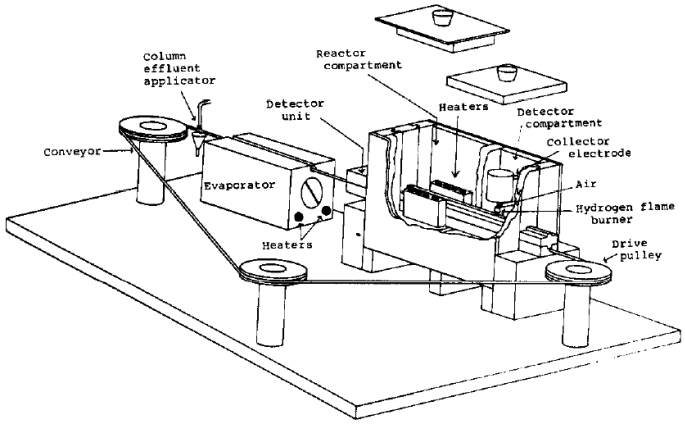

Figure 2.1. Wire based conveyor type interface according to Privett and Erdahl (1978) [26].

Within the first decades, analysis by moving wire interfaces focused on non-volatile compounds such as squalene [23], synthetic rubber samples and polystyrene [31], albumin, glucose and cholesteryl [26] or diphosphatidylglycerol, phosphatidyl-ethanolamine or sphingomyelin in environmental samples [33]. The first application of LC/FID interfaces

for volatile compounds was reported by Karmen [34]. In contrast to former systems, the author used the nitrogen steam inside the drying tube as carrier gas to transport volatile analytes into the FID. A summary of the investigated compounds and the corresponding references is given in Table 2.1.

One of the last publications of wire based LC/FID systems was published in 1986 using the Pye LCM 2, a development of the Pye LCM system [25]. The Pye instruments were produced between 1968 and 1974, after that Young et al. patented a nebulizer spray chamber based system, however the Pye systems are known to be the only commercially available LC/FID systems.

2.2.2 Rotating disk interfaces

Cobler et al. (1968) patented a second type of conveyor interface: the rotating disk [35]. In the setup a rotating perforated metal disc carried the eluent from a gel permeation column into the FID flame. Except for the difference between disk and belt (or wire) the major three compartments of solvent application, evaporation and pyrolysis stayed the same (Figure 2.2). In contrast to wire based systems, the disk relied on low flow rates and required cleaning before further uptake of eluent. The authors successfully applied the system to the detection of, e.g., polystyrenes [27].

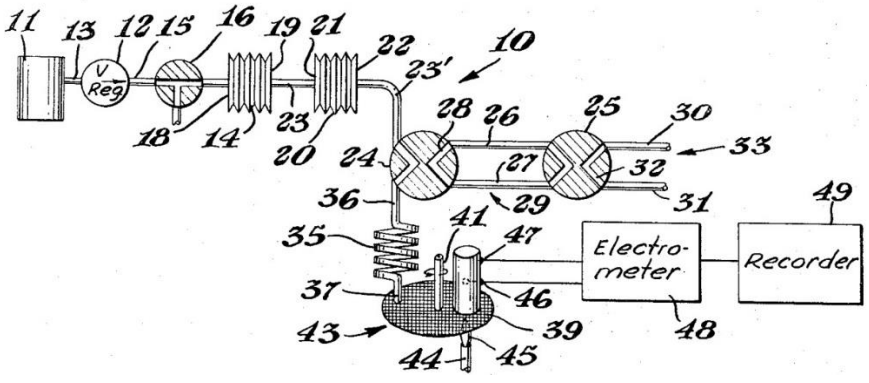

Figure 2.2. Disk based conveyor type interfaces according to Cobler et al. (1968) [35].

Further disc type interfaces used a ceramic disc, heated by an infrared lamp to evaporate the solvent and a two part detector in which the flame was located below the disc and the

electrodes were placed above [36] or a vertically spinning porous alumina disc, other systems used a ceramic coated ring instead of a disc [37].

A more sophisticated type of disk interface was presented in 1989 (Figure 2.3a) [27]. The transport mechanism was made of a two-part disc mounted on the shaft of a stepper motor fixed to the main chassis of the instrument. 40 quartz rods were connected to the disc, as shown in Figure 2.3b. The eluent was deposited at the delivery point onto the FS rods. The disc mechanism was positioned at a slight angle from the horizontal, so that the liquid tends to flow towards the end of the rod. Once liquid was deposited onto a rod, the rod moved over the evaporation air flow. The volatile eluent was completely evaporated and the rod was stepped into the center of the flame, where any carbon containing residue was combusted. After cooling down, the rod then reaches the liquid uptake stage again [27].

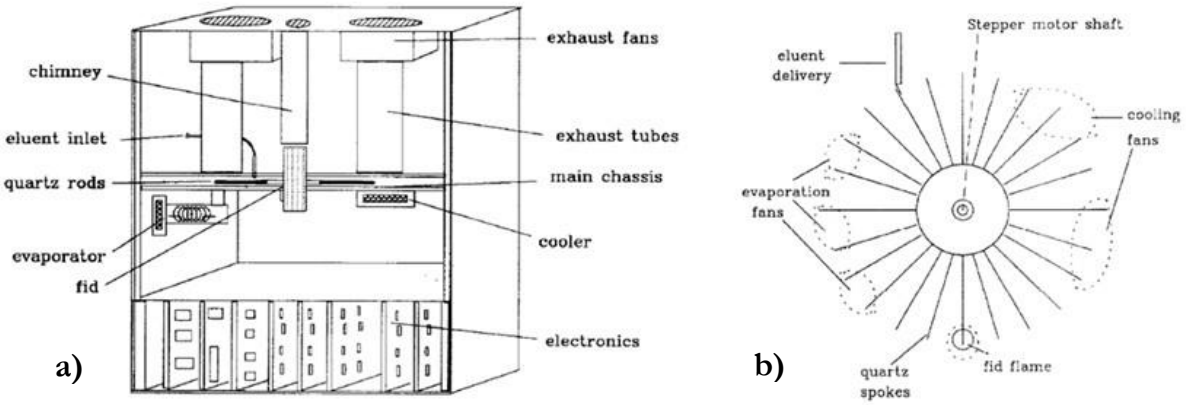

Figure 2.3. Quartz rod assembly by Malcome-Lawes and Moss (1989) [27].
a) Complete detector unit; **b)** Quartz rod solvent transport system.

The system linearity was examined using pyrene, whereby the detector was observed to be overloaded at 20 μg applied. In further experiments the authors used a homologues series of alkanes (C12 - C40). The response was found to reach a plateau at C22 - C40, indicating a non-linear response behavior [27].

Table 2.1. Type of LC/FID systems with corresponding literature (Ref.) and exemplary investigated compounds, sample type and LODs.

Analytes	LOD	Sample Type	Ref.
Conveyor type interfaces (Wire or Belt)			
Squalene, cholesteryl palmitate, oleyl alcohol	n/a	Human sebum, human serum	[23]

Table 2.1. (Continued) Type of LC/FID systems with corresponding literature (Ref.) and exemplary investigated compounds, sample type and LODs.

Analytes	LOD	Sample Type	Ref.
Conveyor type interfaces (Wire or Belt)			
Polystyrene	n/a	Synthetic rubber	[31]
Squalene	n/a	Squalene mixture	[24]
C12 to C40 alkanes, pyrene	n/a	Alkane mixture	[27]
Methyl esters	n/a	Soybean oil glycerolysis mixture	[15]
Triolein and phospholipids	n/a	Blood serum, liver and kidney tissue	[33]
Cholesteryl oleate and triolein	n/a	Cholesteryl oleate and triolein mixture	[26]
Fatty acid methyl esters, sterole esters and tri glycerides	n/a	Fatty acid methyl esters, sterole esters and tri glycerides mixtures	[34]
Xylose, glucose, sucrose, maltose and lactose	110 - 400 ng	Sugar standard mixture	[25]
Conveyor type interfaces (Disk)			
Gel permeation chromatography	n/a	Standard mixtures	[35]
No application mentioned	n/a	Parathion, methyl parathion and diazinon mixture	[38]
No application mentioned	n/a	-	[36]
n-eicosane	2 ng/sec	Tetradecane mixture	[37]
Hanging drop interface			
Volatile organic compounds	0.5 - 9 ppm	Standard mixtures	[16]
Phenols, aliphatic alcohols, methylene chloride, bromochlormethane, 1,2-dichloroethane, chloroform	240 ng[1]	Standard mixtures	[17]
Capillary jet interface			
Parabens and phenols	10 ng ethanol, 25 ng phenol, 36 ng acetic acid	Standard mixtures	[13]
Alcohols (C1 – C5)	0.1 to 1 ng[2]	Standard mixture	[19]
Alcohols (C4 - isomers)	3 to 10 ng	Standard mixture	[39]
Alcohols and aldehydes	0.2 mg/mL 3 - 10 ng	Standard mixture	[18]
Alcohols	1 ng	Standard mixtures	[20]
Alcohols (C1 – C4)	26 - 57 ng	Wine	[40]
Alcohol in beverages	n/a	Alcoholic beverages	[12]

Table 2.1. (Continued) Type of LC/FID systems with corresponding literature (Ref.) and exemplary investigated compounds, sample type and LODs.

Analytes	LOD	Sample Type	Ref.
Capillary jet interface			
Carbohydrates, amino acids, organic acids and bases	n/a	Standard mixtures	[41]
Nebulizer/Spray chamber interface			
i.e. alcohols, glycols	0.23[3] - 10.23[4] µg	Standard mixtures	[21, 22]

[1]Lowest concentration measured; [2]Expected LOD according to [40]; [3]Benzyl alcohol; [4]Aniline; n/a authors mentioned no detection limits

2.2.3 Solvent limitations

The solvent became the limiting factor of former LC/FID couplings. Organic solvents still had been the only choice in reversed phase (RP) LC analysis until the first publication of subcritical water high temperature liquid chromatography by Smith and Co-workers [42]. Smith et al. addressed the observations of Hawthorne et al. [43], who exploited the ability of water to extract non-polar compounds at elevated temperatures. In experiments, Hawthorne et al. showed that the dielectric constant of water is lowered by a simple raise in temperature (Figure 2.4a).

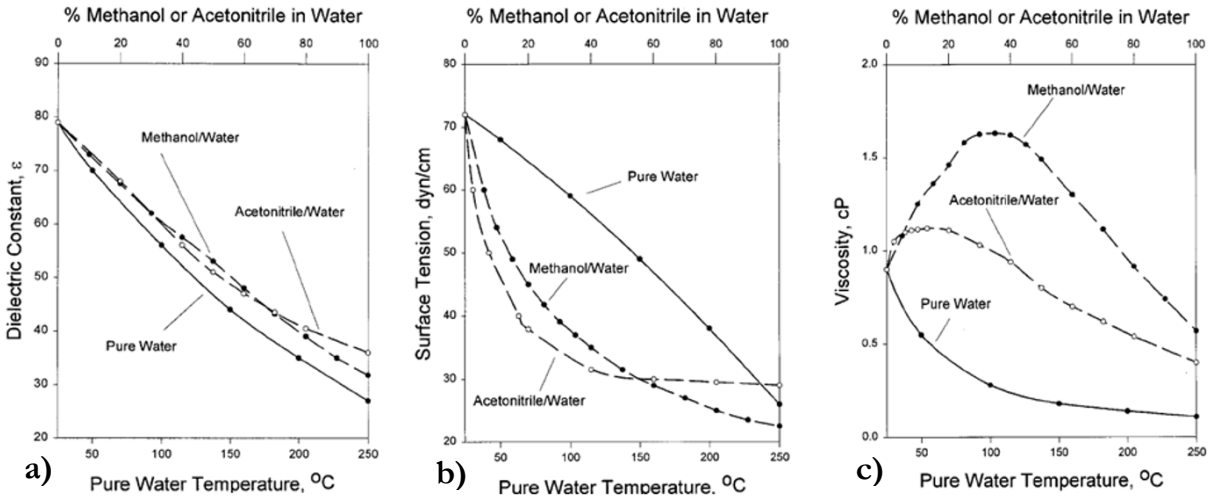

Figure 2.4. Physicochemical properties of Water, Methanol/Water and Acetonitrile/Water mixtures between 0 and 250°C [45]. **a)** dielectric constant, **b)** surface tension and **c)** viscosity.

The authors subsequently extracted polar, moderately polar, and non-polar organics from environmental solids by sequentially increasing the extraction temperature from 50°C (for polar organics, e.g., chlorophenols) to 400°C (for very non-polar organics, e.g., >C20 alkanes) [43]. Smith used the results and created a method for separation of parabens, phenols, barbitones by only water LC [44].

The fundamental work of Hawthorne and Smith resulted in the investigation of analytes suitable for high temperature only water LC. In 1999, Yang et al. [11] conducted separation of BTEX by conventional C18 RP columns. Chienthavorn and Smith published the successful separation of sulfonamides in 1999 using buffered water as eluent [46]. Recent publications show the potential of high temperature liquid chromatography and the range of possible analytes that can be investigated by the technique [47].

2.2.4 Capillary column interfaces

Based on water as solvent, a novel interface type evolved: the capillary jet interface. The fundamentals of capillary jet interfaces originate from coupling experiments of supercritical fluid chromatography (SFC) to FID. A modified FID jet was used to improve the flame stability and increase the sensitivity of detection [48]. The first direct capillary-based interfacing of LC and FID was presented by Miller and Hawthorne [20] and Hooijschuur et al. [39] (Figure 2.5a and b).

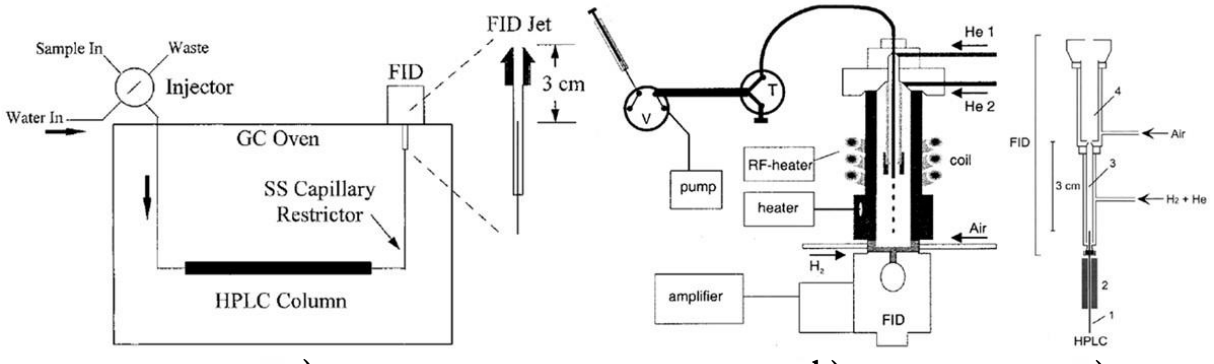

Figure 2.5. Scheme of capillary based interfaces: a) Setup of the LC/FID jet interface by Miller and Hawthorne (1997) [20], **b)** Up-side-down LC/FID interface by Hooijschuur et al. (2000) [39] **c)** Jet interface by Yarita et al. (2002) [12].

Miller and Hawthorne [20] used a small internal diameter SS restriction capillary to prevent mobile phase flash evaporation. The effect occurs by entrance of the liquid into the heated capillary and causes spontaneous expansion of the former liquid into the gaseous phase. In addition, the capillary serves as an evaporation jet to introduce the analyte directly into the flame. The authors adjusted the capillary 3 cm beneath the FID jet (Figure 2.5a) and created a thermo-spray of 300 to 400°C [20]. Hooijschuur et al. developed a μLC/FID system and placed an inductive pre-heated stainless steel capillary up-side-down (Figure 5b) into the FID to improve the transport of the generated aerosol by means of gravitation [39]. Guillarme et al. [19] used a fused silica tubing, preheated by a GC oven to directly link the LC to the FID. A comparable interface was built by Yarita et al. [12] and Nakajima et al. [40] where the authors used an external heating device (Figure 2.5c).

In contrast to conveyor type interfaces, the analytical focus was extended from non-volatile to volatile compounds, too. The first capillary jet interfaces focused on parameter optimization and investigation of ethanol in beverages [20], alcohols and aldehydes [18]. Later ones successfully separated and quantified samples containing, e.g., methanol, ethanol and aldehydes using a 0.5mm ID PRP-1 LC column with a flow of 50 μL min^{-1} [18]. The method was adapted by Yarita et al. [12] and Nakajima et al. [40] for analysis of ethanol in beverages, whereby the SS capillary was replaced by a FS capillary that additionally functioned as a passive split for the LC eluent. Yang et al. used conventional 2 or 4 mm ID columns [41] and split of a column flow of 1.24 mL min^{-1} down to 48 μL min^{-1} to support complete evaporation of the eluent. The interface was capable to introduce amino acids, carboxylic acids and carbohydrates for quantification into the FID. A post-column split was also used by Fu et al. for separation of alcohols, phenols and carboxylic acid on a Polymer RP-1 column with 4.6 mm I.D and 150 mm length [13].

2.2.5 Drop headspace interface

The hanging drop interface was developed beside capillary based LC/FID interfaces [16, 17] and functions by drops formed at the tip of a FS tubing that fall unobstructed into a waste reservoir. A linear flow of helium passes the growing drop and enhances analyte evaporation. The analyte enriched helium stream flows through a deactivated fused silica

transfer tubing into the FID (Figure 2.6a). In contrast to Bruckner et al. who investigated 1-butanol, 1,1,2-trichloroethane, butanone, chlorobenzene, toluene, ethylbenzene and o-xylene, Quigley et al. used the interface for the analysis of e.g. resorcinol, benzyl alcohol, phenol, phenyl-ethyl alcohol, o-cresol and p-cresol [17].

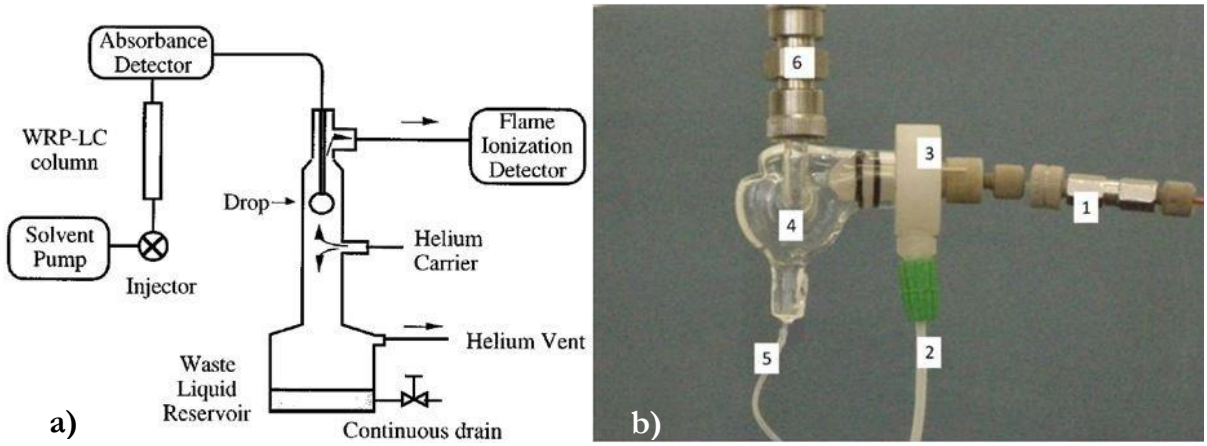

Figure 2.6. a) Scheme of the hanging drop device developed by Bruckner in 1997 [16] (WRP-LC column: water only reverse phase column). b) nebulizer/spray chamber assembly by Young et al. (2012): (1) carrier flow, (2) nebulizing gas, (3) nebulizer, (4) spray chamber, (5) condensate to drain, (6) connection to detector base [21].

2.2.6. Concentric micro flow nebulizer

The micro flow nebulizer interface by Young et al. presents the latest development in LC/FID hyphenation [21, 22]. The setup contains a modified micro-concentric nebulizer adapted to a centrifugal spray chamber with a dimple. The column effluent is nebulized by use of a nebulizer gas at ambient temperatures. Samples are not directly introduced into the FID, in contrast, the sample aerosol is transferred via a carrier gas through a glass tube into a modified FID (Figure 2.6b) [21]. To avoid flash evaporation, a restrictive capillary is used to keep a sufficient backpressure in the system and in addition to work as capillary jet of the micro flow nebulizer. Alcohols, aliphatic and aromatic ketones, acids, amines and glycols were successfully separated by RP-C18 columns and measured by the micro flow nebulizer spray chamber interface. The broad spectra of investigated volatile and semi-volatile analytes are presented in two major publications [21, 22].

2.3 Advantages and limitations of LC/FID interfaces

Table 2.2 summarizes the main advantages and disadvantages of the different interfaces.

Table 2.2. Advantages and Disadvantages of the different types of LC/FID interfaces.

Type of Interface	Advantages	Disadvantages
Conveyor	- Analysis of non-volatile analytes - Organic solvent mobile phase - Linear response - Low LOD for non-volatiles	- Bulky Setup - Susceptible to failures - Additional drying gas required - Additional gas for analyte transfer required
Drop Headspace Cell	- Analysis of volatile analytes - Linear response - Low LOD for volatiles	- Only water mobile phase - Analytes require high air/water partitioning coefficient - Additional gas for analyte transfer required
FS Capillary Jet	- Analysis of non-volatile analytes - Analysis of volatile analytes - Linear response - Low LOD for volatiles - No additional nebulizer gas required	- Only water mobile phase - Silica induced clogging
SS Capillary Jet	- Analysis of non-volatile analytes - Analysis of volatile analytes - Linear response - Low LOD for non-volatiles - Low LOD for volatiles - No additional nebulizer gas required	- Only water mobile phase
Nebulizer Spray Chamber	- Analysis of non-volatile analytes - Analysis of volatile analytes - Linear response for volatile analytes	- Only water mobile phase - Non-linear response for non-volatile compounds - Matrix effects - Additional nebulizer gas required

A substantial advantage of the conveyor type interfaces is the ability to be used for high molecular non-volatile analytes such as bio-polymers. The analyte can be introduced as solid compound into the FID by the belt, disk or wire. In contrast, analysis by nebulizer based interfaces depend on the ability to transfer the analyte molecules into the gaseous state or by the generated solvent spray into the FID. The fast evaporation of the solvent can cause crystallization of the analyte at the tip of the nebulizer capillary. However, most capillary jet interfaces are heated up to 400°C, which supports the evaporation of the analyte. The spray chamber type interface works at ambient temperature, therefore only compounds which can be transferred by the solvent spray can be introduced into the FID as shown by the non-linear response of, e.g., carboxylic acids. The order of applicability for non-volatile analytes is conveyor > capillary jet > nebulizer spray chamber > hanging drop.

The lowest LODs of volatile analytes are obtained by capillary based interfaces. Likewise to non-volatile analytes, the thermospray of capillary jet interfaces supports the evaporation of volatile analytes. Therefore, these types of interfaces show substantially lower LODs of, e.g., alcohols (0.1 - 1 ng), followed by the hanging drop interface (240 ng) or nebulizer spray chamber (230 ng). Conveyor type interfaces cannot be used for volatiles' analysis.

The conducted studies on LC/FID systems showed that a linear response is obtained by each of the different types of LC/FID interfaces. Only the nebulizer spray chamber was found to have a non-linear response for, e.g., ethylene glycol at high concentration levels. According to the authors, it appeared that volatility was a major factor and discrimination in the spray chamber can be a reasonable factor for lower relative responses of compounds that were solid. Due to that, analytes which volatilize during the nebulization process are carried into the flame as a vapor, whereas less volatile analytes which would be transmitted in the droplets of the spray were lost to a more significant extent during transfer and detection [22].

Concerning the applicability of interfaces, the bulky disk and wire based conveyor type interfaces were known to be separate instruments which required a high amount of drying and carrier gas. Furthermore, the conveyor and pre-evaporation units were susceptible to failures. In contrast, most capillary based interfaces as well as the nebulizer spray chamber are designed to be easily installed into existing FID systems.

An undesired side effect of FS based jet interfaces is the occurrence of blockage as result of silica deposition. The silica is washed out of the glassware, column and FS capillary and by evaporation of the solvent, the silica particles can remain inside and at the tip of the capillary and form crystalline deposits (Figure 2.7). These crystals can cause two substantial problems: first - complete blockage of the capillary and second - crystal break-off. The crystal break-off can hit the detector electrode and result in undesirable spiking. A possible solution to partially overcome the problem was done by Miller and Hawthorne by use of SS capillaries with larger IDs [20].

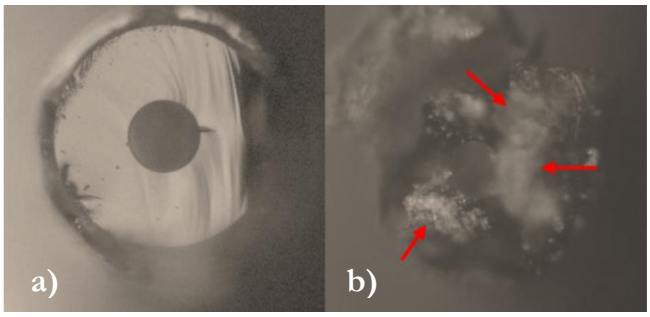

Figure 2.7. Silica formation at a FS capillary tip after 72 hours. a) End of a new FS capillary, **b)** end of the FS capillary after 72 hours nebulization, with a water flow of 50 µL min^{-1}.

Data about the reproducibility of the analytical separation and recorded standard deviations are rare. The calculated standard deviation for a capillary based LC/FID system was found to range from 3 - 6% for flow injection analysis [39] and 1% for the separation of an alcohol standard mixture [12]. However, as internal standard are used to quantify a sample, each system can be considered to produce reproducible results.

2.4 Conclusions and perspectives

Coupling of LC/FID could become a complement to established LC detection methods such as ELSD, UV detectors and MS. Based on the required solvents for chromatographic separation, possible LC/FID target compounds have changed over time. The change of the FID sensitive organic solvents (e.g. methanol, acetonitrile) to aqueous LC resulted in the design of advanced direct interfaces.

Analysts are no longer restricted to high boiling non-volatile compounds, capable to pass through the evaporation chamber of conveyor LC/FID interfaces. Hyphenation of LC/FID by capillary jet interfaces resulted in novel applications. The broad range of UV insensitive analytes such as alcohols and aliphatic hydrocarbons can be quantified by LC/FID nowadays. The use of pre-heated capillaries to support the evaporation of the mobile phase and introduction of analytes into the FID led to limits of detection close to those known from modern GC/FID systems. Fast semi-quantitative analysis of solvents in pharmaceutical products without use of MS systems is possible by using LC/FID systems.

Nevertheless, LC/FID coupling holds the potential to be improved within the next decades. Novelties need to address the different FID systems of GC instrument manufacturer and should be designed to be easily installed to existing GC systems. Even more, the development of small interface-detector units should be addressed in future. A universal, cost effective and simple add-on detector for LC systems is not available until now.

Furthermore most systems are affected by clogging of transfer capillaries, as known from LC/MS probes. The exchange of these capillaries is difficult and requires experience. Novel systems might use robust, exchangeable capillaries ready to install such as known from LC/MS.

A substantial advantage of the FID in contrast to other detectors, is the semi-quantitative analysis of carbon containing materials. However, to date only response studies and prediction models for GC/FID analysis are available. From the beginning of LC/FID until now, comparison of GC/FID and LC/FID response data was hardly studied. Research should therefore focus on the response mechanism in LC/FID to provide a reliable data base for semi-quantitative response prediction as known in GC/FID.

2.5 References

[1] S. Ahuja, Assuring quality of drugs by monitoring impurities, Adv. Drug Deliv. Rev., 59 (2007) 3-11.
[2] S.D. McCrossen, D.K.Bryant, B. R.Cook, J. J.Richards, Comparison of LC detection methods in the investigation of non-UV detectable organic impurities in a drug substance, J. Pharm. Biomed. Anal., 17 (1998) 455-471.
[3] S. Almeling, D. Ilko, U. Holzgrabe, Charged aerosol detection in pharmaceutical analysis, J. Pharm. Biomed. Anal., 69 (2012) 50-63.
[4] T. Vehovec, A. Obreza, Review of operating principle and applications of the charged aerosol detector, J. Chromatogr. A, 1217 (2010) 1549-1556.
[5] A. Clement, D. Yong, C. Brechet, Simultaneous identification of sugars by HPLC using evaporative light scattering detection (ELSD) and refractive index detection (RI). Application to plant tissues, J. Liq. Chromatogr., 15 (1992) 805-817.
[6] P.A. Asmus, J.B. Landis, Analysis of steroids in bulk pharmaceuticals by liquid chromatography with light-scattering detection, J. Chromatogr. A, 316 (1984) 461-472.
[7] I. Adouani, M.L. Du, T.J. Hang, Identification and determination of related substances in diosmin bulk drug and pharmaceutical formulations by HPLC and HPLC-MS, Chromatographia, 76 (2013) 499-508.
[8] J.Y. de Saint Laumer, E. Cicchetti, P. Merle, J. Egger, A. Chaintreau, Quantification in gas chromatography: prediction of flame ionization detector response factors from combustion enthalpies and molecular structures, Anal. Chem., 82 (2010) 6457-6462.
[9] A.D. Jorgensen, K.C. Picel, V.C. Stamoudis, Prediction of gas chromatography flame ionization detector response factors from molecular structures, Anal. Chem., 62 (1990) 683-689.
[10] M. Kállai, J. Balla, The effect of molecular structure upon the response of the flame ionization detector, Chromatographia, 56 (2002) 357-360.
[11] Y. Yang, Subcritical water chromatography: A green approach to high-temperature liquid chromatography, J. Sep. Sci., 30 (2007) 1131-1140.
[12] T. Yarita, R. Nakajima, S. Otsuka, T. Ihara, A. Takatsu, M. Shibukawa, Determination of ethanol in alcoholic beverages by high-performance liquid chromatography-flame ionization detection using pure water as mobile phase, J. Chromatogr. A, 976 (2002) 387-391.
[13] Y. Fu, R.J. Song, N. Yao, Y.D. Long, T.B. Huang, Separation of some alcohols, phenols and caboxylic acids by coupling of subcritical water chromatography and flame ionization detection with post-column splitting, Chin. J. Anal. Chem., 35 (2007) 1335-1338.
[14] I.D. Wilson, Investigation of a range of stationary phases for the separation of model drugs by HPLC using superheated water as the mobile phase, Chromatographia, 52 (2000) S28-S34.
[15] W.E. Neff, M.A. Jackson, G.R. List, J.W. King, Qualitative and quantitative determination of methyl esters, free fatty acids, mono-, di-, and triacylglycerols via HPLC coupled with a flame ionization detector, J. Liq. Chromatogr. Related Technol., 20 (1997) 1079-1090.
[16] C.A. Bruckner, S.T. Ecker, R.E. Synovec, Simultaneous flame ionization and absorbance detection of volatile and nonvolatile compounds by reversed-phase liquid chromatography with a water mobile phase, Anal. Chem., 69 (1997) 3465-3470.

[17] W.W.C. Quigley, S.T. Ecker, P.G. Vahey, R.E. Synovec, Reversed phase liquid chromatography with UV absorbance and flame ionization detection using a water mobile phase and a cyano propyl stationary phase - Analysis of alcohols and chlorinated hydrocarbons, Talanta, 50 (1999) 569-576.
[18] B.A. Ingelse, H.G. Janssen, C.A. Cramers, HPLC-FID with superheated water as the fluent: Improved methods and instrumentation, J. High. Resolut. Chromatogr., 21 (1998) 613-616.
[19] D. Guillarme, S. Heinisch, J.Y. Gauvrit, P. Lanteri, J.L. Rocca, Optimization of the coupling of high-temperature liquid chromatography and flame ionization detection application to the separations of alcohols, J. Chromatogr. A, 1078 (2005) 22-27.
[20] D.J. Miller, S.B. Hawthorne, Subcritical water chromatography with flame ionization detection, Anal. Chem., 69 (1997) 623-627.
[21] E. Young, R.M. Smith, B.L. Sharp, J.R. Bone, Liquid chromatography-flame ionisation detection using a nebuliser/spray chamber interface. Part 1. Design and testing, J. Chromatogr. A, 1236 (2012) 16-20.
[22] E. Young, R.M. Smith, B.L. Sharp, J.R. Bone, Liquid chromatography-flame ionisation detection using a nebuliser/spray chamber interface. Part 2. Comparison of functional group responses, J. Chromatogr. A, 1236 (2012) 21-27.
[23] E. Haahti, T. Nikkari, Continuous Detection of Fractions in Effluents of Silicic Acid Chromatography., Acta. Chem. Scand, 17 (1963) 2565-2568.
[24] R.J. Maggs, A commercial detector for monitoring the eluent from liquid chromatographic columns, Chromatographia, 1 (1968) 43-48.
[25] H. Veening, P.P.H. Tock, J.C. Kraak, H. Poppe, Microbore high performance liquid chromatography with a moving wire flame ionization detector, J. Chromatogr., 352 (1986) 345-350.
[26] O.S. Privett, W.L. Erdahl, An improved flame ionization detector for high performance liquid chromatography, Anal. Biochem., 84 (1978) 449-461.
[27] D.J. Malcolme-Lawes, P. Moss, Novel Transport Detector for Liquid Chromatography - I. Preliminary Experiments, J. Chromatogr., 482 (1989) 53- 64.
[28] J.E. Stouffer, T.E. Kerstens, P.M. Kruger, A New Method for the Detection of Substances Separated by Liquid Chromatographic Systems, Biochim. Biophys. Acta, 93 (1964) 191.
[29] R.P.W. Scott, J.G. Lawrence, An improved moving wire Liquid chromatography detector, J. Chromatogr. Sci., 8 (1970) 65-71.
[30] R.P.W. Scott, U.K. Pat., 998 107 (1965).
[31] H.W. Johnson, E.E. Seibert, F.H. Stross, Belt-detector for quantitative application in the fractionation of polymers by liquid chromatography, Anal. Chem., 40 (1968) 403-408.
[32] J.H.v. Dijk, Sensitivity Improvement of a Moving Wire Liquid Chromatography Detector, J. Chromatogr. Sci., 10 (1972) 31.
[33] F.C. Phillips, W.L. Erdahl, O.S. Privett, Quantitative analysis of lipid classes by liquid chromatography via a flame ionization detector, Lipids, 17 (1982) 992-997.
[34] A. Karmen, Flame Ionization Detector for Liquid-Liquid Chromatography, Anal. Chem., 38 (1966) 286.
[35] J.G. Cobler, H.H. Gill, W.E. Hatton, I.E.G. Owens, Method and apparatus for gel permeation chromatography, U.S. Pat., US3376694A (1968).
[36] H. Dubský, A disc detector for liquid chromatography, J. Chromatogr. A, 72 (1972) 395-403.

[37] J.J. Szakasits, R.E. Robinson, Disk conveyor flame ionization detector for liquid chromatography, Anal. Chem., 46 (1974) 1648-1652.
[38] J.B. Dixon, R.C. Hall, Detection unit with solute detector and transport system, U.S. Pat., US4215090A (1981).
[39] E.W.J. Hooijschuur, C.E. Kientz, U.A.T. Brinkman, Potential of flame ionization detection coupled on-line with microcolumn liquid chromatography using aqueous eluents and an eluent-jet interface, J. High. Resolut. Chromatogr., 23 (2000) 309-316.
[40] R. Nakajima, T. Yarita, M. Shibukawa, Analysis of alcohols by superheated water chromatography with flame ionization detection, Bunseki Kagaku, 52 (2003) 4.
[41] Y. Yang, T. Kondo, T.J. Kennedy, HPLC separations with micro-bore columns using high-temperature water and flame ionization detection, J. Chromatogr. Sci., 43 (2005) 518-521.
[42] R.M. Smith, R.J. Burgess, Superheated water - A clean eluent for reversed-phase high-performance liquid chromatography, Anal. Commun., 33 (1996) 327-329.
[43] S.B. Hawthorne, Y. Yang, D.J. Miller, Extraction of Organic Pollutants from Environmental Solids with Subcritical and Supercritical Water, Anal. Chem., 66 (1994) 2912-2920.
[44] R.M. Smith, R.J. Burgess, Superheated water as an eluent for reversed-phase high-performance liquid chromatography, J. Chromatogr. A, 785 (1997) 49-55.
[45] Y. Yang, M. Belghazi, A. Lagadec, D.J. Miller, S.B. Hawthorne, Elution of organic solutes from different polarity sorbents using subcritical water, J. Chromatogr. A, 810 (1998) 149-159.
[46] O. Chienthavorn, R.M. Smith, Buffered superheated water as an fluent for reversed-phase high performance liquid chromatography, Chromatographia, 50 (1999) 485-489.
[47] T. Teutenberg, Potential of high temperature liquid chromatography for the improvement of separation efficiency—A review, Analytica Chimica Acta, 643 (2009) 1-12.
[48] M.G. Rawdon, Modified flame ionization detector for supercritical fluid chromatography, Anal. Chem., 56 (1984) 831-832.

Chapter 3

A thermospray nebulizer interface for liquid chromatography / flame ionization detection: development and optimization

Within this study, a novel Liquid Chromatography (LC)/ Flame Ionization detector (FID) interface is presented. In contrast to previously presented interfaces, the main nebulizer body and the transfer capillary is made of stainless steel (SS). Previously reported problems such as blocking of the transfer capillary were investigated and solved. The simple design of the here presented nebulizer interface allows a convenient handling and the exchangeability of all nebulizer parts targets fast maintenance during routine analysis.

A significant advantage is the capability to implement the novel interface into most common Gas Chromatography (GC)/FID systems. The effects of the working parameters such as backpressure, gas flow, distance between nebulizer nozzle and FID collector or FID temperature on the signal were analyzed and optimized. The influence of the nebulizer material on flame stability and capillary blockage, a well-known problem of former coupling systems, was investigated, too. Finally, the novel interface was validated for selected compounds known from literature. Obtained results for chromatographic separation of the alcohols propanol, butanol, pentanol and hexanol, used within previous studies in the field of LC/FID coupling are presented.

Limits of Detection (LOD), sensitivity and linearity found within this work are compared with LC/FID interfaces developed in the past.

3.1 Introduction

In the past, coupling of LC to FID was limited by the need to remove organic eluents before detection. Bulky and expensive compartments for the evaporation of solvents had to be implemented. The first interfaces used a moving wire or disk for solvent uptake, combined with an oven for evaporation of the mobile phase. These complex systems were susceptible to failures and only applicable for non-volatile high molecular weight compounds [1].

In the early 1990´s the introduction of subcritical aqueous LC paved the way for LC/FID couplings in the coming decades [1]. In contrast to organic solvents, water causes no detector overload. Direct connection of LC and FID without a solvent evaporation compartment became possible. Valuable methods for superheated water based LC/FID analysis of, e.g., alcohols [2], pharmaceuticals [3] or lipids [4] have been reported. Using supercritical water high temperature LC methods, the coupling require the application of a high backpressure to keep the mobile phase in a liquid state at elevated temperatures [5]. Previously invented capillary based interfaces, used the capillary itself or restriction capillaries to produce the required backpressure.

The drop headspace cell, fused silica (FS) based capillary interfaces, SS capillary interfaces or the nebulizer spray chamber are promising interfaces, capable to detect a wide variety of compounds [1]. Miller and Hawthorne demonstrated that a liquid flow of up to 200 µL min^{-1} can be applied for the analysis of lower alcohols without significant losses of detection sensitivity [6]. In 2012 Young et al. introduced a nebulizer spray chamber interface based on a micro flow nebulizer [7]. The interface was capable of introducing volatile compounds, e.g., methanol and ethanol, as well as non-volatile compounds, e.g., carbohydrates and amino acids into the FID. The obtained signal of volatile analytes was found to be linear over 2 orders of magnitude, but a poor linear range was observed for non-volatile compounds.

The low linear range observed for non-volatile compounds by most LC/FID interfaces needs to be addressed in future. Also the low durability of FS based capillary interfaces, which are well known for clogging, needs to be solved. Until now interfaces are rather be

developed as unique systems, e.g., the upside-down LC/FID interface or the hanging drop, then a simplified add-on analytical tools to provide a novel technique to a broad spectrum of analytical laboratories.

Research in the past showed the potential of LC/FID as low cost universal and robust detectors for semi-quantitative analysis of different compound groups. LC/FID can be a promising tool to accomplish semi-quantitative analysis of analytes without paying attention on their volatility or photochemical properties. Solving the low sensitivity and durability of present interfaces, LC/FID can become a green complement to organic solvent based LC methods and conventional detectors such as UV-, Refractive Index- (RI) or Evaporative Light Scattering- (ELS) detectors.

3.2 Experimental section

3.2.1 Reagents

The alcohols methanol (C1) to hexanol (C6) (p.a., purity >99%), acetonitrile (99.8%), indole (99.8%), iso-quinoline (>97%), N-methylpyrrole (>99%) pyridine-N-oxide (>95%), pyrimidine-N-oxide (>97%), pyrrole (>98%), 2-pyrrolidone (>99%), quinoline (>97%), quinoxaline (≥99%) and s-triazine (97%), were purchased by Sigma Aldrich (Seelze, Germany). Pyridazine-3(2*H*)-one (>97%) was purchased by Alfa Aesar (Heysham, UK). Morpholine (99%), piperazine (99%), piperidine (99%), pyrazine (99%), pyridazine (98%), pyridine (99.5%), pyrimidine-2(*1H*)-one and pyrimidine (99%) were purchased by Merck (Darmstadt, Germany).

Sulfuric acid (purity ≥95%) was supplied by Fischer Scientific (Loughborough, U.K.) and *ortho*-phosphoric acid (purity >85%) purchased from Merck (Darmstadt, Germany) was used for capillary preparation.

Hydrogen (purity 5.0), nitrogen (purity 5.0) and synthetic air (purity 5.0) for FID operation were purchased from AirLiquide (Oberhausen, Germany).

Samples and stocks were prepared using analytical grade water from an ELGA PURELAB purification system (Celle, Germany).

Stock solutions were prepared at total carbon concentrations γ_{TC} of 100 mg L^{-1}. Whereby, γ_{TC} represents the absolute concentration of carbon within the solution. Standard solutions were prepared by dilution from the stock solution at ten different levels in a range of 0.1 to 100 mg L^{-1} using Hamilton microliter syringes (Bonaduz, Switzerland). Solutions for response analysis were prepared by dilution of the stock solution to γ_{TC} of 30 mg L^{-1}.

Aqueous samples of methanol, ethanol, propanol, butanol, pentanol and heptanol and nineteen heterocycles and acetonitrile, respectively were measured by Flow Injection Analysis (FIA). In the lower range, concentrations were distributed at $\gamma_{TC.}$ = 0.1, 2, 4, 6, 8, 10 and 12 mg L^{-1}. Linearity was investigated by measurement of further concentrations at $\gamma_{TC.}$ = 15, 20, 25, 50, 75 and 100 mg L^{-1}, whereby all heterocyclic compounds and acetonitrile were measured up to concentrations of 50 mg L^{-1}.

3.2.2 Setup of the LC/FID system

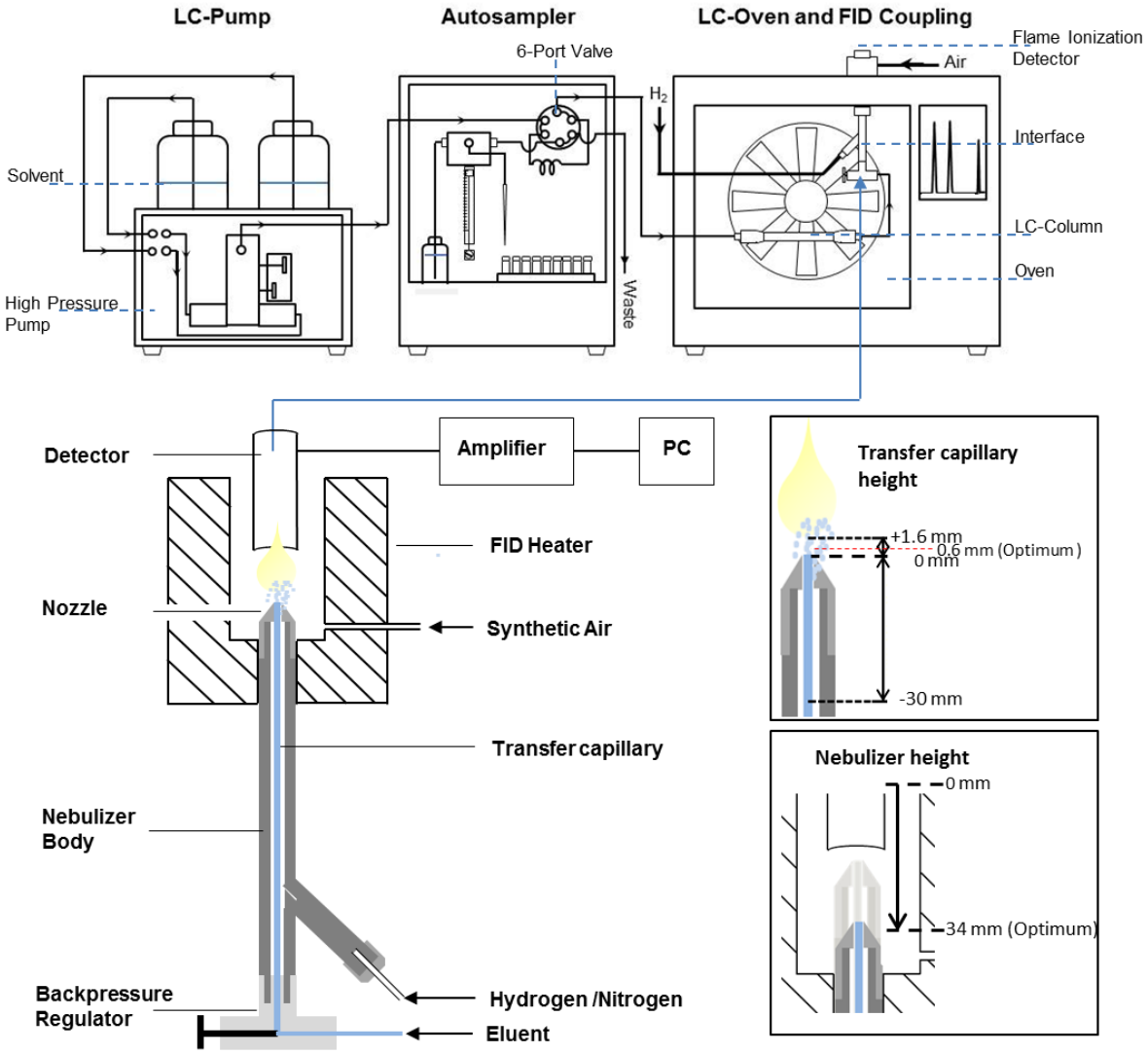

Figure 3.1. Schematic set up of the LC/FID system and scheme of the implemented nebulizer with description of its main parts. The two pictures on the lower right hand side show the experimental variation of the capillary height (upper picture) and the variation of the nebulizer height (lower picture).

The LC/FID system consisted of a Rheos Allegro pump of Flux Instruments (Basel, Switzerland), operated in isocratic mode with analytical grade water as mobile phase. Sample injection was carried out by an AS1 autosampler of the PLATINblue® series from Knauer (Berlin, Germany). The AS1 was equipped with a 1 µL sample loop. Chromatographic separation was performed with a Hypercarb® column (100 mm x 1 mm, 3 µm particle size) from Thermo Scientific (Waltham, MA, USA). Otherwise, FIA with a

direct link between autosampler and interface was carried out. The connections from pump to AS1 and further on to column and the LC/FID interface were realized by 1/32" SS capillaries with an inner diameter (ID) of 0.12 mm of BGB Analytik GmbH (Rheinfelden, Germany). The liquid transfer within the nebulizer was accomplished by a self-modified SS capillary. LC pressure was regulated with an adjustable back pressure regulator (BPR) from IDEX (Oak Harbor, WA USA). The system setup is schematically depicted in Figure 3.1.

FID analysis was performed with a Dani Master GC® provided by Axel Semrau (Sprockhövel, Germany). To temperate the LC column, the oven temperature was set to 50°C for optimization experiments and 90°C for chromatographic separation of alcohols. The FID temperature T_{FID} was set to 275°C. A hydrogen and synthetic air flow ($F_{Hydrogen}$) of 50 and (F_{Air}) of 450 mL min^{-1} was used, respectively. The signal was recorded with the Clarity software (DataApex, Prague, Czech Republic).

3.2.3 Preparation of inner capillary

A commercially available SS capillary (1 m x 0.32 mm OD x 0.16 mm ID) from Hamilton (Reno, NV, USA) was pulse electrochemically polished (PECP). The PECP was performed according to Ishihama et al. in a 1:1:1 solution of sulphuric acid, phosphoric acid and deionised water [8]. Prior to electro polishing, the SS capillary was cut into 12 cm long pieces. Two platinum electrodes were employed as cathodes and the capillary as the anode.

PECP was carried out with a TGP 110 pulse generator from Thurlby Thunder Instruments (Cambridgeshire, UK). The pulse generator was set to a 10 ms pulse period with a 5 ms duty cycle and an applied voltage of 2 V. Depending on the experiment, polishing was performed from an OD of 0.32 mm to 0.29-0.27 mm within 20 minutes. In a second step, the head of the SS capillary was conically shaped. To that end, the SS capillary head was brought into contact with the surface of the etch solution, until a capillary fringe was visible. The pulse generator was operated for about 10 to 15 min until the capillary fringe disappeared. In a final step the tip was polished with 2000 mesh wet sand paper to remove the fringy parts of the conical tip. The sequence of capillary production is depicted in figure 3.2.

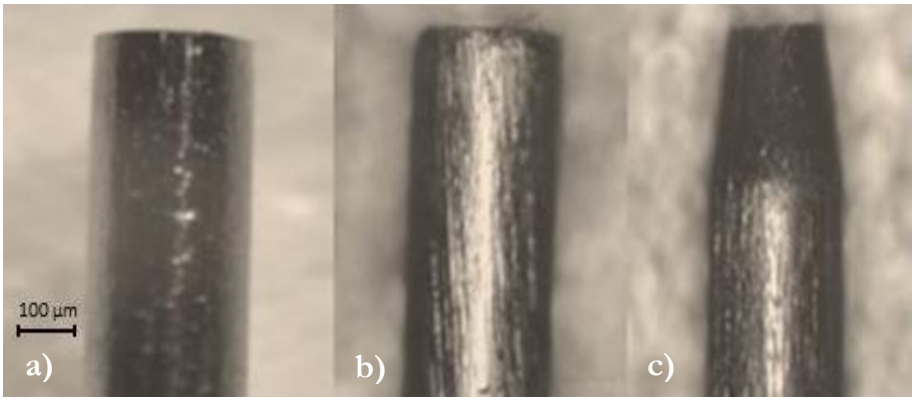

Figure 3.2. Change of a PECP treated SS capillary. a) untreated, **b)** after 20 min PECP treatment and **c)** final capillary with conical tip.

3.2.4 Optimization experiments

Optimization was carried out at eluent flows of 10 to 65 µL min^{-1} and focused on four different parameters: the backpressure, the nebulizer height within the FID, the transfer capillary outer diameter (OD) and height within the nebulizer, respectively. The impact of the backpressure was investigated between 20 to 35 MPa in steps of 5 MPa. The height of the implemented nebulizer was varied between 30 to 34 mm (in steps of 1 mm). The transfer capillary (OD) was varied from 0.27 to 0.29 mm in steps of 0.01 mm. The capillary height within the nebulizer was varied between –5 mm to +1.6 mm, measured from the nebulizer nozzle orifice. The implemented interface and the nebulizer and capillary parameter changes are schematically depicted in Figure 3.1 (right).

Quantitative evaluation of the signal alteration on the influence of the FID hydrogen flow and operation temperature, nitrogen and mobile phase flow was achieved by injection of a caffeine solution (c_{TC} = 1 mg L^{-1}). All other optimization experiments were performed using a methonl solution of c_{TC} = 30 mg L^{-1}). The signal alteration was analyzed after each parameter change. Optimization of FID parameters was performed with an eluent flow of 50 µL min^{-1} and a GC oven temperature of 50°C. The hydrogen flow was increased in steps of 50 mL min^{-1} in a range of 50 to 200 mL min^{-1}. For cooling purposes and to stabilize the FID flame, the nitrogen flow was varied in steps of 25 mL min^{-1} in a range of 0 to 100 mL min^{-1}. The nitrogen was introduced together with H_2 as indicated in Figure 3.1.

The influence of the FID Temperature was investigated between 225°C and 350°C at intervals of 25°C. FID optimization was evaluated by injection of 100µL of an aqueous caffeine solution of c_{TC} = 1 mg L^{-1}. All experiments were carried out in quintuplicate.

3.2.5 Statistical evaluation

Linearity of the calibration curve was tested by diluting the stock solutions to ten working concentrations. The standard deviation (SD), limits of detection (LODs) and limits of quantification (LOQs) were evaluated statistically [9]. The sensitivity was derived from the slopes of the measured calibration curves. The repeatability of the measurements was evaluated using inter-day variations, measured over three days with an injection period of 1 hour.

3.3 Results and discussion

3.3.1 Material effects

Replication of FS capillary based LC/FID interfaces experiments revealed a considerable dependence of working performance on the chosen material. The FS capillary system setups ended up in unstable detection signals or extinguishment of the FID flame as result of capillary blockage.

Clogging of the FS capillary is mainly caused by permanent silica wash out of glassware and FS tubing itself. The dissolved silica was observed to precipitate out of solution inside the FS capillary and at the capillary tip (Figure 3.3b), used to introduce the mobile phase into the FID flame.

Replacement of the FS made transfer capillary by a SS transfer capillary prolonged the durability from three days up to one week. A further enhancement of the transfer capillary lifetime was achieved by replacement of all FS capillary connections by SS capillaries. The larger ID of the SS transfer capillary (160 µm in contrast to previous used FS transfer capillaries 25 to 50 µm) supported the avoidance of clogging. Experiments conducted over

several month using the SS system setup and transfer capillary showed no clogging effects over a period of three month.

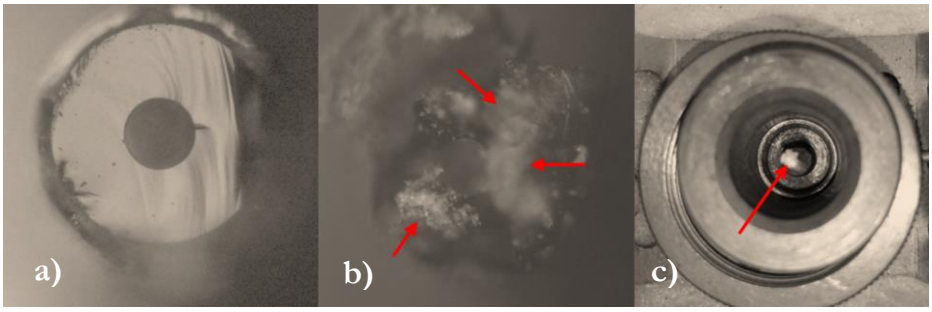

Figure 3.3. Silica formation at a fused silica capillary tip and nebulizer tip after 72 hours. a) End of a new fused silica capillary, **b)** end of the fused silica capillary after 72 hours nebulization, with a water flow of 50 µL min^{-1} and **c)** silica deposits at the nebulizer tip by using fused silica capillaries. Red arrows: precipitated silica.

3.3.2 Optimization of FID parameters

Based on the previously described observations, the optimization experiments were conducted using SS capillaries for connection of LC to FID and the transfer capillary, respectively. The nebulizer interface acts as a FID nozzle as well as nebulizer for the direct introduction of the mobile phase into the interior of the flame, therefore the hydrogen flow needs to fulfill two requirements: first a flow which is capable to keep the flame burning during introduction of the mobile phase and second the flow must be sufficient to generate the required share forces for an adequate nebulization process. In addition, an excess of oxygen is necessary to support a complete combustion of the analytes into CHO^+. According to literature, the synthetic air flow was set to 450 mL min^{-1} [10] within all experiments.

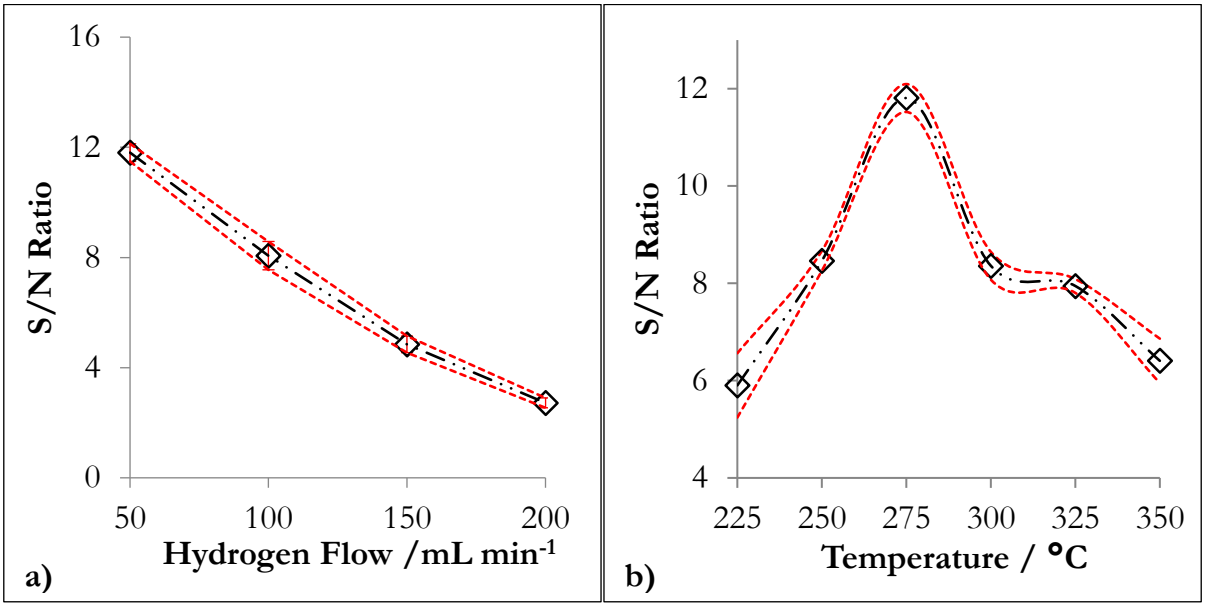

Figure 3.4. Influence of the FID hydrogen flow and operation temperature on the signal to noise ratio of the recorded signal. Test solute: caffeine at c = 1 mg L^{-1}. a) S/N ratio of caffeine from 50 to 200 mL min^{-1} hydrogen flow, FID temperature was set to 275°C. **b)** S/N ration of caffeine between 225°C to 350°C increased in steps of 25°C. LC conditions: F_{Mobile} (H_2O) = 50 µL min^{-1}; FID conditions: $F_{Hydrogen}$ 50 mL min^{-1}, T_{Oven} = 50°C; F_{Air} = 450 mL min^{-1}; $F_{Nitrogen}$ = 0 mL min^{-1}.

Hydrogen flow experiments were performed within 50 to 200 mL min^{-1} for two reasons: First a hydrogen flow below 50 mL min^{-1} resulted in an incomplete evaporation of the solvent and blow out of the flame. Second, operation of the FID with a hydrogen flow higher than 200 mL min^{-1} emits an excess of thermal energy and results in a glowing FID collector tube. The observed decrease of the Signal to Noise (S/N) ratio of 12 (50 mL min^{-1}) down to 3 (200 mL min^{-1}) as depicted in Figure 3.4a is likely due to the increasing electrical resistance of the collector tube at elevated temperatures.

Literature reports a FID temperature of, e.g., 400°C for LC/FID coupling [11]. Previously developed LC/FID interfaces typically used the original FID nozzle and transfer capillaries which were placed up to 3 cm below the nozzle [1]. Thus, the instrumental parameters can be suggested to be different for each setup. Here a decrease of the S/N ratio from 12 observed at 275°C down to 6 at 350°C (figure 3.4b) was noticed. At temperatures below 275°C the flame became instable, as the eluent was not evaporated efficiently.

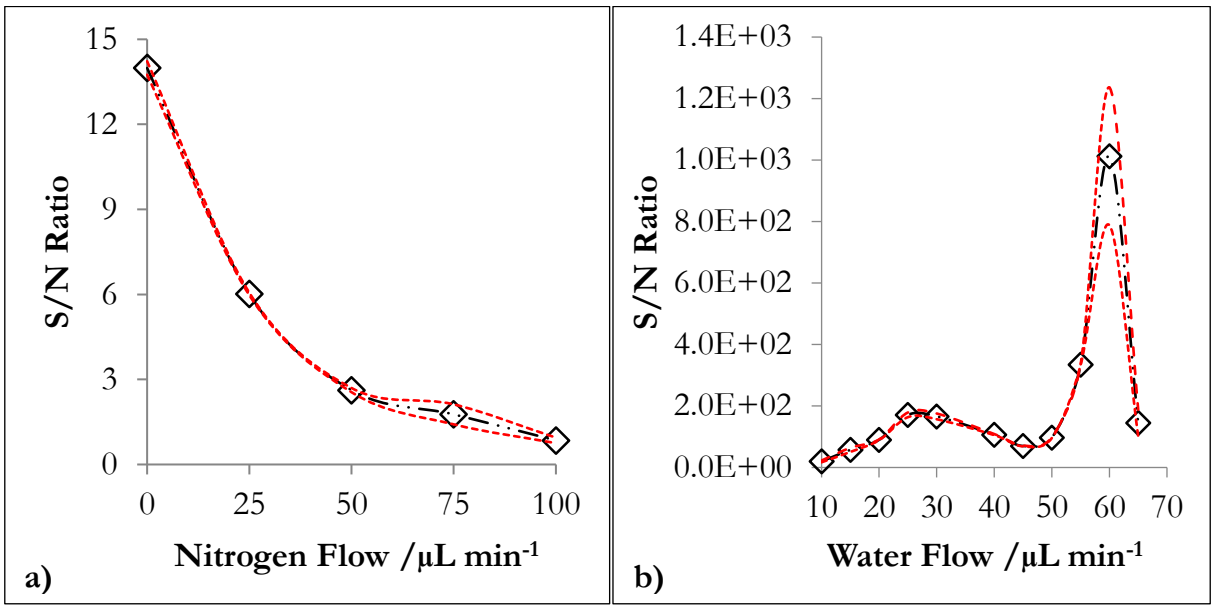

Figure 3.5. Influence of the nitrogen and mobile phase flow on the S/N ratio of the recorded signal. T_{Oven} = 50°C. FID conditions: $F_{Hydrogen}$ 50 mL min-1, F_{Air} 450 mL min-1; T_{FID} = 275°C. Test solute: caffeine at c = 1 mg L-1. a) S/N ratio of caffeine for 0 to 100 mL min-1 nitrogen flow LC conditions: F_{Mobile} (H_2O) = 50 µL min-1. **b)** S/N ratio of caffeine for mobile phase flow rates between 10 and 65 µL min-1.

The influence of the nitrogen flow was investigated between 0 to 100 mL min-1 in intervals of 25 mL min-1. In contrast to other authors [7,12], use of nitrogen make-up gas result in the reduction of the signal (Figure 3.5a). Therefore, no make-up gas was applied during further experiments. Guillarme et al. worked with a solvent flow of 50 µL min-1 by applying comparable system settings [10].

3.3.3 Optimization of LC conditions and backpressure regulation

The introduced interface was capable to maintain a solvent flow of 65 µL min-1 without significant loss of sensitivity. Peak shape and height changed in dependency of the mobile phase flow, as described in literature [13]. Therefore the S/N ratio increased from 10 to 65 µL min-1 by a factor of ~500 (Figure 3.5b). Except the flow range of 10 to 20 µL min-1, the recorded peak area of the test solute remained stable at ~2700 mV s-1.

Almelling and Holzgrab [14] made contrary observations using ELSD. The authors found that the evaporation at elevated liquid flows deteriorate the signal intensity in ELSD by a factor of 2 significantly. In case of ELSD, the intensity loss can result from incomplete

evaporation [15] and larger droplets formed [16]. These droplets hit the drift tube and an attenuation of the signal is observed. Since the LC/FID contains no drift tube at all, the droplets are not able to settle down before reaching the detector (as observed in ELSD).

The water droplets at flows >60 µL min^{-1} hit the FID collector and cause a faulty detection. This problem becomes visible in form of spikes within the whole chromatogram. The occurring spikes result in faulty peak heights or an increased background signal and thus reduce the quality of the signal and S/N ratio, as depicted by the recorded chromatogram of a five time injection of methanol sample in Figure 3.6.

To reduce and/or avoid the formation of droplets, the self-made nebulizer was equipped with a backpressure regulator. Several authors reported [2,6,11,10], that restrictive capillaries are useful for prevention of phase transition within the LC column. Another side effect is a better evaporation and reduction of droplet formation of the aqueous mobile phase after leaving the restriction capillary.

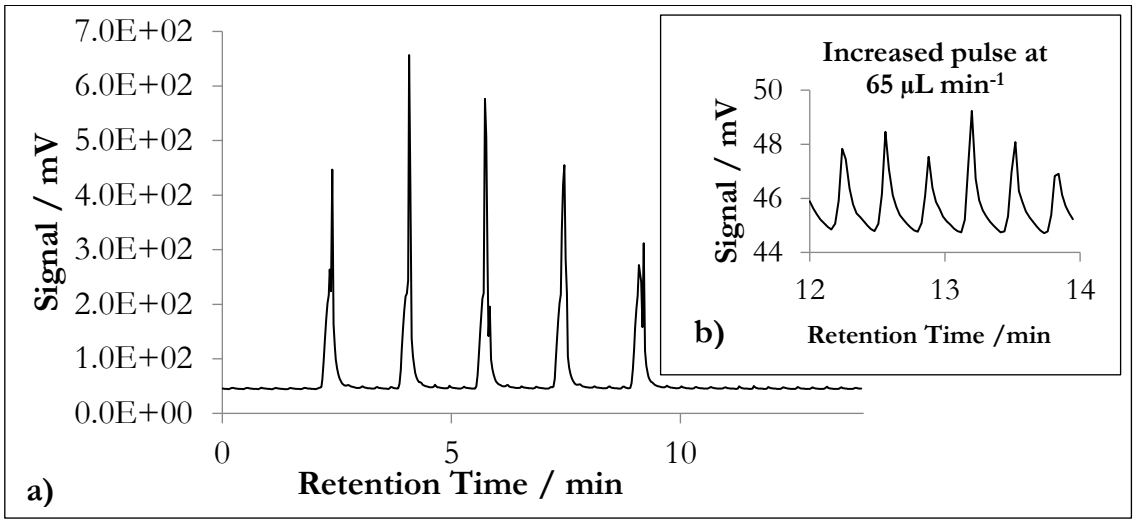

Figure 3.6. Influence of a mobile phase flow of 65 µL min^{-1} on the recorded chromatogram. a) Formation of spikes within the detected methanol peaks. **b)** increased baseline caused by LC pump pulsation. LC conditions:, T_{Oven} = 90°C; backpressure 35 MPa. FID conditions*:* F_{H2} = 50 mL min^{-1}; F_{Air} = 450 mL min^{-1}; T_{FID} = 275°C. Test solute: methanol at c_{Abs} = 30 mg L^{-1}.

Miller and Hawthorne [6] used a SS supercritical fluid extraction restrictor with an 57 µm ID and a backpressure of ~2 MPa at 40°C. Ingelse et al. [11] connected the column outlet of LC to FID by a 100 cm x 50 µm ID FS capillary restrictor. Calculating the backpressure with the Hagen-Poiseuille equation, the backpressure used by Ingelse et al. ranged from 9.9

MPa (F_{Mobile} = 50 µL min^{-1} and T_{Oven} = 50°C) to 15.3 MPa (F_{Mobile} = 50 µLmin^{-1} and T_{Oven} = 100°C). A self-modified FS capillary was used by Hooijschuur et al. [17]. The authors reported backpressure of 4.0 to 5.0 MPa at F_{Mobile} = 5 to 15 µL min^{-1}. The experimental setup by Yarita et al. [2] proposed a split of the mobile phase from 1 mL min^{-1} down to 7 µL min^{-1} and reported a backpressure of 0.4 MPa using a restrictor of 50 mm length x 0.1 mm ID and an FID introduction capillary of 2.7 cm length x 40 µm ID A comparison of the applied backpressures and theoretical backpressure required to prevent phase transition reveals that the influence of the backpressure on evaporation or in particular the introduction efficiency of the eluent into the FID was negligible.

In this study, the upper and lower pressure limits were chosen according to technical reasons. The upper limit is due to the backpressure regulator itself, which cannot withstand a pressure higher than 36 MPa at 90°C. Below 20 MPa, the hydrogen flame became instable and tended to extinguish, because of pulsed flash evaporation. Here an increase of the backpressure up to 35 MPa caused a reduction of pulse induced background noise at, e.g., F_{Mobile} 10 µL min^{-1} by a factor ~3 from 2.5 mV at 20 MPa down to 0.9 mV at 35 MPa. The influence of the backpressure between 20 to 35MPa on the background signal is illustrated in Figure 3.7. An average pulse suppression factor of 2 was obtained for F_{Mobile} ≤65 µL min^{-1}.

A substantial advantage of a pressure regulation by a BPR can be observed by the analysis of non-volatile compounds. Restriction capillaries with internal diameters smaller 100 µm were found to block as result of silica and analyte deposition. Capillaries of these size are manly used to obtain the required backpressure [2,18,10,6,17]. The BPR therefore allows the implementation of capillaries with a larger diameter. As discussed earlier, larger capillary IDs prevent clogging and furthermore support the introduction of semi-and non-volatile compounds into the FID.

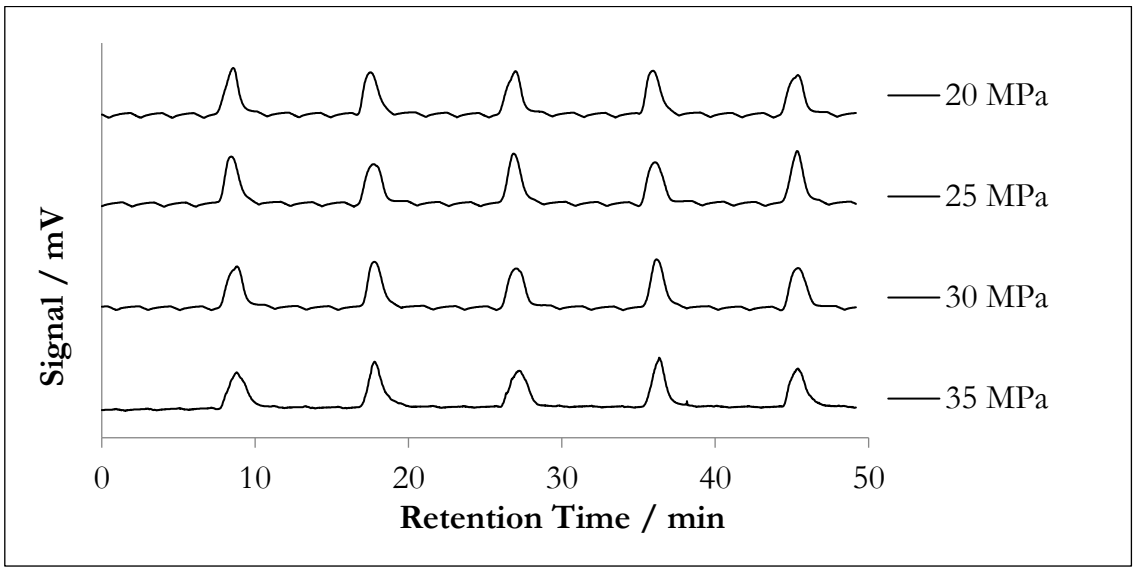

Figure 3.7. Influence of the backpressure on LC pump frequency induced background fluctuations during multiple injection of c_{TC} = 30 mg L^{-1} methanol every 9 min without separation column. LC conditions: F_{Mobile} (H_2O) = 10 µL min^{-1}, T_{Oven} = 90°C; backpressure 20, 25, 30 and 35 MPa. FID conditions: $F_{Hydrogen}$ = 50 mL min^{-1}; F_{Air} = 450 mL min^{-1}; T_{FID} = 275°C.

3.3.4 Influences of the nebulizer and capillary height

In order to meet the technical requirements of the gas vent of the used GC/FID system, the maximum external diameter had to be ≤0.28 mm. Use of thicker capillaries generated excessive backpressures above the flow controller maximum of 0.4 MPa. The nebulizer body and transfer capillary was found to be located in the hot spot of the FID heating device at 34 mm height. Experiments showed, that there was no necessity to test heights below 30 mm. The eluent filled the transfer capillary without being evaporated. This resulted in spontaneous flash evaporation of the eluent [7] and extinguishment of the flame. Beyond 34 mm a rapid decrement of the signal was observed. Improper nebulizer adjustment resulted in incomplete evaporation [14,16] and caused spiking as depicted in Figure 3.8.

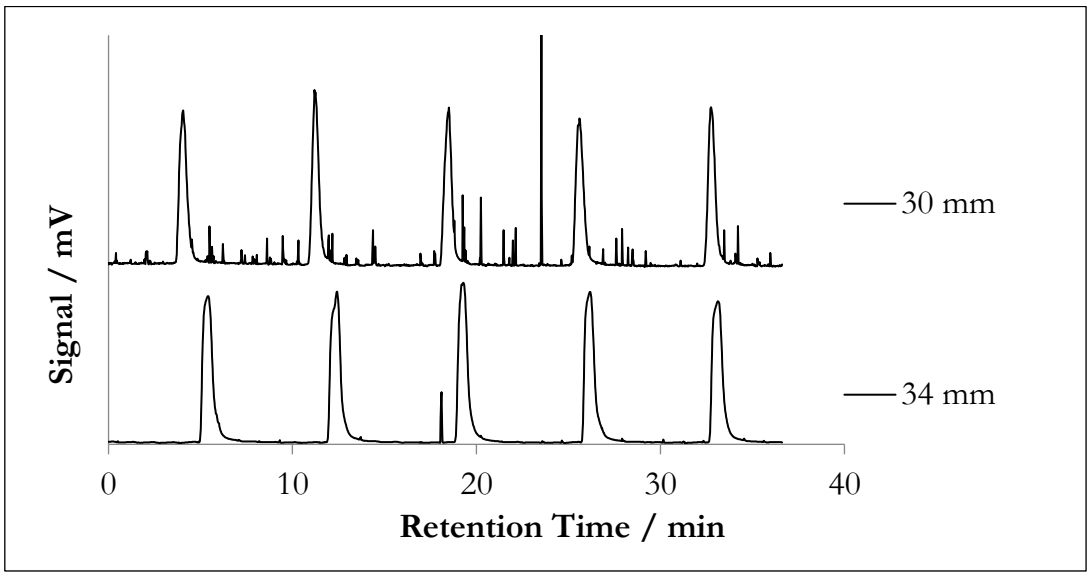

Figure 3.8. Influence of the nebulizer height on the obtained signal during injection of c_{TC} = 30 mg L^{-1} methanol every 7 minutes without separation column. Upper part: 30 mm height where the nebulizer is located outside the hotspot of the FID heater. Incomplete evaporation and spiking is observable Lower part: At 34 mm height the nebulizer is located in the hotspot of the FID heating device, no disturbance by flash evaporation or water droplet is observed here. LC conditions: F_{Mobile} (H_2O) = 25 µL min^{-1}, T_{Oven} = 90°C; backpressure 35 MPa. FID conditions: $F_{Hydrogen}$ = 100 mL min^{-1}; F_{Air} = 450 mL min^{-1}; T_{FID} = 275°C.

Inglese et al. [11] and others [10,6] placed the transfer capillary for the introduction of the mobile phase about 3 cm below the FID jet. Here an optimum with a S/N ratio of ~170 was achieved by passing the capillary +0.6mm thru the orifice of the nebulizer. Further increase to 0.7 and 0.8 mm, respectively, resulted in instability of the flame. In consequence, the S/N dropped down to <5. As depicted in Figure 3.9, further increase of the capillary resulted in unstable baselines and spiking.

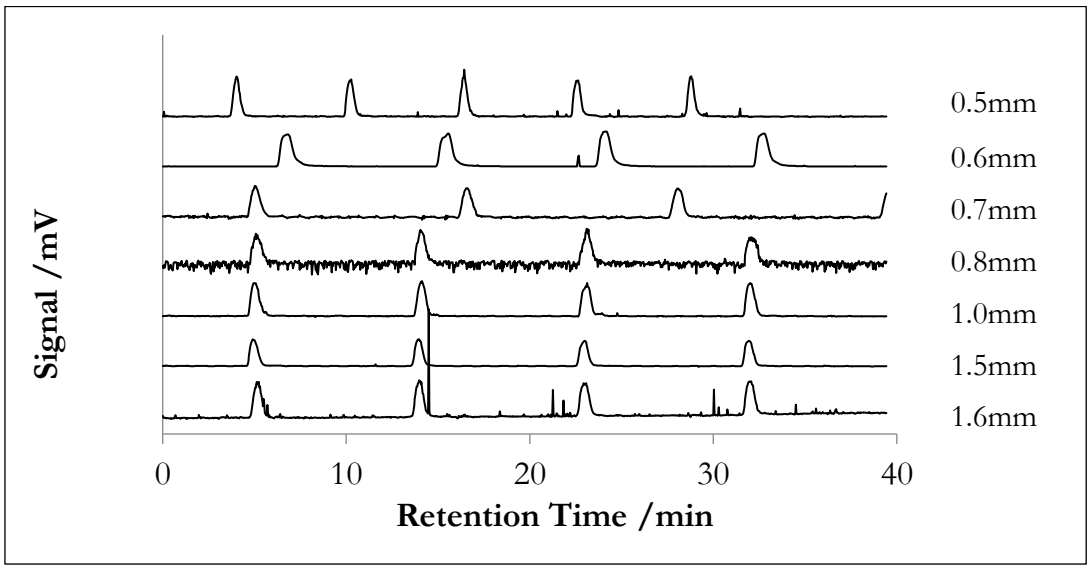

Figure 3.9. Influence of the distance between transfer capillary tip and orifice on the signal during injection of c_{TC} = 30 mg L^{-1} methanol every 9 minutes without separation column. Peaks obtained at selected transfer capillary tip-orifice setups between 0.5 to 1.6 mm. LC conditions: F_{Mobile} (H_2O) = 25 µL min^{-1}, T_{Oven} = 90°C; backpressure 35 MPa. FID conditions: $F_{Hydrogen}$ = 50 mL min^{-1}; F_{Air} = 450 mL min^{-1}; T_{FID} = 275°C. Test solution: methanol c_{TC} = 30 mg L^{-1}.

3.3.5 Validation of the LC/FID system

A main field of application for the invented LC/FID system is the investigation of solvent residues such as acetonitrile, methanol or ethanol in pharmaceutical products. Nitrogen heterocycles like pyridine and pyrimidine are important raw materials for the synthesis of a wide range of pharmaceutics. Therefore the investigation of the linearity, LOD and SD of these N-heterocycles as well as alcohols as solvents in pharmaceutic industries was an important issue.

In compliance to response analysis in GC [19], a linear correlation between carbon content and FID response was observed for the six alcohols and the twenty nitrogen containing compounds. Calibration curves of methanol and quinoline are depicted exemplarily in Figure 3.10a and 3.10b. The robustness and reproducibility was investigated during long term tests performed at an eluent flow of 15 µL min^{-1}. The standard deviation measured for 60 injections (sample interval 1h) over a period of three days was 3%. The deviation between these values and data recorded three weeks before was calculated with 4%.

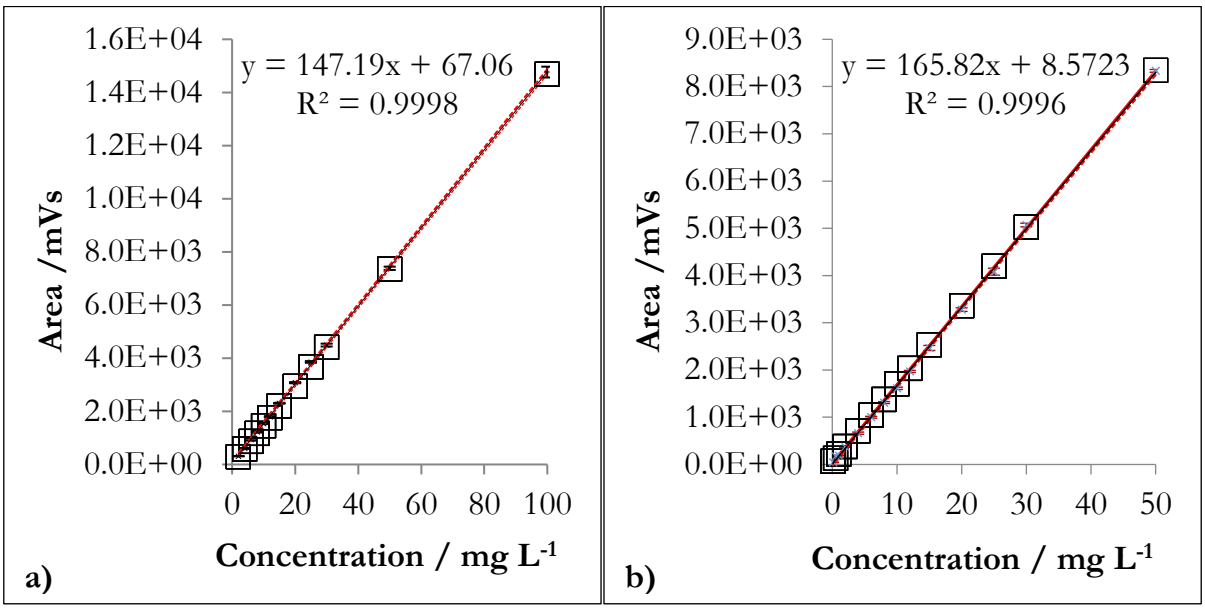

Figure 3.10. Calibration of a) methanol and b) quinoline in a range of 0.1 to 100 mg L^{-1} and 0.1 to 50 mg L^{-1}, respectively with confidence intervals (red). LC conditions: F_{Mobile} (H_2O) = 50 µL min^{-1}, T_{Oven} = 90°C; backpressure 35 MPa. FID conditions: F_{H2} = 50 mL min^{-1}; F_{Air} = 450 mL min^{-1}; T_{FID} = 275°C.

3.3.6 Analysis of N-heterocycles and nitrogen containing compounds

The derived LODs, LOQs and the standard deviation of the procedure for the heterocyclic compounds investigated within this study are summarized in Table 3.1. The calibration curves obtained for heterocyclic compound were found to be linear ($R^2 \geq 0.999$) over the complete calibration range with interceptions close to zero (figure 3.10b). The LODs of pyridine-2(*1H*)-one (0.33 ng), quinoline (0.24 ng) and iso-quinoline (0.28 ng) are markedly below the LOD for, e.g., quinoline in LC/UV (~19 ng) [20] and provide a substantial improvement.

Table 3.1. Statistical evaluation of the analyzed N-heterocycles and nitrogen containing compounds. Correlation coefficient (R^2), Limits of Detection (LOD) and standard deviation (SD) for Flow injection analysis (FIA).

Substance	R^2	LOD / ng	LOQ / ng	SD / %
Pyridine-2(*1H*)-one	0.999	0.33	1.00	3.13
Pyridazine-3(2*H*)-one	0.998	0.40	1.22	4.27
Acetonitrile	0.999	0.39	1.16	4.07
Indole	0.997	0.50	1.62	5.82
iso-quinoline	0.999	0.28	0.83	3.38
Morpholine	0.997	0.50	1.51	5.30

Table 3.1. (Continued) Statistical evaluation of the analyzed N-heterocycles and nitrogen containing compounds. Correlation coefficient (R^2), Limits of Detection (LOD) and standard deviation (SD) for Flow injection analysis (FIA).

Substance	R^2	LOD / ng	LOQ / ng	SD / %
n-methyl-pyrrole	0.995	0.75	2.25	7.33
Piperazine	0.992	0.78	2.34	8.86
Piperidine	0.996	0.56	1.68	6.79
Pyrazine	0.992	0.92	2.72	7.11
Pyridazine	0.985	1.23	3.65	14.75
Pyridine	0.998	0.39	1.16	4.20
Pyridine-N-oxide	0.998	0.39	1.18	4.23
Pyrimidine	0.997	0.59	1.77	5.44
Pyrimidine-N-oxide	0.998	0.24	0.72	3.88
Pyrrole	0.991	0.79	2.33	7.92
2-Pyrrolidone	0.997	0.51	1.53	5.97
Quinoline	0.999	0.24	0.74	2.65
Quinoxaline	0.999	0.27	0.80	2.73
s-triazine	0.985	1.26	3.75	12.23

3.3.7 Analysis of alcohols

According to the different concentration units in LC/FID publications, an alignment of LC/FID response data for a meaningful comparison of previous and the here presented data had to be done. Table 3.2 summarizes the normalized concentrations analyzed by selected LC/FID hyphenations together with data obtained for the optimized nebulizer interface presented within this work. Concentrations are expressed as total carbon concentrations.

Table 3.2. Selected LC/FID hyphenations with investigated target analytes and limits of detection normalized to c_{TC} for some compounds.

Interface	LOD (Analytes)	Compound class	Literature
LC/FID[1]	0.6 - 3.2 ng (Butanol)	e.g. Alcohols	[16]
LC/FID[2]	0.06 - 0.6 ng[3] (Alcohols)	Alcohols	[15]
LC/FID[1]	3 ng (Methanol)	Alcohols and aldehydes	[13]
LC/FID	1 µg (Plant lipids)	Plant lipids	[30]
µLC/FID jet[1]	0.15 ng (Phenol)	e.g. Alcohols, alkanes	[27]
LC/FID[4]	192 ng (Propanol) 195 ng (Butanol)	e.g. Alcohols	[17,18]
LC/FID[1]	Not mentioned	Alcohols	[6]
LC/FID[5]	5.8 ng (Butanol)	Volatile substances	[11]
LC/FID[2]	0.24 ng	N-heterocycles, alcohols	This Study

[1]Fused silica capillary based interface, [2]Stainless steel capillary based interface, [3]calculated for an assumed S/N of 3:1 [4]µFlow nebulizer spray chamber, [5]Hanging drop interface

The statistically derived LODs, LOQs and the standard deviation of the overall six alcohols are summarized in Table 3.3. Each alcohol calibration was found to be linear ($R^2 \geq 0.999$) over the four orders of magnitude with interceptions close to zero (Figure 3.10a).

Table 3.3. Statistical evaluation of alcohols (methanol to hexanol). Linear Range**,** Correlation coefficient (R^2), Limits of Detection (LOD) and standard deviation (SD) for Flow injection analysis (FIA) and LC separation (Hypercarb) of the investigated analytes.

Substance	Linear Range	R^2	LOD / ng		SD / %	
			FIA	Hypercarb	FIA	Hypercarb
Methanol	10^4	0.999	0.51	-	3.0	-
Ethanol	10^4	0.999	0.28	-	2.4	-
Propanol	10^4	0.999	0.28	0.39	2.7	3.2
Butanol	10^4	0.999	0.34	022	2.3	4.7
Pentanol	10^4	0.999	-	0.31	-	4.3
Hexanol	10^4	0.999	-	0.23	-	3.7

A significant increase of the sensitivity by a factor of 800 was achieved in comparison to studies on microflow nebulizers [7,12]. In comparison to FS based capillary interfaces [6,11], the presented SS interface such as the SS interface presented by Guillarme et al. [10], were found to have lower LODs. Among the FS based interfaces, only Hooijschuur et al. [17] presented a competitive interface with likewise limits of detection. Commonly used LC detectors such as UV- and ELS detectors are not able to detect short chained alcohols

sufficiently, the ability of the FID to detect these compounds is a substantial advantage for the residual solvent analysis in pharmaceutical products.

3.3.8 Separation of an alcohol mixture by high temperature LC/FID

The applied separation was a proof of principle for the interface introduced here, rather than an optimized method. The separation was performed isothermal at 90°C by a 100 mm x 2 mm Thermo Hypercarb column within 5 minutes (Figure 3.11).

The S/N ratio was found to be > 30:1 for an alcohol standard solution with c_{TC} = 2 ng propanol, butanol, pentanol and hexanol, respectively. Peak asymmetries of 1.35 (propanol) to 1.04 (hexanol) were obtained using the presented LC/FID system. It can be suggested, that no significant influence on the separation result out of the use of the interface (e.g. creation of an increased dead volume which effects the chromatographic separation). The LOD of, e.g., propanol (0.39 ng) and butanol (0.22 ng) within the applied method as well as the coefficient of variation (≤ 5.4) are comparable to those observed within the previously performed FIA measurements (see table 3.2).

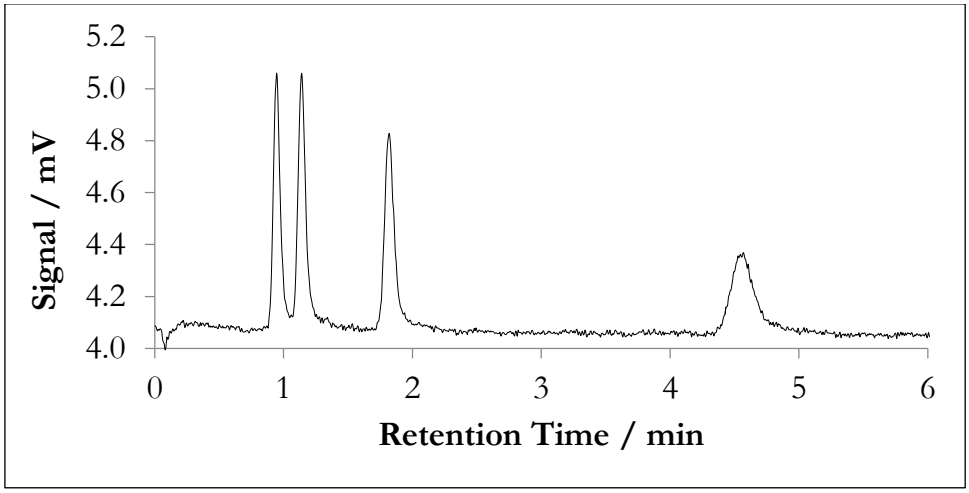

Figure 3.11. Separation of the four alcohols propanol (1), butanol (2), pentanol (3) and hexanol (4). c_{TC} = 2 ng with an S/N of 30:1 for propanol, butanol and pentanol and 20:1 for hexanol. LC conditions: Column: Hypercarb®, F_{Mobile} (H_2O) = 50 µL min^{-1}, T_{Oven} = 90°C; backpressure 35 MPa. FID conditions: $F_{Hydrogen}$ = 50 mL min^{-1}; F_{Air} = 450 mL min^{-1}; T_{FID} = 275°C.

3.4 Conclusion

The successful coupling of LC to FID via a novel nebulizer interface has been demonstrated. The dependence on the material of the restriction and transfer capillary was investigated. Adjustment of the capillary size and height as well as the backpressure resulted in an improvement of the LOD in comparison to most existing interfaces.

A further advantage of the developed interface is the possibility of analyzing volatile as well as non-volatile compounds without loss of linearity or sensitivity. This ability was demonstrated by the analysis of a broad variety of N-heterocycles and can be considered to be a major advantage over former interfaces.

According to the ICH Q3A Guideline the solvent residues depend on the lowest observable effect level and are correlated to the daily exposure by a pharmaceutic product. The guidelines should be viewed as recommendations, and do not establish legally enforceable responsibilities. The limitations are done by the quality control of industries and may vary substantially. Therefore the aim and scope of pharmaceutical residual solvent LODs should provide the lowest possible detection limit to enhance quality control. The presented LC/FID interface provided lower LODs than those observed for traditional LC detectors and can considered being a complement to existing LC detectors.

The applicability for high temperature LC was shown by the successful separation of an alcoholic mixture by use of a Hypercarb column. Likely the usage of a temperature program can shorten the time of analysis and enhance the resolution of the obtained chromatographic separation.

It can be concluded that the novel FID coupling technique offers a promising possibility for an uncomplicated, universal detection in LC. Finally, the linear correlation between carbon content and response might allow a reference free semi-quantitative analysis of residual solvents in future.

3.5 References

[1] C. Becker, M.A. Jochmann, T.C. Schmidt, An Overview of Approaches in Liquid Chromatography Flame ionization Detection, TrAC Trends in Analytical Chemistry, 110 (2018) 143-149.
[2] T. Yarita, R. Nakajima, S. Otsuka, T. Ihara, A. Takatsu, M. Shibukawa, Determination of ethanol in alcoholic beverages by high-performance liquid chromatography-flame ionization detection using pure water as mobile phase, J. Chromatogr. A, 976 (2002) 387-391.
[3] L. Zhang, D.M. Kujawinski, M.A. Jochmann, T.C. Schmidt, High-temperature reversed-phase liquid chromatography coupled to isotope ratio mass spectrometry, Rapid Commun. Mass Spectrom. , 25 (2011) 2971-2980.
[4] W.E. Neff, M.A. Jackson, G.R. List, J.W. King, Qualitative and quantitative determination of methyl esters, free fatty acids, mono-, di-, and triacylglycerols via HPLC coupled with a flame ionization detector, J. Liq. Chromatogr. Related Technol., 20 (1997) 1079-1090.
[5] R. Marek, J. Straub, Analysis of the evaporation coefficient and the condensation coefficient of water, Int. J. Heat Mass Transfer, 44 (2001) 39-53.
[6] D.J. Miller, S.B. Hawthorne, Subcritical water chromatography with flame ionization detection, Anal. Chem., 69 (1997) 623-627.
[7] E. Young, R.M. Smith, B.L. Sharp, J.R. Bone, Liquid chromatography-flame ionisation detection using a nebuliser/spray chamber interface. Part 1. Design and testing, J. Chromatogr. A, 1236 (2012) 16-20.
[8] Y. Ishihama, H. Katayama, N. Asakawa, Y. Oda, Highly robust stainless steel tips as microelectrospray emitters, Rapid Commun. Mass Spectrom. , 16 (2002) 913-918.
[9] ISO_8466-1-1990, Water quality - Calibration and evaluation of analytical methods and estimation of performance characteristics - Part 1 Statistical evaluation of the linear calibration function.
[10] D. Guillarme, S. Heinisch, J.Y. Gauvrit, P. Lanteri, J.L. Rocca, Optimization of the coupling of high-temperature liquid chromatography and flame ionization detection application to the separations of alcohols, J. Chromatogr. A, 1078 (2005) 22-27.
[11] B.A. Ingelse, H.G. Janssen, C.A. Cramers, HPLC-FID with superheated water as the fluent: Improved methods and instrumentation, J. High. Resolut. Chromatogr., 21 (1998) 613-616.
[12] E. Young, R.M. Smith, B.L. Sharp, J.R. Bone, Liquid chromatography-flame ionisation detection using a nebuliser/spray chamber interface. Part 2. Comparison of functional group responses, J. Chromatogr. A, 1236 (2012) 21-27.
[13] P.D. Wentzell, M.R. Bowdridge, E.L. Taylor, C. MacDonald, Random walk simulation of flow injection analysis. Evaluation of dispersion profiles, Anal. Chem. Acta, 278 (1993) 293-306.
[14] S. Almeling, U. Holzgrabe, Use of evaporative light scattering detection for the quality control of drug substances: Influence of different liquid chromatographic and evaporative light scattering detector parameters on the appearance of spike peaks, J. Chromatogr. A, 1217 (2010) 2163-2170.
[15] L.E. Oppenheimer, T.H. Mourey, Examination of the concentration response of evaporative light-scattering mass detectors, J.Chromatogr. A, 323 (1985) 297-304.

[16] G. Guiochon, A. Moysan, C. Holley, Influence of various parameters on the response factors of the evaporative light scattering detector for a number of non-volatile compounds, J. Liq. Chromatogr., 11 (1988) 2547-2570.
[17] E.W.J. Hooijschuur, C.E. Kientz, U.A.T. Brinkman, Potential of flame ionization detection coupled on-line with microcolumn liquid chromatography using aqueous eluents and an eluent-jet interface, J. High. Resolut. Chromatogr., 23 (2000) 309-316.
[18] W.W.C. Quigley, S.T. Ecker, P.G. Vahey, R.E. Synovec, Reversed phase liquid chromatography with UV absorbance and flame ionization detection using a water mobile phase and a cyano propyl stationary phase - Analysis of alcohols and chlorinated hydrocarbons, Talanta, 50 (1999) 569-576.
[19] A.D. Jorgensen, K.C. Picel, V.C. Stamoudis, Prediction of gas chromatography flame ionization detector response factors from molecular structures, Anal. Chem., 62 (1990) 683-689.
[20] M. Mundt, J. Hollender, Simultaneous determination of NSO-heterocycles, homocycles and their metabolites in groundwater of tar oil contaminated sites using LC with diode array UV and fluorescence detection, J. Chromatogr. A, 1065 (2005) 211-218.
[21] R.A. Moreau, P.T. Asmann, H.A. Norman, Analysis of major classes of plant lipids by high-performence liquid chromatography with flame ionization detection, Phytochem., 29 (1990) 2461-2466.
[22] C.A. Bruckner, S.T. Ecker, R.E. Synovec, Simultaneous flame ionization and absorbance detection of volatile and nonvolatile compounds by reversed-phase liquid chromatography with a water mobile phase, Anal. Chem., 69 (1997) 3465-3470.
[23] P.D. Wentzell, M.R. Bowdridge, E.L. Taylor, C. MacDonald, Random walk simulation of flow injection analysis. Evaluation of dispersion profiles, Anal. Chem. Acta, 278 (1993) 293-306.
[24] S. Almeling, U. Holzgrabe, Use of evaporative light scattering detection for the quality control of drug substances: Influence of different liquid chromatographic and evaporative light scattering detector parameters on the appearance of spike peaks, J. Chromatogr. A, 1217 (2010) 2163-2170.
[25] L.E. Oppenheimer, T.H. Mourey, Examination of the concentration response of evaporative light-scattering mass detectors, J.Chromatogr. A, 323 (1985) 297-304.
[26] G. Guiochon, A. Moysan, C. Holley, Influence of various parameters on the response factors of the evaporative light scattering detector for a number of non-volatile compounds, J. Liq. Chromatogr., 11 (1988) 2547-2570.
[27] E.W.J. Hooijschuur, C.E. Kientz, U.A.T. Brinkman, Potential of flame ionization detection coupled on-line with microcolumn liquid chromatography using aqueous eluents and an eluent-jet interface, J. High. Resolut. Chromatogr., 23 (2000) 309-316.
[28] A.D. Jorgensen, K.C. Picel, V.C. Stamoudis, Prediction of gas chromatography flame ionization detector response factors from molecular structures, Anal. Chem., 62 (1990) 683-689.
[29] M. Mundt, J. Hollender, Simultaneous determination of NSO-heterocycles, homocycles and their metabolites in groundwater of tar oil contaminated sites using LC with diode array UV and fluorescence detection, J. Chromatogr. A, 1065 (2005) 211-218.
[30] R.A. Moreau, P.T. Asmann, H.A. Norman, Analysis of major classes of plant lipids by high-performence liquid chromatography with flame ionization detection, Phytochem., 29 (1990) 2461-2466.

Chapter 4

Response analysis: A brief introduction to the applied response factor equations and the most common response factor prediction models‡

Many Gas Chromatography (GC)/Flame Ionization Detection (FID) studies are dealing with response behavior of organic analytes such as alcohols and alkanes. Dietz, Sternberg et al. and others presented comprehensive studies of response data. However, the main focus of previous studies was on investigations of GC relevant analytes. Studies in the field of Liquid Chromatography (LC)/FID mainly focused on volatile analytes as well. In contrast, studies on LC/FID by a conveyor type interface only covered non-volatile substances. The LC/FID system introduced in **Chapter 3** of this work has been shown to be a useful tool for the analysis of volatile and non-volatile substances. The present chapter will highlight the response factor equations applied for the response analysis within the following **Chapter 5 and 6** of this thesis. In addition, it provides a brief introduction to computer based response prediction models and possible uncertainties that may arise in their use.

‡Adapted from: C. Becker, M.A. Jochmann, T.C. Schmidt, An Overview of Approaches in Liquid Chromatography Flame ionization Detection, TrAC, 110 (2019) 143-149.

4.1 Introduction

Simplified, the FID is a carbon counting device giving responses proportional to the number of carbon atoms [1]. The yield of signal causing formylium ions (CHO^+) is approximately one out of 106 carbon atoms and primarily results from chemi-ionization out of the reaction of oxygen with CH to CHO* and further to $CHO^+ + e^-$. The FID is one of the most frequently used detectors in gas chromatography [2]. Its success is based on the robustness, sensitivity and high linear range combined with a carbon dependent response.

Response factors for a broad variety of compounds have been investigated and research showed that hydrocarbon responses follow the equal per carbon rule. The carbon to response proportionality can be applied to estimate the hydrocarbon concentration of, e.g., aliphatic hydrocarbons without knowledge of the structure [3-6]. Deviations arise by heteroatoms, which result in formation of non-formylium ion forming species. By that, heteroatoms diminish the response per carbon significantly [7]. Oxygen containing compounds such as ketons, alcohols and esters for example react to methane, ethane and carbon monoxide. The latter one is known to cause no response in FID and thus reduces the expected response per carbon [3, 7]. Nitrogen containing compounds such as pyridine or amines tend to form undetectable hydrocyanic acid [7]. Therefore, response prediction of complex, heteroatom containing organic compounds becomes difficult and requires advanced prediction models.

Today, a broad variety of response quantification equations are available, e.g., the relative response factor, the molar response factor or relative sensitivity. Even more sophisticated models were established to compensate the influences of heteroatoms or functional groups and obtain more precise estimations [5, 6, 8].

A broad spectrum of abbreviations and calculations for the quantitative analysis of FID response data is available. To gain a more precise impression of the definitions and values obtained by the different response factor models, this chapter will summarize the two response models applied during further experiments, namely the Effective Carbon Number

(ECN) and Relative Sensitivity *(RF)*. In addition a short discussion about theoretical response prediction models is done.

4.2 Response definition and relationship

4.2.1 Effective carbon number *(ECN)*

In 1962, Sternberg et al. published the effects of functional groups and substitutes on the FID response [3]. Pure hydrocarbons were suggested to cause an equal response per carbon within the FID. Sternberg et al. focused on the investigation of the diminishing effects of several functional groups and established the concept of the *ECN* [3].

An important issue of the *ECN* contribution factors published by Sternberg et al. (Table 4.1) is the use for quantitative response prediction for a broad variety of functional group containing organic compounds [9, 10]. Especially if reference materials or pure compounds are not available, response approximation by consideration of the *ECN* delivers suitable semi-quantitative data.

Table 4.1. Effective carbon number contributions according to Sternberg et al. [3].

Atom	Type	Effective carbon number contribution
C	Aliphatic	1.0
C	Aromatic	1.0
C	Olefinic	0.95
C	Acetylenic	1.3
C	Carbonyl	0
C	Carboxyl	0
C	Nitrile	0.3
O	Ether	-1.0
O	Primary Alcohol	-0.6
O	Secondary alcohol	-0.75
O	Tertiery alcohol, esters	-0.25
Cl	Two or more on Aliphatic	-0.12 each
Cl	On olefinic C	+0.05
N	In amines	Similar to O in alcohols

The experimental *ECN* (ECN_{Exp}) is an expression of the response of any compound, compared to a reference compound and can be derived according to:

$$ECN_{Exp} = ECN_{ISTD} \frac{A_{Compound}/A_{ISTD}}{n_{Compound}/n_{ISTD}} \quad \text{Eq.4.1}$$

With ECN_{Exp} the calculated effective carbon number of the sample, ECN_{ISTD}, the effective carbon number of the Internal Standard *(ISTD)*, the peak area *A* and the amount *n* of an analyte and *ISTD*, respectively. GC/FID studies typically use a pure hydrocarbon *ITSD*, e.g., heptane.

Transformation of equation 4.1 allows the calculation of the amount of a known compound by use of the theoretical calculated *ECN* of the compound ($ECN_{Compound}$) according to table 4.1 by:

$$n_{Compound} = \frac{A_{Compound} * ECN_{ISTD} * n_{ISTD}}{A_{ISTD} * ECN_{Compound}} \quad \text{Eq. 4.2}$$

The accuracy of the semi-quantitative analysis of FID responses was already shown in 1961 for methylcyclohexane, n-heptane and benzene [11]. Later on, the validity of the *ECN* concept was shown by many authors [8-10, 12, 13]. The *ECN* can be considered to be one of the most frequently used estimation models and a broad range of *ECN* data for different compound classes and functional groups are available [4, 10, 12].

Within the present study, the ECN_{Exp} and by that the carbon related response of a compound was calculated according to equation 4.1. As methanol was used as *ISTD*, the ECN_{ISTD} was considered to be 0.4 according to the *ECN* contributions listed in Table 4.1. The assumption was made based on the *RF* values obtained by Dietz for GC/FID (*RF* 0.23) [4] and by Young et al. for LC/FID (*RF* 0.22) [14]. Since the *RF* values were observed to be close to each other, the *ECN* observed in GC/FID was considered to be equivalent to the *ECN* observed by LC/FID.

4.2.2 Relative sensitivity *(RF)*

Dietz [4] provided an important contribution by publication of the relative sensitivity *(RF)* of 121 compounds. A novelty of the data published by Dietz was the large number of functional group containing compounds. By that, Dietz provided evidence to the assumption of functional group contributions proposed by Sternberg et al. [3, 4].

The relative sensitivity is defined by using the masses and area counts of a compound and *ISTD* respectively, by:

$$RF = \frac{(m_{ISTD})*(A_{Compound})}{(m_{Compound})*(A_{ISTD})} \qquad \text{Eq. 4.3}$$

The relative sensitivity of the FID is based on a total response of 1 for a pure hydrocarbon compound. A relative sensitivity smaller than 1 means that the detector is less sensitive to the analyte than the pure hydrocarbon reference, and vice versa.

In case that the reference standard has a weaker response than one per carbon, Scanlon and Willis proposed multiplication with a correction factor [10]. Here, methanol was used as reference standard, therefore a correction factor of 0.4 (response of methanol according to Sternberg et al. [3]) was applied to calculate the *RF*. The modification allows a direct comparison of the *RF* values recorded by Dietz and others and the experimental *RF* values obtained for the developed LC/FID system, in the following named RF_{Exp}.

4.2.3 Computer based response factor modelling

Based on the *RF* data recorded by Dietz, Musumarra et al. used a multivariate statistical method for response prediction [5]. The authors recognized uncertainties in response prediction of complex compounds by former models and tried to minimize these uncertainties statistically. The *RF* values were used as dependent variable and the molecular weight and the compound structure (numbers of, e.g., C, H, O, N, S atoms and multiple bonds) were considered for the explanatory variables (descriptors) for prediction (see literature [5]).

Good agreement with experimental data was found by prediction for most studied compounds. However, in case of any type of structural isomers, calculations only matched for some compounds [5]. The experimental data of Dietz show that structural isomers such as 2-picolin, 3-picolin or 4-picolin have different *RF* values. In contrast to that, the predicted data of Musumarra et al. resulted in equivalent responses for all isomers. Combustion of these compounds may result in different fragments leading to different response behavior.

The same flaw in prediction is observed in the model of Katritzky et al. [15] who used a general quantitative structure-property relationship treatment. To achieve high precision and accuracy in prediction, Katritzky et al. extended the formula published by Musumarra et al. to 37 quantum-chemical descriptors and conventional molecular descriptors, respectively. The correlation between experimental and predicted response factors was $R^2 = 0.88$. However, evaluations of the data reveals the same shortcoming as in the model by Musumarra and co-authors: Structural isomers are assumed to cause equal responses [5, 15], even though the data considered for modeling reveal contradictory results [4].

Lučić and Trinajstić extended the number of descriptors and molecular interactions to 296 and thus more attention was paid to the structural isomers [16]. Comparison of the models reveal that deviation of the prediction results for structural isomers such as 2-picoline, 3-picoline and 4-picoline were reduced significantly (Table 4.2). The implemented descriptors and the consideration of molecular interactions seem to be reasonable factors for an overall better correlation and prediction.

Table 4.2. Experimental (*RF*) and predicted (RF_{Pred}) response factors of structural isomers.

Compound	*RF* [4]	RF_{Pred} [5]	RF_{Pred} [15]	RF_{Pred} [16]
2-picolin	0.88	0.83	0.84	0.87
3-picolin	0.86	0.83	0.84	0.87
4-picolin	0.86	0.83	0.84	0.87
Quinoline	0.82	0.76	0.76	0.80
Iso-quinoline	0.82	0.76	0.76	0.80

A combustion enthalpy based model for the prediction of molar response factors (MRF_{Pred}) was applied by De Saint Laumer et al [6]. The author's stated the hypothesis of a direct connection between combustion enthalpies (ΔH_{Comb}) and MRF_{Pred} [6]. Equation 4.4 summarizes the MRF_{Pred} formula, with constant values and descriptors for benzene rings:

$$MRF_{Pred} = -0.071 + 8.57 * 10^{-4} \Delta H_{Comb} + 0.127 \mathrm{n}_{Benz} \qquad \text{Eq. 4.4}$$

De Saint Laumer et al. [6] concluded that this simple approach can well compete with sophisticated calculation models. However, pyrolysis fragments and the further reaction to ions finally causing a signal were not taken into consideration. According to equation 4.5, structural isomers such as 2-picoline, 3-picoline, 4-picoline or 1-propanol and iso-propanol, 1,2-butandiol 1,3-butandiol and 1,4-butandiol result in the same ΔH_{Comb} and MRF values. Therefore It can be suggested that a pure combustion enthalpy based model will cause erroneous results for most structural isomers.

4.3 References

[1] T. Holm, Aspects of the mechanism of the flame ionization detector, J. Chromatogr. A, 842 (1999) 221-227.
[2] B.A. Ingelse, H.G. Janssen, C.A. Cramers, HPLC-FID with superheated water as the fluent: Improved methods and instrumentation, J. High. Resolut. Chromatogr., 21 (1998) 613-616.
[3] J.C. Sternberg, Gallaway, W.S. and Jones, D.T.L., The Mechanism of Response of Flame Ionization Detectors, in: Gas Chromatography: Third International Symposium Held Under the Auspices of the Analysis Instrumentation Division of the Instrument Society of America, June 13-16, 1961, Academic, 1962, pp. 231-267.
[4] W.A. Dietz, Response Factors for Gas Chromatographic Analyses, J. Chromatogr. Sci., 5 (1967) 68-71.
[5] G. Musumarra, D. Pisano, A.R. Katritzky, A.R. Lapucha, F.J. Luxem, R. Murugan, M. Siskin, G. Brons, Prediction of gas chromatographic response factors by the PLS method, Tetrahedron Comput. Methodol., 2 (1989) 17-36.
[6] J.Y. de Saint Laumer, E. Cicchetti, P. Merle, J. Egger, A. Chaintreau, Quantification in gas chromatography: prediction of flame ionization detector response factors from combustion enthalpies and molecular structures, Anal. Chem., 82 (2010) 6457-6462.
[7] T. Holm, Mechanism of the flame ionization detector II. Isotope effects and heteroatom effects, J. Chromatogr. A, 782 (1997) 81-86.
[8] A.D. Jorgensen, K.C. Picel, V.C. Stamoudis, Prediction of gas chromatography flame ionization detector response factors from molecular structures, Anal. Chem., 62 (1990) 683-689.
[9] M. Kállai, J. Balla, The effect of molecular structure upon the response of the flame ionization detector, Chromatographia, 56 (2002) 357-360.
[10] J.T. Scanlon, D.E. Willis, Calculation of Flame Ionization Detector Relative Response Factors Using the Effective Carbon Number Concept, J. Chromatogr. Sci., 23 (1985) 333-340.
[11] I. Halasz, W. Schneider, Quantitative Gas Chromatographic Analysis of Hydrocarbons with Capillary Column and Flame Ionization Detector, Analytical Chemistry, 33 (1961) 978-982.
[12] M. Morvai, I. Pályka, l. Molnár-Perl, Flame Ionization Detector Response Factors Using the Effective Carbon Number Concept in the Quantitative Analysis of Esters, Journal of Chromatographic Science, 30 (1992) 448-452.
[13] C. Cao, P. Huo, Investigation of General Expression to Predict the Molar Response Factor in the GC for Monosubstituted Alkanes, Journal of Chromatographic Science, 45 (2007) 360-368.
[14] E. Young, R.M. Smith, B.L. Sharp, J.R. Bone, Liquid chromatography-flame ionisation detection using a nebuliser/spray chamber interface. Part 2. Comparison of functional group responses, J. Chromatogr. A, 1236 (2012) 21-27.
[15] A.R. Katritzky, E.S. Ignatchenko, R.A. Barcock, V.S. Lobanov, M. Karelson, Prediction of Gas Chromatographic Retention Times and Response Factors Using a General Qualitative Structure-Property Relationships Treatment, Analytical Chemistry, 66 (1994) 1799-1807.

[16] B. Lučić, N. Trinajstić, S. Sild, M. Karelson, A.R. Katritzky, A New Efficient Approach for Variable Selection Based on Multiregression: Prediction of Gas Chromatographic Retention Times and Response Factors, Journal of Chemical Information and Computer Sciences, 39 (1999) 610-621.

Chapter 5

Determination of liquid chromatography/flame ionization detection response factors for alcohols, ketones and sugars‡

In the past, the main focus of Flame Ionization Detector (FID) response studies was set on investigations of Gas Chromatography (GC) relevant analytes such as aliphatic hydrocarbons and selected functional groups. Only a few data are available for Liquid Chromatography (LC)/FID responses. Within this Chapter the FID response factors for a LC/FID system with an aqueous eluent as mobile phase are presented. The study focus on the most common analytes of LC/FID studies in the past as well as several compounds that are not directly GC compatible because of their polarity. Furthermore the range of substances was extended to isomers, poly-alcohols and sugars to obtain more detailed information of the influence of hydroxyl groups on the recorded response. The data show a group specific correlation of responses factors with a correlation coefficient (R^2) for e.g. alcohols and ketones of 0.99.

Constant contribution factors of functional groups as mentioned in several GC/FID response studies and prediction models were observed to a limited extend. Interactions of sugar analytes with water showed that transfer of GC/FID to LC/FID data cannot be done in general. The underlying mechanisms revealed several new aspects, which have to be taken into account for future response prediction models, especially of small molecules. Interactions between eluent and analytes show, that LC/FID response prediction is more complex and requires more than simple addition of functional group contributions.

‡Adapted from: C. Becker, M.A. Jochmann, T.C. Schmidt, Determination of liquid chromatography/flame ionization detection response factors for alcohols, ketones and sugars, ABC Journal, Accept (19.02.2019).

5.1 Introduction

The fast and sensitive quantitative analysis of synthetic by-products during the production of pharmaceuticals or pesticides is an unsolved analytical problem in all fields of Life Science. Especially during production of new pharmaceuticals or pesticides, unwanted by-products can occur. Since no universal detector for reference material free quantification is available for LC, a sensitive, easy applicable, low cost instrumentation is required. The FID, typically used for GC, is known to be a universal detector for fast and precise analysis of carbon containing analytes and by-products. In contrast to UV-, Diode Array (DA)-, Refractive Index (RI)- and Evaporative Light Scattering (ELS)- detectors, the FID signal is not limited by the volatility of a compound or presence of chromophores. The signal is correlated to the carbon content of the analyte and allows the estimation of an analyte concentration directly from the obtained signal [1-3].

To establish the FID as common detector in LC laboratories, several aspects need to be considered, such as a response data base as known for GC and the proof of concept. Today, a broad variety of GC response quantification equations are available such as the Relative Response Factor (*RRF*), the Molar Response Factor (*MRF*) or the relative sensitivity (*RF*). Even more, sophisticated models were established to compensate and calculate the influences of heteroatoms or functional groups to gain more precise estimations [2-4]. Tong and Karasek discussed the differences in experimental GC/FID response factors and figured out that these values are limited by the instruments and conditions used. The relative standard deviation of the instrument in use for, e.g., PAH varied by up to 8.4%, whereas C14 to C32 alkanes showed a deviation of 1.4% [5].

However, all models rely on sets of data obtained by GC/FID studies. Models based on LC/FID response data are not known yet. Even more, LC/FID response studies were never taken into consideration for response prediction models up to day. The development of LC/FID systems, which are capable to deal with a broad spectrum of GC and LC compatible analytes, can be considered to be the limiting factor. Furthermore, studies on the intramolecular reactions during combustion of compounds were not taken into consideration up to now [6, 7].

In the past, coupling of LC to FID was limited by the need to remove organic eluents before detection. In the early 1990´s the introduction of high temperature LC [8-12] paved the way for LC/FID couplings in the coming decades. Direct connection of LC and FID without a pre-evaporation of the organic eluent became possible [13]. Valuable methods for high temperature only water LC/FID analysis of, e.g., alcohols [12, 14], pharmaceuticals [11, 15] or lipids [16, 17] have been reported.

As described above, high temperature aqueous LC is capable to investigate many non-volatile compounds by FID. The obtained response data of the mainly LC feasible analytes such as alcohols, ketones and sugars, can help foster our understanding of response factors for an improvement of current response models. Errors and uncertainties in predictions of substituted compounds caused by lack of experimental data in established prediction models can be corrected.

In the present study, we investigated LC/FID specific response factors of a broad variety of compounds. To this end, we employed a self-made LC/FID system that was established to overcome some of the limitations with previously described interfaces [13]. The employed LC/FID system possesses a linear dynamic range (ng to µg) of at least 10^6. Additionally, the system delivered precise results with ≤4 % deviation of the peak area over one month. In case of pharmaceutical analysis, method validation values such as the reached LODs of 0.28 to 5 ng and LOQs of 0.84 to 1.5 ng are sufficient to meet the regulatory requirements of Class 2 or Class 3 solvent residues in pharmaceutical products of 0.5%.

Aim of this work is to set up the fundamental for establishing LC/FID as common analytical tool. Therefore a response data base as known for GC/FID is required. Since a first step needs to be done, the study focuses on the first groups of compounds investigated by GC/FID. Like in GC, the influence of functional groups and positioning of those was investigated more in detail and was explained by the inflame processes. Due to the complex structure behind most prediction formulas, we rather tried to investigate the reason of compound specific response deviations by consideration of present literature than establishing a novel formula which encounters all possible responses relevant in flame ionization.

5.2 Experimental section

5.2.1 Reagents

D-arabinose (>99%), ascorbic acid (>99%), butane-1,2,3-triol (>99 %), butane-1,2,4-triol (>95%), butane-2,3-diole (>98%), ethylenglycol (≥99.8%), 3-methyl-1-butanole (>98%), 3-methyl-1-pentanole (>99%), 1-butanol (≥99.7%), D-(-)-fructose (>99%), D-(+)-glucose (>99%), D-(+)-mannose (>99%), L-(+)-rhamnose (>99%), D-(-)-ribose (>99%), lactose-monohydrate (>99%), maltose-monohydrate (>99%), *meso*-erythrit (>99.8%), 1-heptanol (>99.5%), 1-hexanol (>99%), 2-hexanone (≥99%), 1-pentanol (>99%), 1-propanol (>99.9%), propane-1,2-diol (≥99.7%), propane-1,3-diol (>98 %), propane-1,2,3-triol (>99%), sorbitol (≥99%) were purchased by Sigma Aldrich (Seelze, Germany). 2-Heptanone (≥98%), 2-pentanone (≥99%), 3-ethyl-3-hexanol (≥99%), 2-propanol (≥99.8%), *β*-D-fructose (>99.8%), 2-butanol (≥99%), 2-butanone (>99%), xylit (≥99%), were purchased by Merck (Darmstadt, Germany). Methanol (>99.8%) and acetone (≥99.9%) was purchased by Fischer-Scientific (Schwerte, Germany). Ethanol (>99.7%) was purchased by LGC Standards GmbH (Wesel, Germany).

Hydrogen (purity 5.0) and synthetic air (purity 5.0) for FID operation were purchased from AirLiquide (Oberhausen, Germany).

Samples and stocks were prepared using analytical grade water from an ELGA PURELAB purification system (Celle, Germany).

Stock solutions were prepared at total carbon concentrations γ_{TC} of 100 mg L^{-1}. Whereby, γ_{TC} represents the absolute concentration of carbon within the solution. Standard solutions were prepared by dilution from the stock solution at ten different levels in a range of 0.1 to 100 mg L^{-1} using Hamilton microliter syringes (Bonaduz, Switzerland). Solutions for response analysis were prepared by dilution of the stock solution to γ_{TC} of 30 mg L^{-1}.

5.2.2 LC/FID analysis

FID analysis was performed with a Dani Master GC® provided by Axel Semrau (Sprockhövel, Germany). The FID temperature T_{FID} was set to 275°C. A hydrogen and synthetic air flow ($F_{Hydrogen}$) of 50 and (F_{Air}) of 450 mL min^{-1} was used, respectively. The signal was recorded with the Clarity software (DataApex, Prague, Czech Republic). For a detailed description of the LC/FID system and the experimental set up, please see **Chapter 3**: *"A Thermospray Nebulizer Interface for Liquid Chromatography - Flame Ionization Detection: Development and Optimization"*.

5.2.3 Response calculation

The experimental Effective Carbon Number (ECN_{Exp}) and the experimental relative sensitivity (RF_{Exp}) were calculated as explained in detail in **Chapter 4**: *"Response Analysis: A brief introduction to the applied response factor equations and the most common response factor prediction models"*.

5.3 Results and discussion

The ECN_{Exp} of the present study, theoretical responses from increments according to Sternberg et al. (ECN_{Theo}), the relative sensitivity values reported in literature (RF) and within this study (RF_{Exp}) are summarized in Table 5.1. The ECN_{Theo} is calculated from the increments according to the effective carbon number contributions [18]. The ECN values are the data published by Halaz and Schneider [19]. The RF_{Exp} was calculated based on the ECN_{Exp} values and used to compare the experimental data obtained here with the ones recorded by Dietz [20].

Table 5.1. Theoretical *ECN* (ECN_{Theo}) according to Sternberg et al. [18], experimental *ECN* values according to literature *(ECN)*, recorded *ECN* values of the present study (ECN_{Exp}) and the experimental *RF* values according to Dietz [20] *(RF)* and this study (RF_{Exp}).

Substance	ECN_{Theo}[18]	*ECN* [19]	ECN_{Exp}	*RF* [20]	RF_{Exp}
Alcohols					
Methanol	0.4	0.751	-[1]	-[1]	-[1]
Ethanol	1.4	-	1.97	0.46	0.55
1-propanol	2.4	2.561	2.33	0.6	0.50
1-butanol	3.4	3.381	3.51	0.66	0.61
1-pentanol	4.4	-	4.44	0.71	0.64
1-hexanol	5.4	-	5.64	0.74	0.71
1-heptanol	6.4	-	6.75	-	0.74
3-methyl-1-butanol	4.4	-	4.65	-	0.68
2-propanol	2.25	2.191	2.09	0.53	0.52
2-butanol	3.25	3.78	2.71	-	0.56
3-methyl-1-pentanol	5.4	-	4.57	0.65	0.55
3-ethyl-3-hexanol	7.75	-	7.11	-	0.50
Diols, Triols and Alditols					
Ethylenglycol	0.5	-	0.87	-	0.18
Propane-1,2-diol	1.65	-	1.52	-	0.26
Propane-1,3-diol	1.8	-	1.67	-	0.28
Butane-2,3-diol	2.5	-	2.01	-	0.29
Propane-1,2,3-triol	0.9	-	1.5	-	0.21
Butane-1,2,4-triol	2.05	-	1.96	-	0.24
Butane-1,2,3-triol	1.9	-	1.84	-	0.22
meso-erythrit	1.3	-	1.83	0.579	0.19
Xylit	2.05	-	2.15	0.577	0.18
Sorbitol	2.8	-	2.57	0.598	0.18
Ketones					
Acetone	2	-	2.6	0.49	0.57
2-butanone	3	-	3.49	0.61	0.62
2-pentanone	4	-	4.36	-	0.65
2-hexanone	5	-	5.21	-	0.67
2-heptanone	6	-	6	-	0.67

[1] the ECN_{Exp} of methanol cannot be calculated since methanol is the internal standard arbitrarily set to 1.

Table 5.1. (Continued) Theoretical *ECN* (ECN_{Theo}) according to Sternberg et al. [18], experimental *ECN* values according to literature (*ECN*), recorded *ECN* values of the present study (ECN_{Exp}) and the experimental *RF* values according to Dietz [20] (*RF*) and this study (RF_{Exp}).

Substance	ECN_{Theo}[18]	$ECN_{Lit.}$[19]	ECN_{Exp}	RF_D [20]	RF_{Exp}
Pentose					
D-arabinose	2.8	-	2.25	-	0.19
D-(-)-ribose	2.8	-	2.55	0.58*	0.22
Hexose					
β-D-fructose	1.8	-	2.39	-	0.17
D-(-)-fructose	1.8	-	2.51	-	0.11
D-(+)-mannose	2.4	-	1.27	-	0.09
D-(+)-glucose	2.4	-	2.64	-	0.09
L-(+)-rhamnose	2.4	-	2.77	-	0.10
Sorbitol	2.8	-	2.57	0.598	0.18
Lactose	5.6	-	4.63	-	0.17
Maltose	5.6	-	3.73	-	0.14
Vitamins					
Ascorbic acid	2.65	-	1.20	-	0.09

5.3.1 Primary alcohols

In the present study the averaged contribution factor of ethanol to 1-heptanol is encountered with -0.4 for the hydroxyl group carrying C-atom. Literature proposes a constant decrease of the *ECN* of primary alcohols by a value of -0.6 and encounter the response of the primary carbon with an *ECN* of 0.4 [18]. Figure 5.1a depicts the response data of C3 to C7 primary alcohols obtained within this study (Figure 5.1a; diamonds) and the theoretically derived response values according to literature (Figure 5.1a; squares) [20]. The gap between experimental and theoretical derived response values becomes larger by prolongation of the carbon chain. The here conducted experiments show that the OH induced influence on the ECN_{Exp} of primary alcohols ≥C6 decreases substantially, and is confirmed by the experimental data recorded by Dietz [20] and Kosch [22].

Plotting of the Δ*RF* values (Δ*RF* = *(RF* of pure Hydrocarbon*)* – *(RF* of primary alcohol*))* recorded by Dietz [20] (Figure 5.1b; triangles) and within this study (Figure 5.1b; squares) reveal that the effect of primary alcohols on the response is reduced by extension of the

carbon chain. Furthermore, the Δ*RF* values obtained by GC/FID and the Δ*RF* values obtained by LC/FID follow the same function. Young et al. [21] reported experimental LC/FID response values close to those observed by Dietz and within this study, too (see Table 5.1).

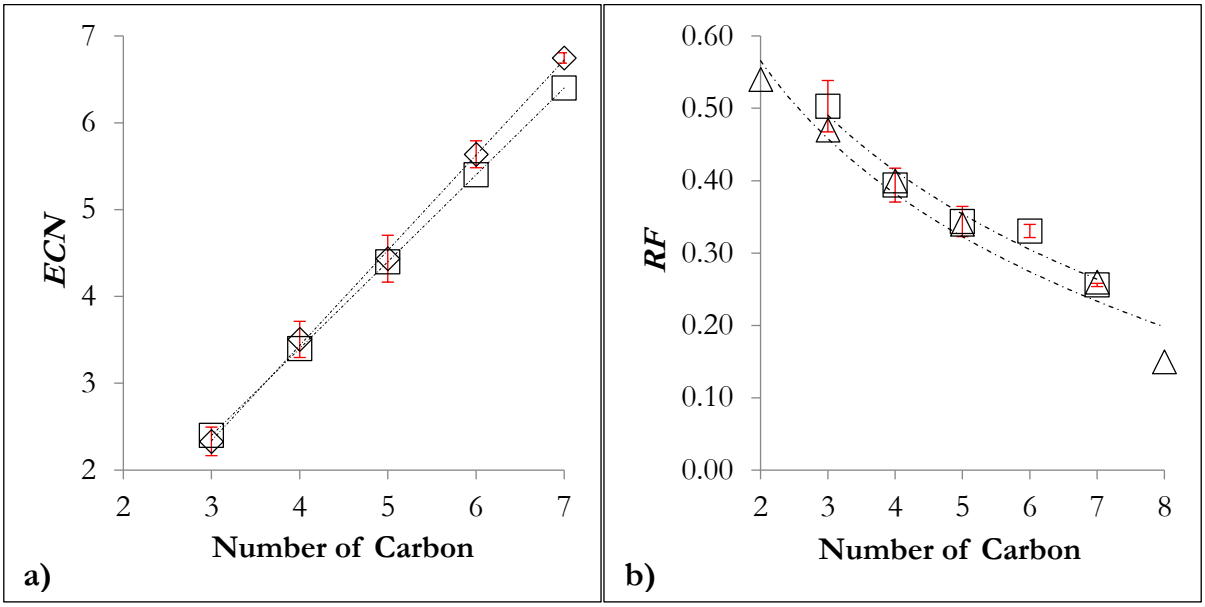

Figure 5.1. Effect of carbon number on *ECN* and the effect of hydroxyl in dependents of the carbon chain length. a) Diamonds indicate the experimental ECN_{Exp} of a homologous series of alcohols (C3 to C7) and squares show ECN_{Theo} according to Sternberg et al. **b)** Triangles show the Δ*RF=(1-RF)* reduction of the data recorded by Dietz and squares indicate the experimentally derived Δ*RF* values. Note: ethanol was not taken into consideration since literature and experimental values show a non-characteristic response behavior.

Differences in the response of alcohols were already noted in early studies and it was mentioned that primary alcohol response were not diminished by a constant value in contrast to alkanes [23]. The chain length was not conclusively mentioned a reason for the diminishing effect. However, the responses published in literature suggest that prolongation of the primary alcohol carbon chain favor the hydrogenation of the hydroxyl group (Eq. 5.1) as discussed by Holmes et al. [24]. The same effect can also be observed for the branched primary alcohol 3-methyl-1-butanol (Table 5.1). According to Holmes, the *ECN* is diminished to the same extent to which CO formation by bond cleavage and hydrogen abstraction at the *a*-position takes place (Eq. 5.1) [24].

5.3.2 Secondary alcohols

Secondary alcohol responses are found to be significantly lower than primary alcohol responses. This effect is not taken into account in prediction models of e.g. de Saint Laumer [2] or Musumarra et al. [4]. The structural configuration of secondary alcohols favors hydrogen abstraction and is a major pathway after the initial chain cleavage (Eq. 5.2). In case of secondary alcohols hydrogen abstraction is rather possible than hydrogenation. Cleavage of secondary alcohols starts as indicated in equation 5.3 by abstraction of methane. The remaining $^{\bullet}COHCH_3$ reacts further into a methyl radical and carbon monoxide (Eq. 5.4).

$$CH_3OH + 2H^{\bullet} \rightarrow CH_4 + H_2O \quad \text{(Eq. 5.1)}$$

$$CH_3OH + 2H^{\bullet} \rightarrow CH_2O + 2H_2 \rightarrow CO + 3H_2 \quad \text{(Eq. 5.2)}$$

$$CH_3CHOHCH_3 + 2H^{\bullet} \rightarrow CH_4 + {}^{\bullet}COHCH_3 + H_2 \quad \text{(Eq. 5.3)}$$

$$^{\bullet}COHCH_3 \rightarrow {}^{\bullet}CH_3 + CO \quad \text{(Eq. 5.4)}$$

The suggested abstraction and formation of CO during combustion becomes clearer by comparison of the experimental response data of 1-propanol (2.33) to 2-propanol (2.09) and 1-butanol (3.51) to 2-butanol (2.71) and can be confirmed by comparison of the *RF* values of 2-prpanol published in literature (*RF* 0.53) and within this study (RF_{Exp} 0.53). Furthermore, the response of 3-ethyl-3-hexanol suggests the same reaction pattern for tertiary alcohols as observed for secondary alcohols (see Table 5.1).

5.3.3 Polyols and alditols

Looking at the theoretical data provided in literature, the congruency of data obtained for the influence of mono-substituted hydroxyl groups becomes clear: secondary > tertiary > primary [18]. However, none of the publications deals with poly-substituted alcohols. Therefore, it seems to be doubtful, that theoretical data, derived by use of contribution factors obtained by mono- substituted alcohols lead to a suitable response prediction.

The presence of two hydroxyl groups were found to cause elevated deteriorative effects on the ECN_{Exp}. Furthermore, the positioning of the hydroxyl group within the analytes was found to have a direct influence on the recorded response. The response decrease of 1-propanol to propane-1,2-diol and ethanol to ethylene glycol was found to be ΔECN_{Exp} 1.48 and 1.13. This observation for propane-1,2-diol suggests to the assumption that decomposition starts at the non-substituted end of the molecule as indicated in Eq. 5.3, earlier. Further decomposition results in dehydrogenation within the reducing part of the flame and conversion into carbon monoxide as shown in Eq. 5.2.

It can be suggested that hydrogen abstraction becomes more feasible with an increasing number of OH groups. Since both C atoms of ethylene glycol contain a hydroxyl group, hydrogenation is the major initial reaction. On the one hand the initial reaction results in CH_4 abstraction (Eq. 5.1) and on the other hand, the remaining $CH_2O\cdot$ radical tends to convert into non-detectable carbon monoxide (Eq. 5.2). However, the observed ECN_{Exp} of 0.87 reveals that hydrogenation as well as hydrogen abstraction occurs; otherwise the ideal conversion would result in a theoretical and experimental *ECN* of 1. It cannot be excluded, that the aqueous mobile phase influences the reaction pattern and thus the response of the compound.

A substantially higher reduction of the ECN_{Exp} by ~2 was observed for butan-2,3-diole. Initial decomposition at the C1 carbon favors dehydrogenation at the hydroxyl carrying C atom of the CH3CHOHCHOH· radical. The radical further reacts as indicated in Eq. 5.4. Therefore, the hydroxyl group positioning at C2 and C3 results in almost complete formation of carbon monoxide.

The discussed deteriorative effect of secondary alcohols was also observed for propan-1,2-diol, butane-2,3-diol, butane 1,2,3-triol and butane 1,2,4-triol. The latter ones were found to have an ECN_{Exp} of 1.90 and 2.05. Using previously mentioned prediction models consequently result in equal responses for these two analytes as well as propane-1,2-diol (ECN_{Exp} 1.65) and propane 1,3-diole (ECN_{Exp} 1.8).

The ECN_{Exp} of alditols rises by the number of carbon atoms almost linearly (Figure 5.2), whereby a substantial suppression of the signal by the formation of non-detectable species can be observed.

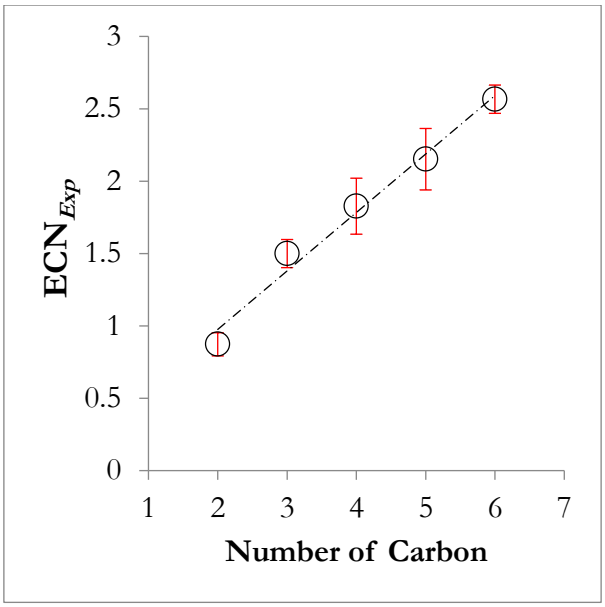

Figure 5.2. ECN_{Exp} of ethylene glycol and C3 to C6 alditols. Cycles present the calculated ECN_{Exp} of ethylene glycol and C3 to C6 alditols.

Table 5.2. Average effect per hydroxyl group (OH) in C3 to C6 alditols.

Substance	ECN_{Exp} reduction per OH	*RSD* (%)
Propan-1,2,3-triol	0.50	6.5
meso-Erythrit	0.54	11
Xylit	0.57	9.9
Sorbitol	0.57	3.8

The average ECN_{Exp} reduction of alditols increased by the carbon chain length from 0.5 (propan-1,2,3-triol) to 0.57 (sorbitol) per hydroxyl group (see Table 5.2). Considering the high standard deviation *(RSD)* of the obtained data, the observation confirms theoretical data. Prediction models of Musumarra et al.[4], Saint Laumer et al.[2] or Sternberg et al.[18] suggest constant contributions for each hydroxyl group.

5.3.4 Ketones

The experimentally determined ketone response factors as function of the carbon number are shown in Figure 5.3a.

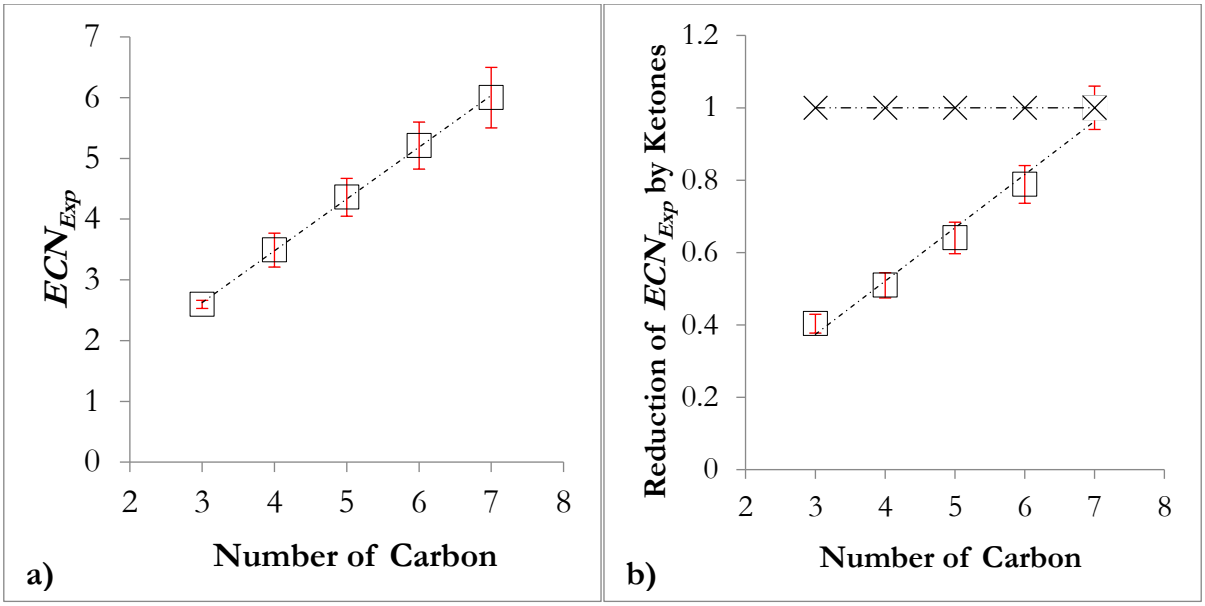

Figure 5.3. Influence of the carbon number on ECN_{Exp} of C3 to C7 ketones. (a) Triangles represent the observed ECN_{Exp} values of ketones (C3 to C7) **(b)** squares indicate the observed influence of the ketone group on the response and crosses the contribution factor of ketones published by Sternberg et al. [18].

In 2011, Veloo et al. published experimental data for the partially formed amount of carbon monoxide during combustion of ketones [25]. The reported increase of carbon monoxide formation by extension of the carbon chain is in good agreement with the observations within this study. The depicted squares of Figure 5.3b show the experimental observed successive reduction of the response by extension of the carbon chain in contrast to the theoretical proposed constant values (crosses, Figure 5.3b).

Lam et al. [26] and Swarc and Watson [27] identified two major reaction pathways in the pyrolysis of acetone. Within the first pathway, acetone is decomposed into a methyl and an acetyl radical (Eq. 5.5), followed by a rapid acetyl radical decomposition into a second methyl radical and carbon monoxide as shown in equation 5.6. In the second reaction, the previously formed methyl radical initiates formation of ketene according to reactions 5.7 and 5.8, respectively.

$$CH_3COCH_3 \rightarrow CH_3^{\bullet} + CH_3CO^{\bullet} \quad \text{(Eq. 5.5)}$$

$$CH_3CO^{\bullet} \rightarrow CH_3^{\bullet} + CO \quad \text{(Eq. 5.6)}$$

$$CH_3^{\bullet} + CH_3COCH_3 \rightarrow CH_4 + CH_3COCH_2^{\bullet} \quad \text{(Eq. 5.7)}$$

$$CH_3COCH_2^{\bullet} \rightarrow CH_2CO + CH_3^{\bullet} \quad \text{(Eq. 5.8)}$$

The formation of the radical and further reaction to carbon monoxide was found to be the dominant reaction [25]. The here published data confirm the experimental data of Veloo [25], the ECN_{Exp} response was found to be diminished by 0.4 in acetone up to 1 for 2-heptanone (Table 5.1).

It can be concluded, that only partial conversion of the ketone group into CO occurs in acetone and complete conversion of the ketone group into carbon monoxide takes place in 2-heptanone. In contrast, the prediction models of, e.g., Sternberg et al. [18] encounter the response of the carbonyl group carbon with zero. This assumption can be considered to be valid only for alkanes ≥ C7.

5.3.4 Pentoses and hexoses

Comparative FID response studies of pentoses and hexoses were not published yet. Only a few response data of carbohydrates were published in literature using a LC/FID system [21]. Reasons are the low volatility and the required derivatization for GC/FID analysis. Using LC/FID requires no specific treatment before analysis. In total, two pentose and seven hexoses, sorbitol and xylit were investigated. Sugars mainly differ in the structural configuration of the hydroxyl groups, therefore response prediction models result in equal responses for all structural isomers of pentose and hexose sugars by GC/FID. The recorded data reveal the invalidity of the theoretical assumption for hexoses and pentoses (Table 5.1). Furthermore, an unequally distributed ECN_{Exp} between 1.21 (Glucose) and 2.68 (β-D-Fructose) was noticed.

In aqueous solutions sugars are present in three structural configurations: pyranose form, furanose form and open chain form (Figure 5.4a to c). The structural distribution mainly depends on the sugar (Table 5.3). Thus, a reasonable influence on the response deviations can only be derived from structural characteristics and the resulting physicochemical properties.

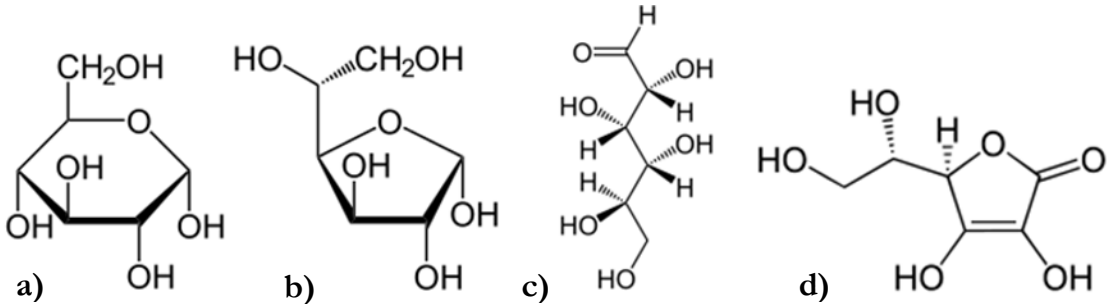

Figure 5.4. Structure of sugars and ascorbic acids: a) α-D-glucopyranose, **b)** α-D-glucofuranose, **c)** α-D-glucose open chain structure and **d)** ascorbic acid.

When sugars are present in crystalline pyranose ring structure, current response prediction modelling suggests that they will be converted into same amounts of CHO^+, CO_2 and CO, respectively. However, this is not the case as the shift of the ECN_{Exp} for the structural isomers of hexose and pentose sugars shows (Figure 5.5a).

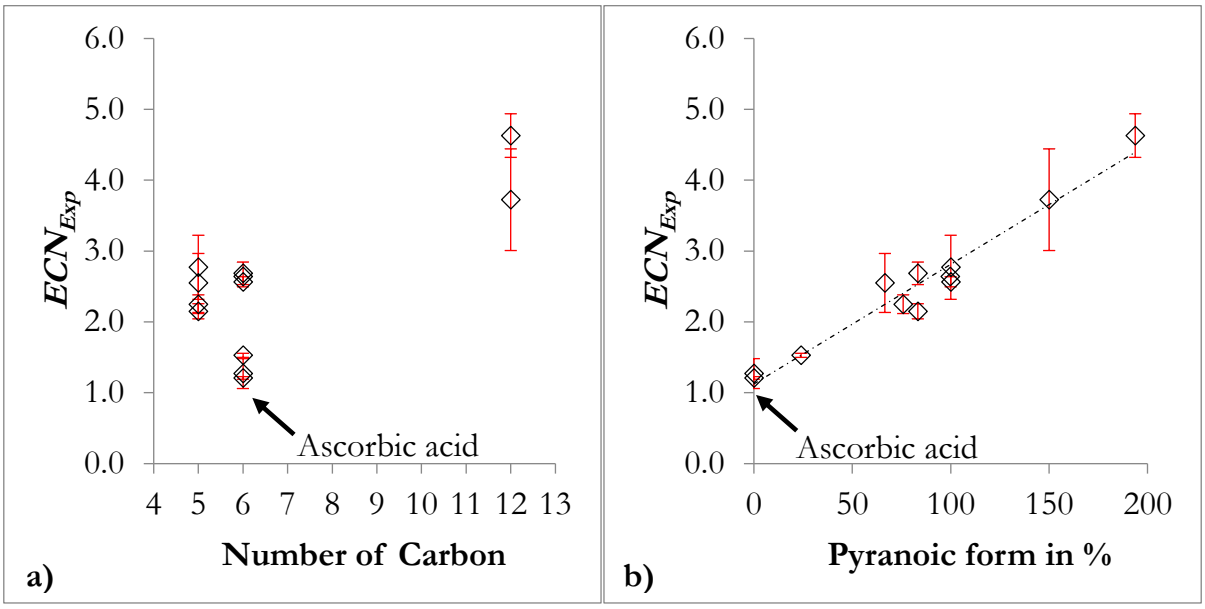

Figure 5.5. ECN_{Exp} values of sugars. a) Experimental ECN_{Exp} values of sugars and ascorbic acid plotted against the carbon number **b)** Experimental ECN_{Exp} plotted in dependency of the pyranose form observed in water. Hexose sugars are set as 100%. Disaccharides may lead to values exceeding 100 %.

Considering the structural distribution of sugar molecules in water can provide a linear correlation. Combustion of the pyranose ring structure can be suggested to result in a significantly lower amount of non-detectable carbon monoxide. Hydrogenation at the C6 position of the pyranose form favors formation of detectable species. The ether bridge can be converted into a double bond at the C1 or C5 position and results in a chain structure of the molecule.

In contrast, hydrogenation of the C6 atom of furanose mainly results in formation of CO at the C5 position, as observed for aliphatic polyalcohols. The assumption is underlined by the ECN_{Exp} clusters formed for each group of sugars. Figure 5.5a shows that pentose sugars are located within the same ECN_{Exp} range. The same observations are found for hexoses which are mainly present in pyranose form or furanose form, respectively.

Table 5.3. Structural distribution of sugars in water in % [28].

Sugar	Pyranose form	Furanose form	Chain	C-Atoms	Contribution factor[1] for pyranoic form
D-arabinose	91	8.8	0.03	5	0.83
D-(-)-ribose	80	20	0.05	5	0.83
β-d-fructose	83.34	16.66	-	6	1
D-fructose	70-77	25-28	0-0.07	6	1
D-(+)-mannose	99.1	0.9	0.005	6	1
D-(+)-glucose	99.75	0	0.25	6	1
L-(+)-rhamnose	100	-	-	6	1
Sorbitol	-	-	100	6	1
Xylit	-	-	100	5	0.83
Lactose	96.87[2]	3[2]	0.135[2]	12	2
Maltose	99.75[3]	0[3]	0.25[3]	12	2

[1] Contribution factor was multiplied with the pyranoic form in % to weight the obtained ECN_{Exp} with regard to the number of carbons of a compound
[2] Lactose consists of one molecule D-galactose and D-glucose
[3] Maltose consist of two molecules D-glucose

Plotting of the response data versus the total occurrence of the pyranose form in water, results in a linearization of the ECN_{Exp} values of sugars (Figure 5.5b). To consider the total amount of carbon, hexose sugar configurations were nominally encountered with 1 and pentose sugar with 0.83. Since lactose and maltose consist of two sugar molecules, the configurations of both sugars were summed up. This leads for lactose to 1 x 94% (pyranose

form of galactose in water) + 1 x 99.75% (pyranose form of D-glucose in water) = 193.75%. In the same way, for maltose 199.5% are calculated.

To provide evidence to the assumption of the *ECN* structural relationship, the ECN_{Exp} of ascorbic acid was calculated out of the measured response, too. The analyte structure is close to the furanoic structure of hexose sugars (Figure 5.4d), therefore a significant reduction in comparison to pyranoic sugars was assumed. The observed ECN_{Exp} of 1.20 confirms the assumption. The correlation of the plotted data (R^2 0.96) let assume a correlation between response and structural configuration of sugars.

5.4 Conclusion

Most FID response studies rely on data recorded by GC/FID. Therefore the main focus of previous research was on typical GC analytes such as alcohols, ketones and benzenes. Only rare data are available for LC/FID based *RF* values, and due to lack of GC/FID obtained *RF* values for non-volatile analytes, a direct comparison of, e.g., sugars, pharmaceuticals and acids becomes difficult.

The presented response study demonstrates the relevance of LC/FID analysis, enabling the determination of volatile and non-volatile analytes. Combustion studies of a broad variety of compounds are available today and the impact seems to be neglected in modern prediction models, as shown for ketones. These studies can provide helpful information to understand the response behavior of isomers.

Literature and presented response data suggest the limited validity of response prediction models not only for isomers. Furthermore, such deviations likely occur for other functional groups and structural isomers as well and need to be addressed in future.

Interactions of, e.g., sugars and organic acids with water showed that transfer of GC/FID data cannot be done in general. These interactions between eluent and analyte show that LC/FID response prediction is more complex and requires more than simple addition of functional group contributions. The underlying mechanisms revealed several new aspects, which have to be taken into account for future LC/FID response models.

5.5 References

[1] R.G. Ackman, Fundamental Groups in the Response of Flame Ionization Detectors to Oxygenated Aliphatic Hydrocarbons, Journal of Chromatographic Science, 2 (1964) 173-179.
[2] J.Y. de Saint Laumer, E. Cicchetti, P. Merle, J. Egger, A. Chaintreau, Quantification in gas chromatography: prediction of flame ionization detector response factors from combustion enthalpies and molecular structures, Anal. Chem., 82 (2010) 6457-6462.
[3] A.D. Jorgensen, K.C. Picel, V.C. Stamoudis, Prediction of gas chromatography flame ionization detector response factors from molecular structures, Anal. Chem., 62 (1990) 683-689.
[4] G. Musumarra, D. Pisano, A.R. Katritzky, A.R. Lapucha, F.J. Luxem, R. Murugan, M. Siskin, G. Brons, Prediction of gas chromatographic response factors by the PLS method, Tetrahedron Comput. Methodol., 2 (1989) 17-36.
[5] H.Y. Tong, F.W. Karasek, Flame ionization detector response factors for compound classes in quantitative analysis of complex organic mixtures, Anal. Chem., 56 (1984) 2124-2128.
[6] R.J. Maggs, A commercial detector for monitoring the eluent from liquid chromatographic columns, Chromatographia, 1 (1968) 43-48.
[7] R.P.W. Scott, J.G. Lawrence, An improved moving wire Liquid chromatography detector, J. Chromatogr. Sci., 8 (1970) 65-71.
[8] R.M. Smith, R.J. Burgess, Superheated water - A clean eluent for reversed-phase high-performance liquid chromatography, Anal. Commun., 33 (1996) 327-329.
[9] O. Chienthavorn, R.M. Smith, Buffered superheated water as an fluent for reversed-phase high performance liquid chromatography, Chromatographia, 50 (1999) 485-489.
[10] Y. Yang, Subcritical water chromatography: A green approach to high-temperature liquid chromatography, J. Sep. Sci., 30 (2007) 1131-1140.
[11] I.D. Wilson, Investigation of a range of stationary phases for the separation of model drugs by HPLC using superheated water as the mobile phase, Chromatographia, 52 (2000) S28-S34.
[12] T. Yarita, R. Nakajima, S. Otsuka, T. Ihara, A. Takatsu, M. Shibukawa, Determination of ethanol in alcoholic beverages by high-performance liquid chromatography-flame ionization detection using pure water as mobile phase, J. Chromatogr. A, 976 (2002) 387-391.
[13] C. Becker, M.A. Jochmann, T.C. Schmidt, An Overview of Approaches in Liquid Chromatography Flame ionization Detection, Trends Anal. Chem., (2018).
[14] Y. Fu, R.J. Song, N. Yao, Y.D. Long, T.B. Huang, Separation of some alcohols, phenols and caboxylic acids by coupling of subcritical water chromatography and flame ionization detection with post-column splitting, Chin. J. Anal. Chem., 35 (2007) 1335-1338.
[15] L. Zhang, D.M. Kujawinski, M.A. Jochmann, T.C. Schmidt, High-temperature reversed-phase liquid chromatography coupled to isotope ratio mass spectrometry, Rapid Commun. Mass Spectrom. , 25 (2011) 2971-2980.
[16] W.E. Neff, W.C. Byrdwell, Soybean oil triacylglycerol analysis by reversed-phase high performance liquid-chromatography coupled with atmospheric-pressure-chemical-ionization mass spectrometry, J. Am. Oil Chem. Soc., 72 (1995) 1185-1191.

[17] W.E. Neff, M.A. Jackson, G.R. List, J.W. King, Qualitative and quantitative determination of methyl esters, free fatty acids, mono-, di-, and triacylglycerols via HPLC coupled with a flame ionization detector, J. Liq. Chromatogr. Related Technol., 20 (1997) 1079-1090.
[18] J.C. Sternberg, Gallaway, W.S. and Jones, D.T.L., The Mechanism of Response of Flame Ionization Detectors, in: Gas Chromatography: Third International Symposium Held Under the Auspices of the Analysis Instrumentation Division of the Instrument Society of America, June 13-16, 1961, Academic, 1962, pp. 231-267.
[19] I. Halasz, W. Schneider, Quantitative Gas Chromatographic Analysis of Hydrocarbons with Capillary Column and Flame Ionization Detector, Analytical Chemistry, 33 (1961) 978-982.
[20] W.A. Dietz, Response Factors for Gas Chromatographic Analyses, J. Chromatogr. Sci., 5 (1967) 68-71.
[21] E. Young, R.M. Smith, B.L. Sharp, J.R. Bone, Liquid chromatography-flame ionisation detection using a nebuliser/spray chamber interface. Part 2. Comparison of functional group responses, J. Chromatogr. A, 1236 (2012) 21-27.
[22] J. Kosch, Total Hydrocarbon Analysis Using Flame Ionization Detector, in: Environmental Instrumentation and Analysis Handbook, Wiley, 2005, pp. 147-156.
[23] G. Perkins, R.E. Laramy, L.D. Lively, Flame Response in the Quantitative Determination of High Molecular Weight Paraffins and Alcohols by Gas Chromatography, Analytical Chemistry, 35 (1963) 360-362.
[24] T. Holm, Aspects of the mechanism of the flame ionization detector, J. Chromatogr. A, 842 (1999) 221-227.
[25] P.S. Veloo, Studies of Combustion Characteristics of Alcohols, Aldehydes and Ketons, University of Southern California, (2011) 1-221.
[26] K.-Y. Lam, W. Ren, S.H. Pyun, A. Farooq, D.F. Davidson, R.K. Hanson, Multi-species time-history measurements during high-temperature acetone and 2-butanone pyrolysis, Proceedings of the Combustion Institute, 34 (2013) 607-615.
[27] M. Szwarc, J.W. Taylor, Pyrolysis of Acetone and the Heat of Formation of Acetyl Radicals, The Journal of Chemical Physics, 23 (1955) 2310-2314.
[28] J. Falbe, M. Regitz, RÖMPP Lexikon Chemie, 10. Auflage, 1996-1999: Band 2: Cm - G, Thieme, 2014.

Chapter 6

Determination of liquid chromatography/flame ionization detection response factors for N-heterocycles, carboxylic acids, halogenated compounds and others

Many Gas Chromatography / Flame Ionization Detection (GC/FID) studies are dealing with response behavior of analytes such as alcohols and alkanes. Studies in the field of liquid chromatography (LC)/FID mainly focused on volatile analytes. In contrast, studies on LC/FID by conveyor type interface covered high molecular non-volatile biopolymers, whereby no response factors were calculated. With this study we fill the gap and present response factors of volatile and non-volatile analytes by LC/FID.

In the present study 56 different compounds such as carboxylic acids, N-heterocycles, halogenated acids, pharmaceuticals and other compounds were investigated. In some cases the obtained response factor data confirmed aspects known from GC/FID studies. But this study also disproves several assumptions done in previous response studies as well as the prediction models based upon the experimental data and literature.

Especially relative sensitivity *(RF)* and effective carbon number (*ECN*) values of structural isomers such as pyrazine, pyridazine and pyrimidine are assumed to be equal in current response prediction models. Contradictory to this assumptions, the experimental response factors and *ECN* values of, e.g., the structural isomers pyrazine (RF_{Exp} 0.59; ECN_{Exp} 3.66), pyridazine (RF_{Exp} 0.66; ECN_{Exp} 4.1) and pyrimidine (RF_{Exp} 0.63; ECN_{Exp} 3.93) reveal different experimental response factors and *ECN* than proposed by response factor prediction models (*RF* 0.64; *ECN* 4).

6.1 Introduction

The FID is one of the most frequently used detectors in GC [1]. Its success is based on the robustness, sensitivity and high linear range, combined with a carbon dependent response [2]. The yield of signal causing formylium ions is approximately one out of 10^6 carbon atoms. The formylium ions primarily result from ionization by the reaction of oxygen with CH to $CHO^{\bullet}$ and further to $CHO^+ + e^-$ [2].

Response factors for a broad variety of compounds are known and research showed that hydrocarbon responses follow the equal per carbon rule. The proportionality allows the calculation of hydrocarbon concentrations without knowledge of the structure [3-6]. Carbon atoms were suggested to cause an equal response within the FID and several authors confirmed validity of the assumption for a broad variety of hydrocarbons [3, 7]. Further investigations showed the diminishing effects of several functional groups on the detector response and based on that, the model of the effective carbon number was developed [3].

An important issue of *ECN* contribution factors is the use for quantitative response prediction [8, 9]. Especially if reference materials or pure compounds are not available, response approximation by consideration of the *ECN* delivers suitable semi-quantitative approaches in GC/FID analysis. The *ECN* can be considered to be one of the most frequently used estimation models and a broad range of *ECN* data for GC relevant compound classes and functional groups are available [4, 9, 10]. However, disadvantages arise when heteroatoms are involved. In such cases, the formation of non-methane forming species occurs and diminishes the response per carbon significantly [11]. Oxygen containing compounds such as ketones, alcohols and esters react to methane, ethane and carbon monoxide. The latter one is known to cause no response in FID and thus reduces the expected response per carbon [3, 11]. Nitrogen containing compounds such as pyridine or amines tend to form undetectable hydrocyanic acid [11]. Thus, prediction of FID response for complex, heteroatom containing organic compounds becomes difficult and requires advanced prediction models.

A novelty was the investigation of many functionalized analytes by use of the relative sensitivity [4] and the later on derived theoretical response prediction models based up this values [5]. The validity of the most common GC/FID response prediction models for LC/FID responses can only be proved by comparison of experimental data. Therefore, the determination of LC/FID response data for functional groups and heteroatom containing compounds is obligatory. In the past only the response data of the most common compounds such as alcohols were investigated by LC/FID and compared to GC/FID data [12, 13]. Experimental studies revealed similarities in the responses of, e.g., ethanol and propanol as well as differences for LC/FID responses of ketones [14]. Due to the lack of data, a more detailed comparison of LC/FID to GC/FID response data is not possible until today.

Within this chapter, we focus on a broad range of N-heterocyclic compounds, halogen substituents and other compounds, to get a more detailed view on LC/FID responses and extend the range of data for a better comparability to GC/FID. Therefore, the experimental response data of 56 different compounds were measured and compared to GC/FID data if available. Furthermore, the effects of the structure, functional groups and heteroatoms were discussed under consideration of combustion processes known from literature.

6.2 Experimental section

6.2.1 Reagents

1,3 dichloro-2-prpanol (98%), 2,2,2-trifluorethanol (>99%), 2-chlorethanol (>99%), 2-hydroxybenzoic acid (>98%), 2-hydroxypyrazine (>97%), 3-chloropropanol (>99%) 4-methylbenzaldehyde (>96%), 4-aminoantipyrine (>98%), acetic acid (>99%), acetylsalicylic acid (>98%), acetonitrile (99.8%), butanoic acid (>99%), caffeine (≥99%), campherchinone (>97%), campher (≥95%), chloroacetic acid (>99%), cumarine (≥99%),dichloroacetic acd (>99%), formic acid (98%), heptanoic acid (>99%), hexanoic acid (>99.5%), hydroxycortisone (≥98%), iso-quinoline (>97%), N-methylpyrrole (>99%), nicotinic acid (>99%), octanoic acid (>99.5%), perfluoroheptanoic acid (>99%), perfluorononanoic acid (>97%), perfluorooctanoic acid (>96%), propanoic acid (>99%), pyridine-N-oxide

(>95%), pyrimidine-N-oxide (>97%), pyrrole (>98%), pyrrolidine (>99%), quinoline (>97%), quinoxaline (≥99%), s-triazine (97%), theophylline (>99%), sulfamethoxazole (>99.5%), trichloroacetyl chloride(>99%), uracil (>99.5%), urea (>99%) were purchased by Sigma Aldrich (Seelze, Germany). 1,8- cineole (>99%), ammonium formiate (>99%), and pyridazine-3(2*H*)-one (>97%) was purchased by Alfa Aesar (Heysham, UK). Morpholine (99%), piperazine (99%), piperidine (99%), pyrazine (99%), pyridazine (98%), pyridine (99.5%), pyrimidine (99%), toluene (>99%), trichloroacetic acid (>99%), were purchased by Merck (Darmstadt, Germany). Pentanoic acid (>99%) was purchased by Fisher Scientific GmbH (Schwerte, Germany).

Hydrogen (purity 5.0) and synthetic air (purity 5.0) for FID operation were purchased from AirLiquide (Oberhausen, Germany).

Stock solutions were prepared at total carbon concentrations c_{TC} of 100 mg L^{-1}. Whereby, c_{TC} represents the absolute concentration of carbon within the solution. Standard solutions were prepared by dilution from the stock solution at ten different levels in a range of 0.1 to 100 mg L^{-1} using Hamilton microliter syringes (Bonaduz, Switzerland). Solutions for response analysis were prepared by dilution of the stock solution to c_{TC} of 30 mg L^{-1}.

6.2.2 LC/FID analysis

FID analysis was performed with a Dani Master GC® provided by Axel Semrau (Sprockhövel, Germany). The FID temperature T_{FID} was set to 275°C. A hydrogen and synthetic air flow ($F_{Hydrogen}$) of 50 and (F_{Air}) of 450 mL min^{-1} was used, respectively. The signal was recorded with the Clarity software (DataApex, Prague, Czech Republic). For a detailed description of the LC/FID system and the experimental set up, please see **Chapter 3**: *"A Thermospray Nebulizer Interface for Liquid Chromatography - Flame Ionization Detection: Development and Optimization"*.

6.2.3 Response calculation

The experimental Effective Carbon Number (ECN_{Exp}) and the experimental Relative Sensitivity (RF_{Exp}) were calculated as explained in detail in **Chapter 4**: *"Response Analysis: A*

brief introduction to the applied response factor equations and the most common response factor prediction models".

6.3 Results and discussion

6.3.1 Response factors by LC/FID analysis

Twenty N-heterocycles, acetonitrile and ammonium formate, a homologues series of nine carboxylic acids (formic to pelargonic acid), tartaric and citric acid, the four perfluorinated acid perfluorohexanoic to perfluorononanoic acid, seven halogenated short chained acids, six aromatic acids, seven pharmaceutical substances and nine other compound were investigated. The experimental derived *ECN* values *(ECN_{Exp})*, the calculated theoretical responses according to Sternberg et al. *(ECN_{Theo})*, the relative sensitivity according to literature *(RF)* and this study *(RF_{Exp})* are summarized in table 6.1.

Table 6.1. Theoretical effective carbon number according to literature *(ECN_{Theo})*, recorded *ECN_{Exp}* of the present study, and experimental *RF* values according to literature and *(RF)* and this study *(RF_{Exp})*.

Substance	*ECN_{Theo}*[3]	*ECN_{Exp}*	*RF* [4] / [13]	*RF_{Exp}*
Acids				
Formic acid	0	0.10	0.01/-	0.03
Acetic acid	1	1.14	0.24/0.21	0.24
Propanoic acid	2	2.05	0.40/-	0.35
Butanoic acid	3	2.99	0.48/-	0.43
Pentanoic acid	4	4.03	-/-	0.51
Hexanoic acid	5	5.04	0.63/-	0.56
Heptanoic acid	6	6.18	0.61/-	0.61
Octanoic acid	7	6.88	0.65/-	0.61
Tartaric acid	0.5	0.57	-/-	0.05
Aromatic acids				
Nicotinic acid	5	4.72	-/-	0.49
2-hydroxybenzoic acid	5.4	5.05	-/-	0.47
3-phenylacrylic acid	7.95	7.90	-/-	0.68
Chloro halogenated compounds				
Chloroacetic acid	1.00	0.72	-/-	0.10
Dichloroacetic acid	0.76	0.55	-/-	0.05
Trichloroacetic acid	0.52	0.45	-/-	0.64

Table 6.1. (Continued) Theoretical effective carbon number according to literature *(ECN_{Theo})*, recorded *ECN_{Exp}* of the present study, and experimental *RF* values according to literature and *(RF)* and this study *(RF_{Exp})*.

Substance	*ECN_{Theo}*[3]	*ECN_{Exp}*	*RF* [4] / [13]	*RF_{Exp}*
Chloro halogenated compounds (Continued)				
Trichloroacetyl chloride	0.52	0.34	-/-	0.02
2-chloroethanol	1.40	1.58	-/-	0.25
3-chloropropanol	2.40	1.47	-/-	0.20
1,3-dichloro-2-propanol	2.01	1.35	-/-	0.13
Fluoro halogenated compounds				
Perfluoroheptanoic acid	4.44	3.75	-/-	0.13
Perfluorooctanoic acid	5.20	4.54	-/-	0.14
Perfluornonanoic acid	5.96	6.55	-/-	0.18
2,2,2-trifluoroethanol	1.04	0.97	-/-	0.12
Nitrogen-heterocycles				
Pyridine	5	4.93	0.80/0.90	0.80
Pyrazine	4	3.66	-/-	0.59
Ammonium formate	0	0.09	-/-	0.02
Pyridazine	4	4.10	-/-	0.66
Pyrimidine	4	3.93	-/-	0.63
Acetonitrile	1.3	1.20	0.39/-	0.37
Morpholine	2.8	3.71	-/-	0.55
Piperazine	1.8	3.38	-/-	0.50
Quinoline	9	10.27	0.79/-	1.02
iso-quinoline	9	9.69	0.80/-	0.95
Pyridine-N-oxide	5	4.79	-/-	0.64
2-hydroxypyridine	4.75	4.61	-/-	0.62
Chinoxaline	8	8.75	-/-	0.86
2-hydroxypyrazine	4	2.45	-/-	0.33
Piperidine	5	5.98	-/-	0.90
s-triazine	3	0.97	-/-	0.15
2-pyrrolidone	3	4.73	-/-	0.71
Pyrrole	4	3.60	0.81/-	0.69
N-methyl pyrrole	5	3.65	-/-	0.58
Pyridazine-3(2*H*)-one	3	1.83	-/-	0.24
4-aminoantipyrine	9.4	9.53	-/-	0.60

Table 6.1. (Continued) Theoretical effective carbon number according to literature *(ECN_{Theo})*, recorded *ECN_{Exp}* of the present study, and experimental *RF* values according to literature and *(RF)* and this study *(RF_{Exp})*.

Substance	*ECN_{Theo}*[3]	*ECN_{Exp}*	*RF* [4] / [13]	*RF_{Exp}*
Others				
Toluene	7	7.15	-/-	0.99
1,8-cineole	9	9.57	-/-	0.80
Urea	0	0.07	-/-	0.01
4-methyl-benzaldehyde	7	6.45	-/-	0.69
Campher	9	9.82	-/-	0.83
Campherchinone	8	6.16	-/-	0.47
Sulfamethoxazole	7.75	3.99	-/-	0.20
Theophylline	5	1.84	-/-	0.18
Uracil	2	0.56	-/-	0.06
Hydrocortisone	14.8	10.43	-/-	0.37
Caffeine	1.6	1.86	-/-	0.12
Coumarin	7	4.37	-/-	0.38

6.3.2 Acids

The ECN_{Exp} of formic to nonanoic acid was found to increase linearly with a correlation of R^2 0.995 (Figure 6.1a) by each carbon atom. Table 6.1 shows the increase of the ECN_{Exp} from 0.1 (formic acid) to 8 (nonanoic acid). The RF_{Exp} values are in compliance to those observed by Dietz [4] in GC/FID studies and Young et al. [13] by using an LC/FID system.

The reduction of ECN_{Exp} compared to the number of carbons as depicted in Figure 6.1b indicates formation of a non-detectable species out of the carboxylic group. The thermal decomposition of formic acid and resulting reaction products were investigated by several authors [14-16]. The majority of carboxylic group decomposition takes place via dehydration (Eq. 6.1) and decarboxylation (Eq. 6.2).

$$HCOOH \rightarrow H_2O + CO \quad \text{Eq. 6.1}$$

$$HCOOH \rightarrow CO_2 + H_2 \quad \text{Eq. 6.2}$$

$$HCOOH + H^* \rightarrow COH^* + H_2 \quad \text{Eq. 6.3}$$

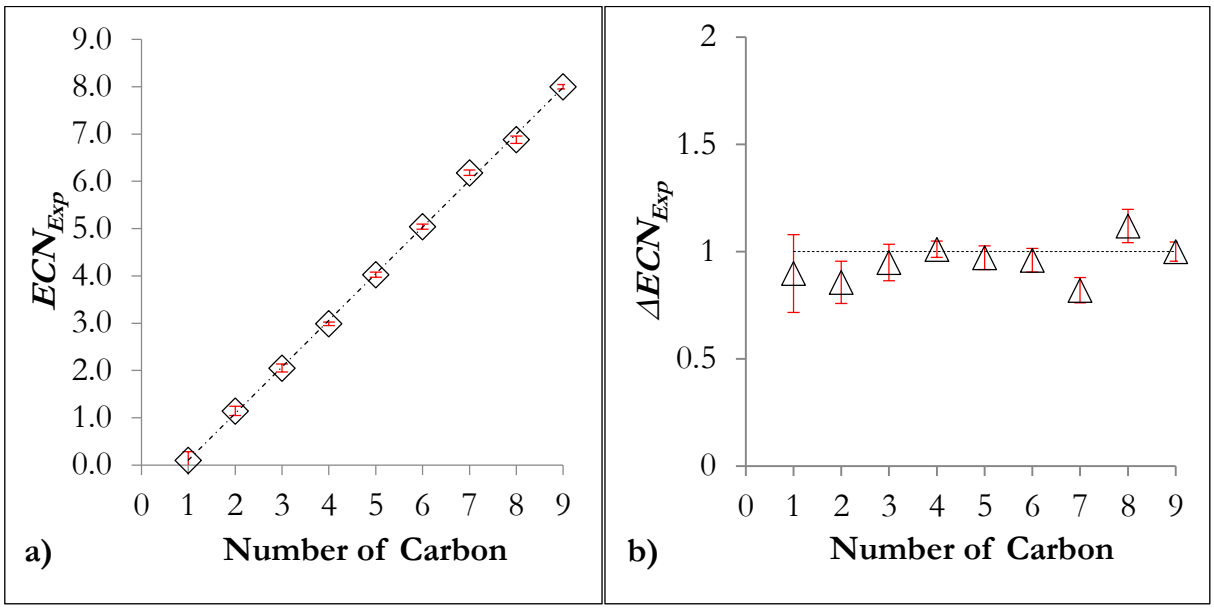

Figure 6.1. Molar response factors and the diminishing effect of a homologues series of carboxylic acids (a) diamonds are the recorded ECN_{Exp} of C_1 to C_9 carboxylic acids and uncertainty. **(b)** triangles show the experimentally observed reduction of the ECN_{Exp} by approximately 1, dashed line indicates the theoretical reduction by one.

Formation of carboxyl radicals (Eq. 6.3) can be considered to be negligible. The ECN_{Exp} values shown in Figure 1b confirm the almost complete reaction of the carboxylic group to FID insensitive CO and CO_2 as proposed for GC/FID by Scanlon [9], Ackerman [15] and Sternberg [3].

An ECN_{Exp} of 0.69 was observed for tartaric acid by LC/FID analysis. Within previous studies, the ECN_{Exp} of butan-2,3-diol was recorded with 2.09. Replacing two methyl groups by two carboxylic groups, the low response of tartaric acid seems to be reasonable.

The recorded ECN_{Exp} of nicotinic acid was 4.72. The ΔECN_{Exp} value of nicotinic acid and non-substituted pyridine (ECN_{Exp} of 4.93) is only -0.21. This shows the complete inactivation of the carboxyl substituent in nicotinic acid. Furthermore, the *meta*-position of the carboxylic group in nicotinic acid possibly results in a higher formation of hydrogen cyanate and causes the diminished response. 2-hydroxybenzoic acid and 3-phenylacrylic acid showed ECN_{Exp} of 5.05 and 7.90, respectively. The reduction of the ECN_{Exp} values by about 1, provides evidence to the assumption that the carboxylic group is almost completely transferred into non-detectable species.

6.3.3 Halogenated compounds

The highest suppression effect on the ECN_{Exp} was observed for mono-substituted chloro-compounds (Table 6.3). Comparison of the non-halogenated analytes ethanol, propanol, and acetic acid to the mono-substituted analytes chloroethanole, chloropropanol and chloroacetic acid reveal a chloro-substitute induced ECN_{Exp} reduction of 0.4, 0.9 and 0.5, respectively.

Addition of further chloro-substituents was noticed to have a minor effect. The ECN_{Exp} reduction of chloroacetic acid to dichloroacetic acid, trichloroacetic acid and trichloroacetyl chloride was about 0.12 each. The same reduction of 0.12 can be observed for mono- to dichloropropanol. Figure 6.2a shows the stepwise ECN_{Exp} decrease of the non-substituted analytes and the chloro-substituted analytes. The data are in compliance to the *ECN* contribution factor of -0.12 encountered for two or more chloro-substituents by Sternberg et al. [3] and close to the average decrease of -0.14 observed for mono-substituted chlorines by Kallai [8].

Considering the low bond dissociation energy of the C-Cl bond of ΔH_{diss}= 327 kJ mol^{-1} the experimental decrease of the ECN_{Exp} seems to be unreasonable and C-Cl bond cleavage should cause a minor, negligible effect on the ECN_{Exp} and RF_{Exp} respectively [8, 9]. A possible reason of the lower ECN_{Exp} values of, e.g., trichloroacetic acid in LC/FID is possibly due to the excess of H_2O and the free radicals generated in the interior of the flame (Equation 6.4). Further reaction of the radicals with water result in formation of FID insensitive species [16] according to Equation 6.5 and 6.7, respectively.

$$CCl_3COO^- \xrightarrow{\Delta H} (CCl_3COO^-)^* \quad \text{Eq. 6.4}$$

$$(CCl_3COO^-)^* \rightarrow CCl_3^* + COO^- \quad \text{Eq. 6.5}$$

$$(CCl_3COO^-)^* \rightarrow Cl^* + CCl_2COO^- \quad \text{Eq. 6.7}$$

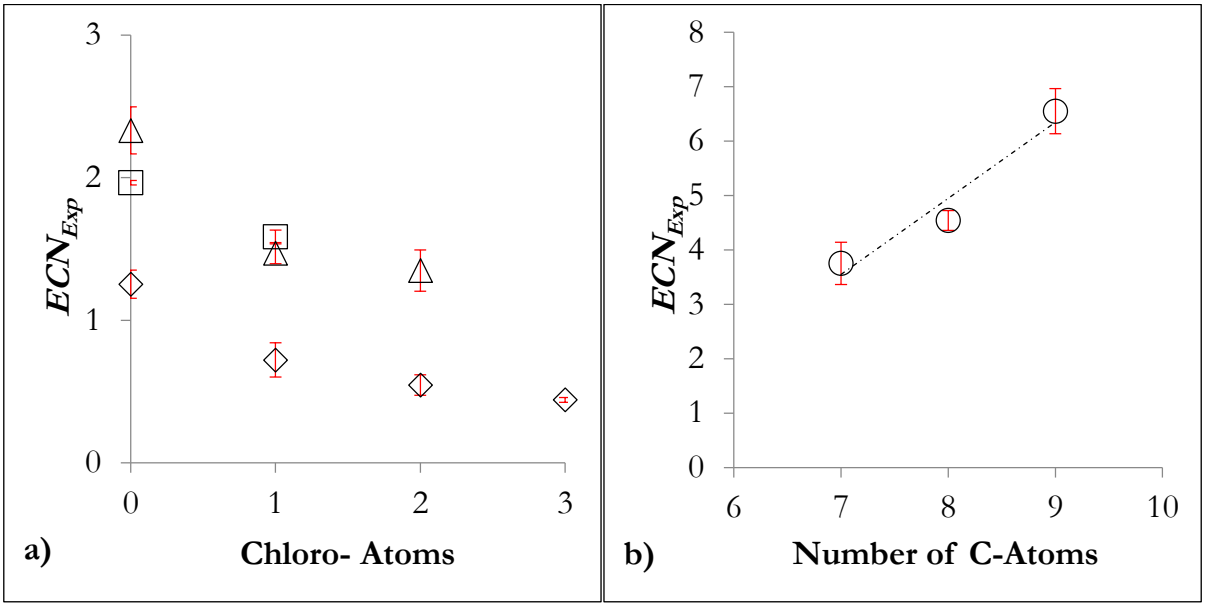

Figure 6.2. Influence of halogen-substitutes on the ECN_{Exp} (a) diamonds show the ECN_{Exp} decrease of acetic acid and the corresponding mono-, di- and tri- chlorinated analytes. Triangles show the ECN_{Exp} decrease of 1-propanol to 3-chloro-1-propanol and 1,3-dichloro-2-propanol. Squares indicate the ECN_{Exp} of ethanol and chloroethanol. **(b)** circles show the ECN_{Exp} of C7 to C9 perfluorocarboxylic acids.

The ECN_{Exp} of 2,2,2-trifluoroethaonol was found to be 0.95 and approximately half of the value recorded for ethanol (ECN_{Exp} 1.98). In a previous study on the reactions of alcohols in the FID, we showed the importance of dehydrogenation for formation of detectable species out of OH substituted carbons. Here, the fluoro atoms support the dehydrogenation reaction and thus formation of detectable CHO^+. It can be suggested, that the tri-substituted carbon atom cannot be transformed into a $CHO^{\bullet}$ -radical. The almost complete inactivation of the fluorine substituted carbon can be derived out of the reaction mechanism published by Arthur and Bell [17] (Equation 6.8 to 6.11).

$$CF_3CH_2O + H^* \rightarrow CF_3CHO^- + H_2 \qquad \text{Eq. 6.8}$$

$$CF_3CHO^- \rightarrow CF_3^- + CHO^+ + e^- \qquad \text{Eq. 6.9}$$

$$H^+ + CF_3^- \rightarrow CF_3H \qquad \text{Eq. 6.10}$$

$$CF_3OH \rightarrow CF_2O + HF \qquad \text{Eq. 6.11}$$

The proposed chain mechanism for decomposition results in two major reaction products: CF_3^- and CHO^+ [17]. In the presence of water CF_3^- reacts to CF_3OH [16-18]. Kinetic studies

on the behavior of CF_3OH reveal the conversion into CF_2O and HF (Equation 6.13) [18-20]. Carbonyl fluoride finally hydrolyzes to carbon dioxide and hydrogen fluoride [20, 21]. Both species are non-detectable by FID.

The situation changes by extension of the carbon backbone in perfluorinated alkanes (PFAs). Askew and Maduskar [22] reported the response of PFAs of more than 6 C-atoms to approach the response values of their hydrocarbon analogs. The authors concluded that the wide variation in response values of perfluoroalkanes and the similarity of high molecular weight perfluoroalkanes and alkanes is due to the stability of the C-F bond, which decreases by the progressive increase of the carbon chain length [22].

The ECN_{Exp} of perfluorinated carboxylic acids (PFCAs) was found to diminish by approximately 3.25 to 3.5 in contrast to PFA analogs, or the corresponding aliphatic hydrocarbons. The carboxylic group reacts into insensitive species such as CO and CO_2 (Eq. 6.2 and 6.3) and thus cause loss of sensitivity or *RF* for the PFCAs. The formation of non-detectable species such as CF_2O may result in the observed reduction of the ECN_{Exp} and RF_{Exp}, respectively. Possibly, the excess of water favors formation of these and other non-detectable species. However studies on the combustion of PFCAs in the presence of H_2O are not available yet and should be part of future research.

6.3.4 Nitrogen containing compounds

Using previously published response calculation models, the structural isomers pyrimidine, pyrazine and pyridazine result in equal responses [5, 6]. In contrast to the former studies, Table 6.1 shows the experimentally obtained decrease of the isomer responses in the order of pyridazine > pyrimidine > pyrazine.

Holmes [11] investigated heteroatom effects in the interior of the flame and found the origin of response variations in formation of hydrogen cyanide (Eq. 6.12).

$$CH_3 - NH_2 + 2H^* \rightarrow (CH_2 = NH + 2H_2) \rightarrow HCN + 3H_2 \qquad \text{Eq. 6.12}$$

A more detailed reaction pathway (Figure 6.3 and 6.4) for the pyrolysis of pyridine and pyrimidine heterocycles was published by Hore et al. in 1998 [23].

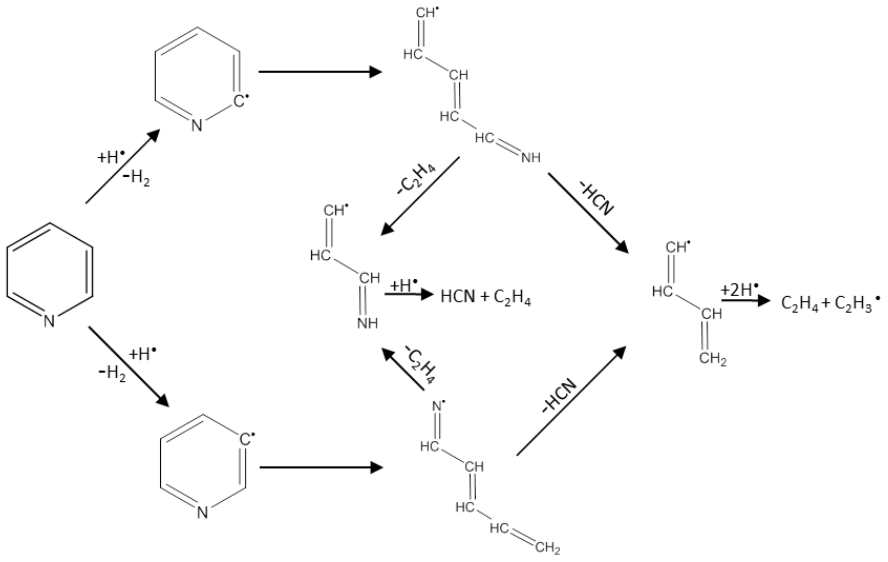

Figure 6.3. Decomposition of pyridine in the interior of the FID [23].

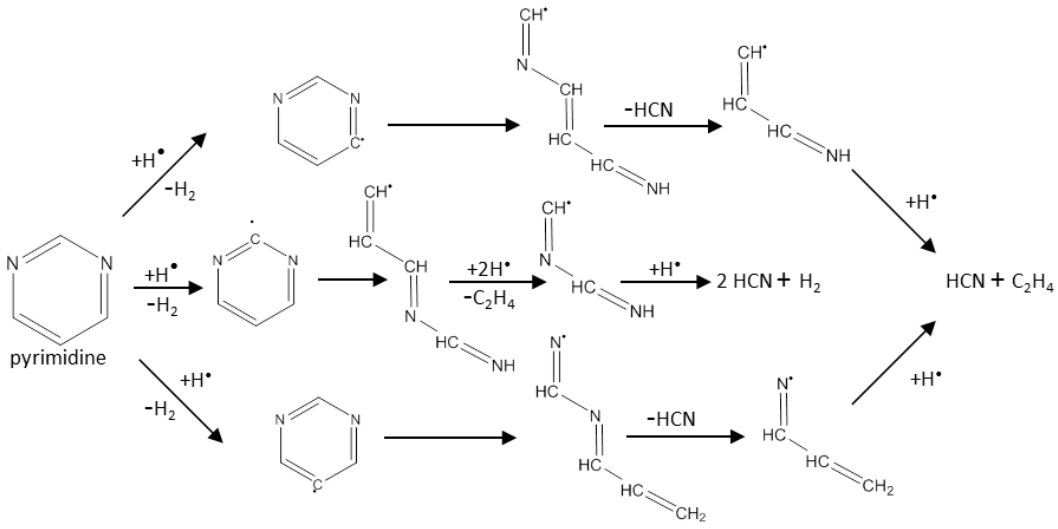

Figure 6.4. Proposed decomposition of pyrimidine in the interior of the FID.

The reaction schedule shows, pyrolysis of pyridine results in formation of a single intermediate with a terminal nitrogen. In contrast, cleavage of the diazines results in formation of two intermediates with terminal nitrogen [23]. The dissociation energy of the terminal C=N bond is ΔH_{diss} = 615 kJ mol^{-1} compared to ΔH_{diss} = 348 and 614 kJ mol^{-1} for C-C and C=C bonds, respectively. Accordingly, formation of HCN out of terminal nitrogen

as shown in Equation 6.12 is favored. The assumption can be confirmed by the response reduction recorded within this work and by others [24]. Also reported in literature is the isomerization of pyrazine to pyrimidine. The equality of both experimental responses might be an evidence of a comparable pyrolytic reaction, which may include the isomerization of pyrimidine/pyrazine as proposed by Doughty et al. [24].

The diazine heterocycle pyridazine showed a higher response (ECN_{Exp} 4.1) than recorded for the isomers pyrazine (ECN_{Exp} 3.66) and pyrimidine (ECN_{Exp} 3.93). Hore and Russel [23] concluded that an intramolecular elimination of the nitrogen to N_2 is the major reaction pathway in pyridazine pyrolysis. The second intramolecular route with formation of 2 HCN as observed for the isomers pyrazine and pyrimidine is feasible, but negligible [23].

The response of s-triazine is influenced by its conversion into ammonium formate in the presence of water [25]. The resulting hydrolysis product results in the FID non-detectable species hydrocyanic acid. The positioning of the nitrogen within the heterocyclic ring and the resulting combustion fragments lead to a comparable response pattern than observed for unsubstituted azines. In comparison to the non-substituted azines the presence of the N^+=O bond as observed in pyridine-1-oxide and pyrimidine-1-oxide resulted in an attenuation of the response by a factor of 1.5. In contrast, reduction of the response by a factor of >2 was observed for the C=O bonds of pyridine-2(1H)-one and pyridazine-3(2H)-one. The increased diminishing effect relates to the increased bond dissociation energy of C=O (ΔH_{diss} = 745 kJ mol^{-1}) in contrast to N=O, C=C and C-O bonds, respectively. According to Nicholson [26], the reaction of carbonyl groups are too endothermic and slow for ionization. Therefore, the oxygen carrying carbon atom is converted into the non-detectable carbon monoxide [26]. Equation 6.13 shows the proposed reaction after cleavage of the ring structure.

$$CH_2O + 2H_2 \rightarrow CO + 3H_2 \qquad \text{Eq. 6.13}$$

Non-aromatic heterocycle responses decrease by the number of heteroatoms within the molecule, too. Whereby, only a minor amount of the carbon bonded nitrogen reacts further to HCN. In contrast to aromatic heterocycles, the nitrogen can also react to ammonia

during reaction in the reductive part of the H_2 flame. Cleavage of the ring structure results in stepwise conversion of the single bonded carbon atoms to CH_4 and further to CHO^+.

Transformation in the interior of the reductive part of the flame involves reduction of the double bonds of heterocyclic aromatics. Pyrimidine and pyrazine as well as piperazine result in similar combustion products (CO, NH_3 and HCN) and thus show a similarity in their response behavior. The ECN_{Exp} of 3.6 measured for pyrrole indicates a partial conversion of the C-N bond into HCN. Zhai et al. reported several nitrogen containing intermediates in a theoretical combustion study of pyrrole, and suggested HCN as an important end product during combustion [27]. The significant decrease of the ECN_{Exp} provides evidence to the assumption that formation of HCN is more relevant in pyrrole combustion.

For 4-Aminoantipyrin a complete conversion to CHO^+ can be considered for the benzene ring as well as the methyl substituents. Combustion of the pyrin ring results mainly in formation of the three species HCN, CO and CHO^+. However, the recorded ECN_{Exp} is close to the theoretical response according to Sternberg.

6.3.5 Others

Toluene was found to have a higher response factor than the number of carbon atoms. Dietz reported a *RF* value of 1.07 for toluene, which indicates that a substantially higher response than the number of carbons was recorded by GC/FID, too. Here and elsewhere a reasonable conclusion for the increased sensitivity is not provided.

The ECN_{Exp} of p-tolylaldehyde was affected more than expected by the ketone group. As previously mentioned, a complete inactivation of the oxygen containing carbon would be reasonable. However, the response was diminished by 1.55. Even more affected was the response of campherchinone, which contains two ketones. Here the ECN_{Exp} response was reduced by 3.84, which is almost two times higher than the reduction of the ECN_{Exp} in aliphatic ketones.

Sulfamethoxazole, theophylline, uracil, caffeine and coumarin were noticed to be detectable by LC/FID, but the response was substantially reduced in contrast to theoretical calculation models (Table 6.1). Most of these compounds are heterocyclic and have more than one

functional group. Correction for the response reducing effect of heterocycles and functional groups on the compounds would result in higher responses than recorded. The complex structures might show the importance of multiple substituents and the final effect on the combustion products and resulting response. Since most analytes of the present study as well as in literature are aliphatic or aromatic compounds with one or two functional groups, comparison was not possible until yet. However, the importance of the influence of multiple substituents and consideration of the basic structure of analytes becomes obvious.

6.4 Conclusion

The presented response study demonstrated the high value of LC/FID analysis, enabling the determination of volatile and non-volatile analytes. Comprehensive response studies on structural isomers by consideration of inflame processes has proven to add important information for the explanation of response behavior of a broad spectra of analytes. Due to the limitation of only water LC methods nowadays, the technique will need to be explored for more analytes. Furthermore, a more detailed database for the FID relevant combustion processes of complex molecules is required.

On the one hand the experimental data confirm the limited validity of prediction models previously published for structural isomers [5, 6]. On the other hand the interaction of perfluorinated analytes with the eluent shows that a direct comparison of GC and LC data only can be done for analytes which are not affected by the eluent, e.g., ketones. Future studies should focus on the interactions of eluent with the analyte to get a more detailed view on the in-flame processes and the occurring differences between LC/FID and GC/FID response data.

6.5 References

[1] B.A. Ingelse, H.G. Janssen, C.A. Cramers, HPLC-FID with superheated water as the fluent: Improved methods and instrumentation, J. High. Resolut. Chromatogr., 21 (1998) 613-616.
[2] T. Holm, Aspects of the mechanism of the flame ionization detector, J. Chromatogr. A, 842 (1999) 221-227.
[3] J.C. Sternberg, Gallaway, W.S. and Jones, D.T.L., The Mechanism of Response of Flame Ionization Detectors, in: Gas Chromatography: Third International Symposium Held Under the Auspices of the Analysis Instrumentation Division of the Instrument Society of America, June 13-16, 1961, Academic, 1962, pp. 231-267.
[4] W.A. Dietz, Response Factors for Gas Chromatographic Analyses, J. Chromatogr. Sci., 5 (1967) 68-71.
[5] G. Musumarra, D. Pisano, A.R. Katritzky, A.R. Lapucha, F.J. Luxem, R. Murugan, M. Siskin, G. Brons, Prediction of gas chromatographic response factors by the PLS method, Tetrahedron Comput. Methodol., 2 (1989) 17-36.
[6] J.Y. de Saint Laumer, E. Cicchetti, P. Merle, J. Egger, A. Chaintreau, Quantification in gas chromatography: prediction of flame ionization detector response factors from combustion enthalpies and molecular structures, Anal. Chem., 82 (2010) 6457-6462.
[7] I. Halasz, W. Schneider, Quantitative Gas Chromatographic Analysis of Hydrocarbons with Capillary Column and Flame Ionization Detector, Analytical Chemistry, 33 (1961) 978-982.
[8] M. Kállai, J. Balla, The effect of molecular structure upon the response of the flame ionization detector, Chromatographia, 56 (2002) 357-360.
[9] J.T. Scanlon, D.E. Willis, Calculation of Flame Ionization Detector Relative Response Factors Using the Effective Carbon Number Concept, J. Chromatogr. Sci., 23 (1985) 333-340.
[10] M. Morvai, I. Pályka, l. Molnár-Perl, Flame Ionization Detector Response Factors Using the Effective Carbon Number Concept in the Quantitative Analysis of Esters, Journal of Chromatographic Science, 30 (1992) 448-452.
[11] T. Holm, Mechanism of the flame ionization detector II. Isotope effects and heteroatom effects, J. Chromatogr. A, 782 (1997) 81-86.
[12] E. Young, R.M. Smith, B.L. Sharp, J.R. Bone, Liquid chromatography-flame ionisation detection using a nebuliser/spray chamber interface. Part 1. Design and testing, J. Chromatogr. A, 1236 (2012) 16-20.
[13] E. Young, R.M. Smith, B.L. Sharp, J.R. Bone, Liquid chromatography-flame ionisation detection using a nebuliser/spray chamber interface. Part 2. Comparison of functional group responses, J. Chromatogr. A, 1236 (2012) 21-27.
[14] C. Becker, M.A. Jochmann, T.C. Schmidt, Determination of Liquid Chromatography/Flame Ionization Detection Response Factors for Alcohols, Ketones and Sugars, Anal Bioanal Chem, (2019).
[15] R.G. Ackman, Fundamental Groups in the Response of Flame Ionization Detectors to Oxygenated Aliphatic Hydrocarbons, Journal of Chromatographic Science, 2 (1964) 173-179.
[16] C. Wu, D. Wei, J. Fan, L. Wang, Photosonochemical degradation of trichloroacetic acid in aqueous solution, Chemosphere, 44 (2001) 1293-1297.

[17] N.L. Arthur, T.N. Bell, The recombination of trifluoromethyl radicals at high temperature, Chemical Communications (London), (1965) 166-167.
[18] W.F. Schneider, T.J. Wallington, R.E. Huie, Energetics and Mechanism of Decomposition of CF3OH, The Journal of Physical Chemistry, 100 (1996) 6097-6103.
[19] M. Zhang, Z. Lin, C. Song, Comprehensive theoretical studies on the CF3H dissociation mechanism and the reactions of CF3H with OH and H free radicals, The Journal of Chemical Physics, 126 (2007) 034307.
[20] L. Pasteris, E.V. Oexler, E.H. Staricco, Reaction of CF3 radicals with H2O and D2O, International Journal of Chemical Kinetics, 15 (1983) 835-844.
[21] M.W. Farlow, E.H. Man, C.W. Tullock, R.D. Richardson, Carbonyl Fluoride, in: Inorganic Syntheses, John Wiley & Sons, Inc., 2007, pp. 155-158.
[22] W.C. Askew, K.D. Maduskar, Response of the Flame lonization Detector to Perfluoroalkanes, Journal of Chromatographic Science, 9 (1971) 702-704.
[23] N. R. Hore, D. K. Russell, Radical pathways in the thermal decomposition of pyridine and diazines: a laser pyrolysis and semi-empirical study, Journal of the Chemical Society, Perkin Transactions 2, (1998) 269-276.
[24] A. Doughty, J.C. Mackie, Kinetics of thermal decomposition of the diazines: shock-tube pyrolysis of pyrimidine, Journal of the Chemical Society, Faraday Transactions, 90 (1994) 541-548.
[25] C. Grundmann, A. Kreutzberger, Triazines. IX. 1,3,5-Triazine and its Formation from Hydrocyanic Acid1,2, Journal of the American Chemical Society, 76 (1954) 5646-5650.
[26] A.J.C. Nicholson, Decomposition reactions in the flame ionization detector, Journal of the Chemical Society, Faraday Transactions 1: Physical Chemistry in Condensed Phases, 78 (1982) 2183-2194.
[27] L. Zhai, X. Zhou, R. Liu, A Theoretical Study of Pyrolysis Mechanisms of Pyrrole, The Journal of Physical Chemistry A, 103 (1999) 3917-3922.

Chapter 7

General conclusions and outlook

7.1 General conclusion

Coupling of LC/FID has evolved to become a complement to established LC detection methods such as light scattering detectors, UV detectors and mass spectrometers. Based on the required solvents for chromatographic separation, LC/FID amenable compounds increased over time from non-volatile to semi-volatile and volatile analytes [1]. The change from the FID sensitive organic solvents (e.g. methanol, acetonitrile) to an only water mobile phase resulted in the design of advanced direct interfaces. Therefore, LC/FID is no longer restricted to high boiling non-volatile compounds.

A broad range of UV insensitive analytes such as alcohols and aliphatic hydrocarbons can be quantified by LC/FID nowadays. Furthermore, modern LC/FID capillary jet interfaces can achieve the limits of detection known from modern GC/FID systems. Even more, residual solvents in pharmaceuticals, which cannot be detected with common LC detectors such as UV- or RI- detectors now can be analyzed using semi-quantitative determination by FID.

The presented LC/FID system successfully targeted the problem of capillary blockage [2] by implementation of a backpressure regulator in combination with a stainless steel capillary of larger internal diameter. By that, problems such as a non-linear response for semi- and non-volatile analytes as discussed by other authors [3] were not observed. The novel system was constructed to be adapted to the most common FID systems used in analytical laboratories, in contrast to former developments that were designed with inductive heating devices or required modifications of the FID [1]. It was shown that many GC and LC relevant analytes can be analyzed using the presented LC/FID interface. Using the interface, it was possible, to set up a substantial database for LC/FID response data.

The great advantage of the FID to be used for response prediction and semi-quantitative investigation of analytes using LC/FID is still not established in laboratories yet. Within this thesis more than 100 different responses of several compound classes such as N-heterocycles, ketones, sugars, and carboxylic acids were studied. This study like others [3]

reveals similarities between LC/FID and GC/FID responses for volatile compounds as well as differences for semi-volatile compounds.

Up to this study, response data of LC/FID systems were rare and not taken into consideration in response models and response prediction yet. Fundamental and sophisticated response prediction models were published by Sternberg [4], Dietz [5], Musumarra [6] and de Saint Laumer [7] for GC/FID. Most of them are not applicable for, e.g., structural isomers, since these models are based on functional group contribution factors. These prediction models were presented without consideration of the relevant in-flame process, and therefore result in equal responses for isomers. Young et al. [3, 8] and the here presented work demonstrated the variations of GC/FID and LC/FID response factors obtained for short chain alcohols, aniline and further compounds. The observed decreasing influence of hydroxyl groups or ketones in contrast to GC/FID related response literature reveal the necessity of a LC/FID related database of group specific contributions to the response.

Interactions of sugars and organic acids with water showed that transfer of GC/FID data cannot be done in general. These interactions between eluent and analyte show that LC/FID response prediction is more complex and requires more than simple addition of functional group contributions.

This thesis contributes to closing the gap between GC/FID and LC/FID response studies. The study of structural isomer responses within this work and literature revealed that the response of a compound cannot be derived by only using the number of hydrocarbons and heteroatoms within a molecule. It likely provides a basis for future LC/FID response studies.

7.2 Outlook

The presented data provide a detailed look on the responses of alcohols, poly-alcohols, ketones, sugars, nitrogen heterocycles, halogenated compounds and several others, however, many more compounds, e.g., pharmaceuticals, polyaromantic hydrocarbons, fatty acids need to be investigated. Future work in the field of LC/FID should focus on compounds which addresses compounds of industrial interest. For the use in pharmaceutical industries, the LC/FID interface should be applied for the analysis of, e.g., class 1 to class 3 residual solvents as described by the ICH guideline [9].

Within the past decade the trend in analytical chemistry is to decrease the amount of organic solvents and change to more environmental friendly analysis. On the one hand this can be done by miniaturized systems, on the other hand this can be achieved using only water liquid chromatography [10, 11]. Therefore, using of only water LC/FID can provide a substantial advantage to routine and pharmaceutical laboratories. Only water LC methods can easily be applied to several LC relevant analytes. The presented interface can be used, to combine the environmental aspects of only water LC with the robustness of the FID.

Today only a few only water LC methods are available and detection methods such as LC/IRMS benefit from the advantages of only water LC methods as shown in publications about, e.g., steroid or pesticide analysis by high temperature only water LC separation [12, 13]. Therefore future work in the field of LC/FID should also target the development of only water LC methods. By that, the acceptance of LC/FID can be significantly increased.

The responses of all compounds investigated by only water LC methods today and in future need to be recorded to extend the response data base of LC/FID. Response models and an appropriate data base are essential to increase the acceptance of LC/FID in laboratories. In addition, a data base of more than the here presented compounds will help to understand the occurring in-flame processes and the resulting responses in LC/FID.

Finally LC/FID can be combined with already existing LC detection methods, e.g., UV or MS. The required flow of the presented LC/FID between 10 to 50 µL min^{-1} allows the analysis of samples within any flow range and splitting of the eluent. By that analysts can take the advantages to gain structural information of the known or unknown compounds

of interest by, e.g., UV or MS combined with a semi-quantitative determination of the concentrations within the samples by FID.

7.3 References

[1] C. Becker, M.A. Jochmann, T.C. Schmidt, An Overview of Approaches in Liquid Chromatography Flame ionization Detection, TrAC, 110 (2018) 143-149.
[2] B.A. Ingelse, H.G. Janssen, C.A. Cramers, HPLC-FID with superheated water as the fluent: Improved methods and instrumentation, J. High. Resolut. Chromatogr., 21 (1998) 613-616.
[3] E. Young, R.M. Smith, B.L. Sharp, J.R. Bone, Liquid chromatography-flame ionisation detection using a nebuliser/spray chamber interface. Part 2. Comparison of functional group responses, J. Chromatogr. A, 1236 (2012) 21-27.
[4] J.C. Sternberg, Gallaway, W.S. and Jones, D.T.L., The Mechanism of Response of Flame Ionization Detectors, in: Gas Chromatography: Third International Symposium Held Under the Auspices of the Analysis Instrumentation Division of the Instrument Society of America, June 13-16, 1961, Academic, 1962, pp. 231-267.
[5] W.A. Dietz, Response Factors for Gas Chromatographic Analyses, J. Chromatogr. Sci., 5 (1967) 68-71.
[6] G. Musumarra, D. Pisano, A.R. Katritzky, A.R. Lapucha, F.J. Luxem, R. Murugan, M. Siskin, G. Brons, Prediction of gas chromatographic response factors by the PLS method, Tetrahedron Comput. Methodol., 2 (1989) 17-36.
[7] J.Y. de Saint Laumer, E. Cicchetti, P. Merle, J. Egger, A. Chaintreau, Quantification in gas chromatography: prediction of flame ionization detector response factors from combustion enthalpies and molecular structures, Anal. Chem., 82 (2010) 6457-6462.
[8] E. Young, R.M. Smith, B.L. Sharp, J.R. Bone, Liquid chromatography-flame ionisation detection using a nebuliser/spray chamber interface. Part 1. Design and testing, J. Chromatogr. A, 1236 (2012) 16-20.
[9] ICH, ICH Harmonised Tripartite Guideline, in: Impurities: Guideline for Residual Solvents Q3C(R5), 2011.
[10] R.M. Smith, Superheated water chromatography - A green technology for the future, J. Chromatogr. A, 1184 (2008) 441-455.
[11] Y. Yang, Subcritical water chromatography: A green approach to high-temperature liquid chromatography, J. Sep. Sci., 30 (2007) 1131-1140.
[12] L. Zhang, D.M. Kujawinski, M.A. Jochmann, T.C. Schmidt, High-temperature reversed-phase liquid chromatography coupled to isotope ratio mass spectrometry, Rapid Commun. Mass Spectrom. , 25 (2011) 2971-2980.
[13] Y. Yang, B. Kapalavavi, L. Gujjar, S. Hadrous, R. Marple, C. Gamsky, Industrial application of green chromatography - II. Separation and analysis of preservatives in skincare products using subcritical water chromatography, Int. J. Cosmetic Sci., 34 (2012) 466-476.

List of figures

List of tables

List of abbreviations

ΔH_{Comb}	Combustion enthalpy
ΔH_{diss}	Dissociation energie
µLC	Micro liquid chromatography
$A_{Compound}$	Peak area of a compound
A_{ISTD}	Peak area of the internal standard
$A_{Reference}$	Peak area of a reference compound
A_{Sample}	Peak area of a sample
BPR	Backpressure regulator
BTEX	Benzene, toluene, ethylbenzene, *meta*-xylene, *ortho*-xylene, *para*-xylene,
cP	Viscosity
c_{TC}	Total carbon concentration
DA	Diode array
dECN	Difference between the ECN of a molecule and the actual carbon atoms number
dyn/cm	Surface tension
ECN	Effective carbon number
$ECN_{Compound}$	Effective carbon number of a compound
ECN_{Exp}	Experimental effective carbon number
ECN_{Theo}	Theoretical effective carbon number
ELSD	Evaporative light scattering detector
Eq.	Equation
F_{Air}	Synthetic air flow in mL min^{-1}
$F_{Hydrogen}$	Hydrogen flow in mL min^{-1}
F_{Mobile}	Mobile phase flow in µL min^{-1}
$F_{Nitrogen}$	Nitrogen flow in mL min^{-1}
FI	Flow injection

FIA	Flow injection analysis
FID	Flame ionization detector
FS	Fused silica
GC	Gas chromatography
HPLC	High performance liquid chromatography
ID	Inner diameter
LC	Liquid chromatgraphy
LOD	Limit of detection
LOQ	Limit of quantification
$m_{Compound}$	Concentration mass of a compound
m_{ISTD}	Concentration mass of an internal standard
MS	Mass spectrometry
n/a	Not available
$n_{Carbon,\ i}$	Actual carbon-atom number of a compound
$n_{Compound}$	Amount of a compound
$n_{Reference}$	Amount of a reference compound
OD	Outer diameter
p.a.	Pro analysis
PAH	Polycyclic aromatic hydrocarbons
PECP	Pulsed electrochemically polished
PFA	Perfluorinated alkanes
PFCA	Perfluorinated carboxylic acids
R^2	Correlation coefficient
RF	Relative sensitivity
RF_{Exp}	Experimental relative sensitivity
RF_{Pred}	Predicted relative sensitivity
RI	Refractive idex

RP	Reverse phase
S/N	Signal to noise ratio
SD	Standard deviation
SFC	Supercritical fluid chromatography
SS	Stainless steel
T_{Oven}	Oven temperature of the gas chromatograph in °C

List of publications and presentations

Publications

C. Becker, M.A. Jochmann, T.C. Schmidt, An Overview of Approaches in Liquid Chromatography Flame ionization Detection, TrAC, 110 (2019) 143-149.

C. Becker, M.A. Jochmann, T.C. Schmidt, Determination of liquid chromatography/ flame ionization detection response factors for alcohols, ketones and sugars, ABC Journal, Accept (19.02.2019).

Presentation

25. Doktorandenseminar Hohenroda 2014 (Hohenroda, Germany)

C. Becker, M.A. Jochmann, T.C. Schmidt,

"Analysis of alcohols and selected compounds by a novel LC/FID interface"

Anakon 2015 (Graz, Austria)

C. Becker, M.A. Jochmann, T.C. Schmidt,

"Development of a LC-FID coupling - Parameter optimization and response analysis"

Poster

Anakon 2013 (Essen, Germany)

C. Becker, M.A. Jochmann

"Development of a LC-FID coupling for the universal detection of semi- and non-volatile compounds"

HPLC 2014 (New Orleans, USA)

C. Becker, M.A. Jochmann, T.C. Schmidt

"Development of a LC/FID coupling: Analysis of selected compounds by high temperature LC/FID"

HTC 2015 (Bad-Herrenalb, Germany)

C. Becker, O. Gassner, S. Wiese, M. A. Jochmann, T. Teutenberg

"Evaluation of a concept hyphenating flame ionization detection with nano- and capillary liquid chromatography"

Curriculum vitae

Aus datenschutzrechtlichen Gründen ist der Lebenslauf in der Online-Dissertation nicht enthalten.

Erklärung

Hiermit versichere ich, dass ich die vorliegende Arbeit mit dem Titel

„ Development of a Thermospray Nebulizer Interface for Liquid Chromatography with Flame Ionization Detection and Detector Response Studies of Volatile and non-Volatile Compounds"

selbst verfasst und keine außer den angegebenen Hilfsmitteln und Quellen benutzt habe, und dass die Arbeit in dieser oder ähnlicher Form noch bei keiner anderen Universität eingereicht wurde.

Essen, im März 2019

Christian Becker

Declaration of scientific contributions

The present thesis includes work that has been published in cooperation with Co-authors, with my own contributions declared as follows:

C. Becker, M.A. Jochmann, T.C. Schmidt, An Overview of Approaches in Liquid Chromatography Flame ionization Detection, TrAC, 110 (2019) 143-149.

Declaration of own contributions: The draft and corrections to the manuscript were written by C. Becker. The manuscript was revised by C. Becker, M.A. Jochmann, T.C. Schmidt.

C. Becker, M.A. Jochmann, T.C. Schmidt, Determination of liquid chromatography/ flame ionization detection response factors for alcohols, ketones and sugars, ABC Journal, Accept (19.02.2019)

Declaration of own contributions: The experiments were conducted by C. Becker. Sample preparation and evaluation of experimental data was performed by C. Becker and M. Funk. The draft and corrections to the manuscript were written by C. Becker. The manuscript was revised by C. Becker, M.A. Jochmann, T.C. Schmidt.

Danksagung

Die hier vorliegende Arbeit hat mich durch Höhen und Tiefen begleitet, wie die zahlreichen Menschen, auf dem langen Weg bis zu diesen abschießenden Worten. Daher möchte ich mir die Zeit nehmen und dies nicht nur als Obligatorium sehen, sondern den Menschen von Herzen danken, die mich mir ihr Vertrauen geschenkt haben und mich unterstützt haben, dass ich diese Arbeit beendenden konnte.

Ein großer Dank gilt Professor Torsten C. Schmidt für die Betreuung und der damit einhergehenden langjährigen und professionellen Betreuung sowie der Begutachtung der vorliegenden Arbeit. Er hat mir nicht nur die Möglichkeit gegeben meine Doktorarbeit in der Arbeitsgruppe der Instrumentellen Analytischen Chemie zu verfassen, sondern hat mich zu einem Teil seiner Ideen und großartigen Arbeit werden lassen. Seine Arbeitsgruppe war und ist wie eine Familie in der man sich unterstützt und für einander da ist.

Für die Übernahme des Zweitgutachtens und für die anregungsvollen und interdisziplinären Diskussionen spreche ich Herrn Professor Oliver J. Schmitz meinen Dank aus. In Seminaren und auf zahlreichen Konferenzen hat er mir immer wieder neue Blickwinkel auf meine Arbeit gezeigt.

Bei Herrn Dr. Maik A. Jochmann möchte ich mich für die moralische und fachliche Unterstützung bedanken. Er hat einen großen Anteil an dieser Arbeit, denn es war sein Projekt und sein Vertrauen in mich, was mir letztlich die Möglichkeit zu dieser Arbeit gegeben hat.

Abschließend möchte ich meinen Eltern danken. Ihr seid immer eine treibende Kraft gewesen und wir haben auf so zahlreichen Spaziergängen über diese Arbeit diskutiert. Ich habe mich immer gefreut, dass ihr meine Freude und Leidenschaft für die Analytik geteilt habt. Es ist mir ein besonderes Anliegen meinen Geschwistern Silke, Stefan und Angie zu Danken. Ein Mensch kann sich keine besseren Geschwister wünschen als euch, vielen Dank für die Unterstützung die ihr mir zuteilwerden lassen habe auf meinem Weg.

Sosehr ich durch die geprägt wurde die schon erwähnt wurden, möchte ich zu guter Letzt dem Menschen danken, der die größten Opfer und die größte Entbehrung bringen musste, Konstantin. Als ich diese Arbeit begonnen habe warst du noch so jung und doch musstest du in den letzten Jahren die größten Opfer bringen. Wir haben uns so oft die Zeit genommen, um Spaß zu haben, zu toben und den anderen zum Lachen zu bringen. Viel zu oft saß ich auch an dieser Arbeit und du hast mir die größte Geduld, die man von einem so kleinen Menschen und jedem Menschen überhaupt erwarten kann entgegengebracht. Du bist und bleibst immer meine treibende Kraft. Dein Wissensschlafler.